Groundwater occurrence and risk of pollution in a mountain watershed of Nicaragua

José Alfredo Mendoza

Engineering Geology
Lund University

Doctoral Thesis
2006

LUND UNIVERSITY

Academic thesis which, by due permission of the Faculty of Engineering at Lund University, will be publicly defended on Friday 12th of May, 2006, at 10:15 a.m. in lecture hall B, in the V-building, John Ericssons väg 1, Lund, for the degree of Doctor of Philosophy in Engineering.

Faculty opponent: Dr. Jiří Krásný, Charles University Prague, Czech Republic.

Author
José Alfredo Mendoza

Title
Groundwater occurrence and risk of pollution in a mountain watershed of Nicaragua

Keywords
Hydrogeology, groundwater, electrical resistivity, surface water, springs, Nicaragua

Published by
Engineering Geology, Lund University

Printed by
KFS AB Lund 2006

ISBN-10 91-973406-8-5
ISBN-13 978-91-973406-8-7
EAN 9789197340687
ISRN LUTVDG/TVTG--1019-SE

Preface

This research contribution constitutes a doctoral thesis developed within an interdisciplinary environmental research program, which aims to improve the capabilities of Nicaraguan universities on evaluating environmental problems. The research was developed during alternating periods of fieldwork in Nicaragua and data processing and analysis in Sweden. In Nicaragua, the responsible institution was the Centro de Investigaciones Geocientíficas, Universidad Nacional Autónoma de Nicaragua (CIGEO/UNAN-Managua). In Sweden, supervision was provided from Engineering Geology, Lund University. The investigations presented here have been performed under the auspices of the Swedish International Development Authority (Sida/SAREC).

This work is dedicated to all the rivers,

including Iyas Joti Alfons who is a continuous flow of energy,

love and

happiness.

Acknowledgments

The first credits go to the Swedes that through their Swedish International Cooperation Development Agency (Sida/ SAREC) show their solidarity with developing countries. I have great hopes that this support becomes less and less necessary in a near future, as Nicaragua develops its own capacities.

The Royal Physiographic Society in Lund provided me with the computer to write this thesis. I have got financial support to perform chemical analyses and participate in conferences from the following funds: Ekedahl-Lundbergska fonden, Stiftelsen Dagny och Eilert Ekvalls premie- och stipendiefond, and Stiftelsen Margit Stiernswärds fond för miljövårdsforskning.

The staffs from Engineering Geology, Lund University and Centro de Investigaciones Geocientíficas (CIGEO/UNAN) have co-operated to assist this research.

Torleif Dahlin and Gerhard Barmen have been excellent supervisors during this work. Torleif has been all the way in this trip, enthusiastically sharing his knowledge on geophysics. The guidance provided by Prof. Leif Bjelm during the first period of work is appreciated.

The logistical support from the personnel at CIGEO is acknowledged, in particular the director Dionisio Rodríguez, Marvin Valle, Verónica Mayorga and Silvia Morales. Doña Rosita and Carmencita supplied me with flavorful Nicaraguan coffee.

I want to express my gratitude to all the PhD-mates and friends from Nicaragua and Lund. I will not forget the camaraderie from current and former staff members at Engineering Geology; Peter Jonsson, Virginie Leroux, Peter Flyhammar, Conny Svensson, Peter Ulriksen and Kjell Andersson.

In the study area many miners provided assistance during fieldwork in Santo Domingo; Julio Guevara, Ramiro Duarte, Sergio Pérez and others.

Several Nicaraguan and Swedish students accompanied me during fieldwork in Santo Domingo. They are sincerely acknowledged for their participation in this research.

I appreciate the advices from many experienced practitioners and scientists. Whenever I had questions on methodology or applications, I got excellent answers and opinions.

More than a thesis I kept and gained several families during this journey. I want to thank families Pichardo Valverde (Managua), Duarte (Santo Domingo) and Upadhayaya (Sweden) for their full time support.

Ines, Javier, Claudia, my mother and relatives always supported me during the field activities in Nicaragua.

Savita supplied me with love and delicious vegetarian food during the writing of the thesis. Iyas went to sleep early so that I could sit and work during the evenings.

Absolutely none of the organizations and people mentioned here is responsible for errors or misinterpretations that might be present in this thesis. However, all of them share the possible success.

Abstract

Hydrogeological and geophysical methods were applied in the Río Artiguas watershed, a mountain basin located in central Nicaragua. This area is under environmental stress from anthropogenic activities like gold mining using mercury and waste disposal into the streams. The aim of this work was to characterise the hydrogeological conditions in the basin with emphasis on understanding the possible connections between streams and groundwater. It was also important to evaluate the vulnerability and risk of groundwater pollution. Hydrogeological mapping, resistivity imaging, hydrological measurements and hydrochemical surveys were combined to meet the aims of the work.

The hydrogeological characterisation permitted identification of a) recharge areas, b) geological units that contribute to the formation of the groundwater system and c) a mechanism of discharge through springs and streams. The geophysical surveys allowed mapping the extension of weathering and tectonic features with hydrogeological significance, e.g. faults, dykes and fractures. A total of 99 perennial springs were documented and classified according to their mechanism of formation. Isotopic data indicate that the recharge occurs very close to the sites where the springs are formed. This is also supported by the relatively low ion concentrations found in the water of the springs.

The weathering layers together with fractures and dykes form shallow aquifers that commonly discharge in a spring or along the streams. The high precipitation regime is an immediate source of water to the system, and in conjunction with the geology and steep topography it generates a constant and rapid circulation of water from recharge areas to discharge zones. The natural implication of this hydrogeological framework is that the formation of large or regional flows is not evident at the current state of knowledge.

The same factors that influence groundwater occurrence are to some extent responsible for the degree of groundwater vulnerability to pollution. The vulnerable areas are situated along the steep valleys of the basin, where the interactions between subsurface and surface water can facilitate the spreading of pollutants. Since the pollution sources are located near the streams the risk of groundwater pollution is concentrated there. The pollutants disposed into the streams are rapidly removed by the river flow, which has a high contribution from precipitation. The pollutants are then transported far away from the sources.

The urgent need to end the pollution of Río Artiguas is obvious. The tools to prevent further deterioration are not only to be found in the hydro geosciences and mining technology sphere, but they are also located in the socio–political arena. In this respect, the research presented in this thesis will gain importance as it reaches and informs local decision makers about the vulnerability and risks of pollution that the current anthropogenic activities represent for the groundwater resources.

Resumen

Métodos hidrogeológicos y geofísicos fueron aplicados en la cuenca del Río Artiguas, una cuenca de montaña situada en Nicaragua central. Esta cuenca está bajo un estrés ambiental por parte de actividades antropogénicas como minería de oro, con uso del método del mercurio, y vertido de desechos domiciliares en los arroyos. El objeto de este trabajo fue caracterizar las condiciones hidrogeológicas de la cuenca con énfasis en el estudio de las interrelaciones entre aguas superficiales y subterráneas. La evaluación de la vulnerabilidad de los acuíferos y el riesgo de contaminación fueron tareas importantes. Mapeo hidrogeológico, imágenes de resistividad eléctrica, mediciones hidrológicas y exploración hidroquímica fueron combinados para cumplir los objetivos.

La caracterización hidrogeológica permitió la identificación de a) las áreas de recarga b) las unidades geológicas que forman los acuíferos y c) los mecanismos de descarga por medio de manantiales y en los arroyos. El método geofísico permitió la delimitación de la meteorización y las zonas tectónicas con importancia hidrogeológica, como diques, fracturas y vetas de cuarzo. Un total de 99 manantiales fueron documentados y clasificados de acuerdo a su mecanismo de formación. Datos isotópicos indican que la recarga ocurre muy cerca de los sitios donde se forman los manantiales. Esto está también respaldado por las relativamente bajas concentraciones de iones que se encontró en el agua de manantiales.

Las zonas de meteorización junto con las fracturas y diques forman acuíferos someros que normalmente descargan sus aguas en los manantiales o a lo largo de los arroyos. El intenso régimen lluvioso es una fuente inmediata de agua en el ciclo hidrogeológico, y en conjunto con la geología y topografía abrupta generan una circulación rápida y constante desde las zonas de recarga a las zonas de descarga. De aquí se desprende que la existencia de acuíferos grandes no es evidente en el estado actual del conocimiento hidrogeológico de la cuenca.

Los mismos factores que son responsables en la formación de sistemas de agua subterránea son también responsables del grado de vulnerabilidad a la contaminación. Las áreas vulnerables están situadas a lo largo de los valles de la cuenca, donde las interacciones entre arroyos y acuíferos pueden facilitar el transporte de contaminantes. Dado que las fuentes de contaminación están situadas a orilla de los arroyos el riesgo de contaminación esta concentrado ahí. Los contaminantes arrojados en los arroyos son rápidamente removidos por los flujos del río bajo las grandes precipitaciones. Entonces los contaminantes son transportados a grandes distancias de las fuentes.

Es obvia la necesidad de detener la contaminación en el Río Artiguas. Las herramientas para detener una mayor contaminación no están sólo en manos de las ciencias de la tierra y la tecnología de minería, sino que están en manos de los actores sociopolíticos. En este sentido, el trabajo presentado en esta tesis ganará importancia en la medida que alcance a los tomadores de decisión en el nivel local y les informe la vulnerabilidad y riesgo que las actividades antropogénicas actuales representan para los sistemas de agua subterránea.

Contents

1. Introduction 3
1.1 Background 3
1.2 Objectives 4
1.3 Limitations 4
1.4 Organisation of the thesis 4
1.5 Description of the Papers 5

2. The Río Artiguas watershed 7
2.1 Geography, Geology, Hydrology and Hydrogeology 7
2.2 History and Economy 9
2.3 Weather 9

3. Hydrogeological characterisation 10
3.1 Hydrogeological importance of weathering and fractures 10
3.1.1 The extent of weathering 11
3.1.2 Influence of tectonics 11
3.2 Hydraulic conductivity tests 12
3.3 Recharge and occurrence of springs 13
3.3.1 Recharge estimations and identification of recharge areas 14
3.3.2 Occurrence and classification of springs 16
3.3.3 Groundwater table 20
3.4 Hydrochemistry 22

4. Geophysical investigation 24
4.1 The resistivity imaging method 24
4.2 Hydrogeological mapping with electrical resistivity 25
4.3 Forward modelling 28

5. Groundwater -surface water interactions 30
5.1 Character of the aquifers' relationship with surface water 30
5.2 Field study of the connections between river and shallow aquifers 31

6. Groundwater Pollution Risk Assessment 36
6.1 Vulnerability evaluation 36
6.2 Pollution sources and contaminant load 37
6.3 Method for the assessment of groundwater pollution risk 39

7. Discussion 41

8. Conclusions 44

9. Ideas for future research 45

10. References 47

Appendix 56

This thesis is based on the following papers:

I
Mendoza JA, Dahlin T, Barmen G (2005) Hydrogeological and hydrochemical features of an area polluted by heavy metals in central Nicaragua. Hydrogeology Journal, DOI: 10.1007/s10040-005-0462-5

II
Mendoza JA, Dahlin T. Resistivity imaging in steep and weathered terrains. Journal of Applied Geophysics, submitted

III
Mendoza JA, Ulriksen P, Picado F, Dahlin T. Aquifer interaction with a polluted mountain river of Nicaragua. Hydrological Processes, submitted

IV
Mendoza JA, Barmen G. (2006) Assessment of groundwater vulnerability in the Río Artiguas basin, Nicaragua. Environmental Geology, DOI 10.1007/s00254-006-0233-1

V
Mendoza JA, Cuadra S, Picado F, Barmen G, Jakobsson K, Bengtsson G. Ecological, groundwater and human health risk assessment in a mining region of Nicaragua. (Manuscript)

Related Papers

Mendoza JA, Dahlin T, Barmen G (2004) Use of resistivity imaging in a surface water – groundwater interactions study. Procc. XXXIII International Association of Hydrogeology IAH & VI ALHSUD Congress 11-15 October, 2004, Zacatecas City, Mexico

Mendoza, JA, Barmen, G. and Dahlin, T. (2002) Hydrogeological and Hydrochemical features of an area polluted by heavy metals in Nicaragua. XXXII International Association of Hydrogeology IAH & VI ALHSUD Congress. Mar del Plata, Argentina. 21-25 October 2002.

Mendoza JA, Dahlin T (2002) Mapping a quartz vein using three electrode arrays at Santo Domingo, Nicaragua. EEGS Procs. Aveiro, Portugal.

Mendoza JA, Bjelm L, Dahlin T (2000) Resistivity Imaging as a tool for Groundwater studies at Santo Domingo, central Nicaragua. EEGS Procs. Bochum Germany.

1. Introduction

The first chapter provides the background information which serves as a justification for the research presented in this thesis. Here, the aim and objectives of the thesis are outlined in combination with the limitations of the thesis. A brief description of the structure of thesis is also presented.

1.1 Background

During the period 1996-1997, the Universidad Nacional Autónoma de Nicaragua through its Centro de Investigaciones Geocientíficas (CIGEO/UNAN) carried out two hydrochemical surveys in the Río Artiguas basin. The surveys attempted to elucidate if there was any evidence of environmental pollution arising from anthropogenic activities, particularly in the water sources of the basin and its surroundings (Romero 1996; André et al. 1997). Those surveys found high concentrations of mercury (Hg) in waters of the basin and even some kilometres outside the basin, mainly along the river courses. Such findings stimulated the development of further research aiming to characterise the extent of the pollution and its effect on the environment and humans.

The problem that motivates this thesis is the increasing threat that economic activities represent for groundwater resources in the Río Artiguas basin, in combination with the lack of knowledge about the origin and nature of the groundwater systems present in the area. This thesis focuses on the hydrogeological features and current water pollution situation of the basin. In the area, gold-mining and household wastes are disposed in the river headwaters contaminating the surface water along its entire length to the Caribbean Sea. Such contamination represents an escalating socioeconomic and environmental problem. For example, pollution sources are diffusely spread in the area, which means that spilling of dangerous substances could occur at practically any point. Water for human consumption is supplied from sources located very close to the polluted streams, and there are no known groundwater reserves for future use. The pollution occurring in the headwaters means that the communities located downstream are unable to fully utilize this resource.

The need to prevent further pollution in the area poses several questions; for example what are the main physical and temporal characteristics of the pollution? Are all watercourses in the basin exposed to pollution sources? Is there any groundwater resource threatened by anthropogenic activities like mining? Answering these questions requires a thorough understanding of the processes controlling groundwater occurrence and its transport throughout the basin.

To understand these processes it is necessary to gather a comprehensive amount of information about the different factors that govern the hydrological cycle in the basin. This requires the characterisation and quantification of factors such as recharge, formation of groundwater systems, and discharge, among others.

This thesis explains the mechanisms that control the formation of groundwater systems and their relationships with the river in the study area. It attempts to provide valuable information to scholars, managers and authorities, not only in the study area, but also in other regions with similar geological settings or areas where water resources and environment are under threat from polluted rivers. Most of the presented research utilises information collected during the period 2000-2005.

1.2 Objectives

The aim of this thesis is to contribute to the knowledge of groundwater resources in the Río Artiguas basin (Figure 1). Three particular objectives can be outlined,

1. Characterise the occurrence of groundwater, identify the recharge areas and describe the mechanisms of discharge.

2. Describe the interactions between surface water and groundwater along the river course.

3. Evaluate the groundwater vulnerability of the basin and assess the groundwater risk of pollution originating from artisanal and small scale mining.

These objectives were fulfilled by analysing information collected through three types of fieldwork. First, hydrogeological and geophysical surveys were performed, including subsurface mapping with the electrical resistivity imaging method. Secondly, a groundwater resources inventory, accompanied by hydrochemical surveys was undertaken. Last, a river - shallow aquifers interaction experiment at a site with characteristic hydrogeological features was conducted. Complementary hydrological and meteorological data were collected.

1.3 Limitations

It is important to state that this study attempts to explain the mechanisms of formation of groundwater systems rather than to make comprehensive estimates of hydraulic parameters.

The groundwater vulnerability and risk assessments are performed assuming that the pollution from artisanal and small scale gold-mining is the main hazard, leaving for future study the assessment of pollution from sewage disposal.

Though some of the baseline research activities were outside the basin, i.e. geological reconnaissance, the main study is restricted to the areas within the basin. Some hydrogeological findings have implications for other areas in central Nicaragua, where similar geological settings may imply a similar hydrogeological framework.

1.4 Organisation of the thesis

The thesis consists of two parts; this summary and the journal articles appended in a methodological order, from the characterisation and discussion of collected data to the overview of vulnerabilities and risk of pollution for water resources in the area. The summary explains the conceptual basis integrating the articles, including relevant hydrogeological considerations and the background of the geophysical method used. It also presents and discusses results that are not necessarily integrated in the articles and are added here to strengthen the aims of the study.

Every section in the summary starts with a concise introduction to important concepts in the addressed subjects. Both background information and investigative results are clearly distinguished in the text. Chapter 2 is a description of the area. Chapter 3 summarises the hydrogeological features of the area. The resistivity imaging method and some results of its application in the area are discussed in chapter 4. The fifth chapter gives an overview of the importance of groundwater - surface water interaction studies and discusses the types of interaction that can be found in the basin. The groundwater resources vulnerability and risk assessment methods are introduced in chapter 6. Chapter 7 is an effort to integrate and discuss the results of this research. Chapter 8 is a synopsis of the main conclusions and chapter 9 outlines some recommendations for further research in the area.

1.5 Description of the Papers

Paper 1:
Hydrogeological and hydrochemical features of an area polluted by heavy metals in central Nicaragua

The paper examines geophysical and hydrochemical information from the study area and interprets these data in a hydrogeological context. The article includes results of a geological reconnaissance, a geophysical survey and hydrochemical analyses of springs' water. A representative group of springs were sampled for chemical analyses, while the geophysical surveys were carried out across five springs. Geophysical results for two springs are presented in the article. The electrical resistivity method was used to map geological materials related to groundwater systems.

Paper 2:
Resistivity imaging in steep and weathered terrains

This paper presents and discusses resistivity surveying as a reliable method for geophysical mapping in areas with steep topography. It includes some examples of the more than 40 2D-resistivity surveys performed in the basin. The goal is to discuss the effectiveness of resistivity imaging as a technique for mapping shallow aquifers in steep terrain and in areas affected by advanced weathering and intense fracturing. This paper includes the mapping of quartz dykes, which was not reliable prior to the recent development of resistivity surveying. The data interpretation was accompanied by numerical modelling to assess the suitability of all used electrode arrays in relation to the expected geological settings.

Paper 3:
Aquifer interactions with a polluted mountain river of Nicaragua

The article focuses on studying the shallow aquifer interactions with a polluted river by means of time series analyses of data collected in piezometers installed in a selected site. The hourly measured parameters were hydraulic heads and temperature. The data was collected during the period from March 2004 to March 2005. The collected data was complemented with resistivity surveys made parallel to and across the river channel, and which reinforce the interpretation of the time series analyses.

Paper 4:
Assessment of groundwater vulnerability in the Río Artiguas basin, Nicaragua.

This article evaluates the intrinsic vulnerability of groundwater in the Río Artiguas basin and provides information for sustainable use of water resources. The DRASTIC and GOD methods were used to analyse the relative pollution potential within the basin. DRASTIC was modified to include the degree of influence that geological structures have on the vulnerability. The resulting vulnerability maps show that the limited groundwater resources are susceptible to surface water pollution as high vulnerability areas converge along the river valleys. This assessment uses different kinds of data collected during this research project as well as geological information from the literature.

Paper 5:
Ecological, groundwater and human health risk assessment in a mining region of Nicaragua

It represents an effort to study an environmental problem from three disciplines; ecotoxicology, human health and hydrogeology. The aim of the article is to evaluate environmental risks associated with mercury pollution from gold mining in the Río Artiguas basin, central Nicaragua. The possible links between presence of mercury in waters, in aquatic biota and in human blood are analysed. This article uses hazard indices as a common tool to compare the three kinds of risk; groundwater risk of pollution, human health risk and ecological risk. The hazard indexes are discussed in order to provide information for protection and prevention of further pollution. The article is in a manuscript form.

2. The Río Artiguas watershed

This chapter describes the generalities of the study area with emphasis on the geological and hydrological features referenced in the literature, mainly in reports related to mining. This information is needed to justify the selection of the research methodology used in this thesis.

2.1 Geography, Geology, Hydrology and Hydrogeology

The Río Artiguas watershed is located 177 km east of the capital of Nicaragua, Managua. Land use in the basin is primarily allocated for cattle while cropping is limited to a few crops for domestic consumption. There are sparse zones with rainforest, mainly located along the stream valleys and around the multiple springs. More than half the population in the basin lives in the countryside areas. These people use water from springs and streams for domestic and human consumption.

Geologically, most of Río Artiguas basin is formed by Late Tertiary volcanic rocks, mainly basalt and andesite lava flows considered to be part of the denominated Coyol Group. The lava flows overly Early Tertiary rhyolitic-dacitic pyroclastic flows towards the south of the area, which corresponds to the Matagalpa Group (Hodgson 1972). There are gold bearing quartz veins cutting these basalt and andesite lava flows, surrounded by hydrothermal alteration aureoles (Darce 1990). Some isolated rhyolitic plugs are found intruding the basalts and andesites of the Coyol Group (Figure 1).

Structurally, there is a distinct trend of subvertical fractures in an east-northeast direction, which are often intruded by silica veins. These veins are often segmented by a semi-perpendicular fracturing trend in a northwest-southeast preferential orientation (Darce 1990; Weinberg 1990, 1992; Ehrenborg 1996). The veins are 0.5-10 m wide and become thinner with depth. The alteration aureoles around the veins are two to ten times wider than their respective veins at the surface (Darce 1990), grading laterally into fresh rock. The combined perpendicular fracturing pattern also affects the morphology of the area, with drainage and hill alignments following the preferential fractures directions. The quartz veins are all located in the most upstream zones of Río Artiguas and extend outside the basin towards east and west.

Following the hydrological classification of Wohl (2000), Río Artiguas can be defined as a mountain river in humid tropical areas. This means that in terms of morphology and hydrology the river has the following features:

1. Steep average channel of approximately 0.04 m/m steepness. The channel has a high roughness, with exposed bedrock accompanied with coarse clasts.

2. Highly turbulent flow and limited sediment supply, which is evidenced by the lack of banks and terraces along the channel.

3. Channel morphology controlled by the geology, and especially by tectonics (in this case).

In contrast with the large aquifers found in the Pacific coast region, aquifers are not abundant in the central region of Nicaragua. A number of intermontane valleys of hydrogeological importance are sparsely distributed in central Nicaragua, occurring mostly in volcanic terrains of Tertiary origin (Krásný 1998; INETER 2004a).

The main sources of hydrogeological information in the basin are the springs, streams, mining galleries and shafts. There are only a few dug wells where no relevant hydrogeological data can be obtained. The closest drilled well is located 11 km west of the village of Santo Domingo.

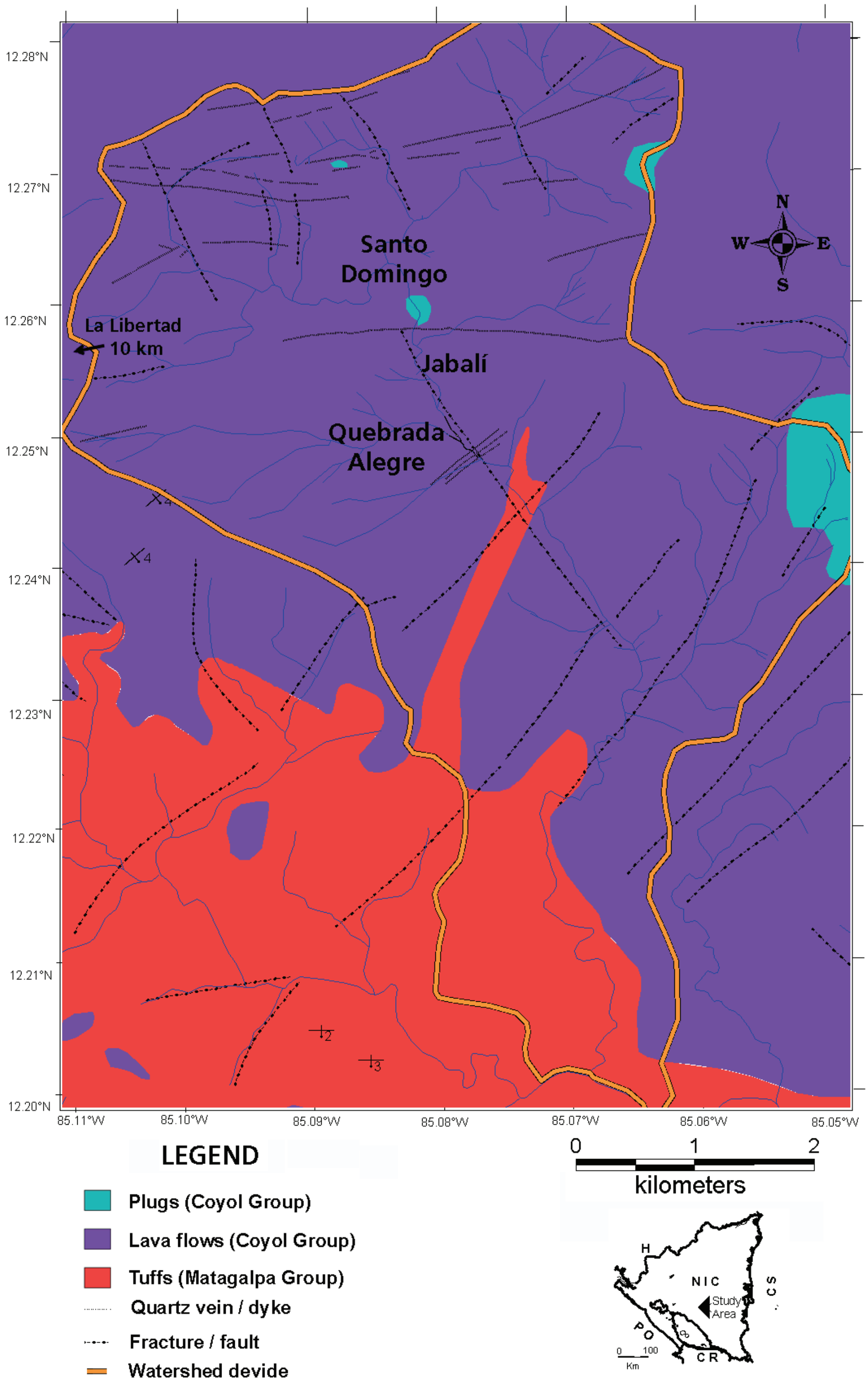

Figure 1. Geology of the Río Artiguas basin and surroundings. Inset: the location in Nicaragua, H:Honduras, CS: Caribbean Sea, CR: Costa Rica, PO: Pacific Ocean.

2.2 History and Economy

The history of the study area is strongly influenced by the gold mining that has been going on since pre-Columbian times. In his fourth trip to the new continent Columbus was informed about the gold rich region east of the *Amerrisque* mountains (Hurlbut 1886; Rea 1964), nowadays known as La Libertad – Santo Domingo gold district. Since the conquest and colonial times the region has undergone continuous mineral exploitation.

The first mining camp was settled around 1880 in the area today known as Jabalí, one kilometre south from the village of Santo Domingo. Since then, amalgamation, using mercury, was the method used for refining the gold (Feust 1912). In 1906 the cyanide method was introduced in Santo Domingo, but it never entirely substituted the mercury method. The latter is easier to use by the approximately 500 small-scale miners working in the area. The effects of anthropogenic activities on the river drainage are so visible that the river has been renamed "*Sucio*", which means dirty, by the locals.

2.3 Weather

A weather station, installed in the basin in November 2004 as part of this project, recorded temperatures between 15°C and 34°C. The climate type is Tropical Mountainous. Historic average precipitations of ca. 2400 mm yr^{-1} has been recorded in the area by INETER (1991). There is precipitation throughout the year and despite the limited size of the basin (28 Km^2), a spatial variability in precipitation has been observed. Figure 2 presents the precipitation during the period March 2004 to March 2005.

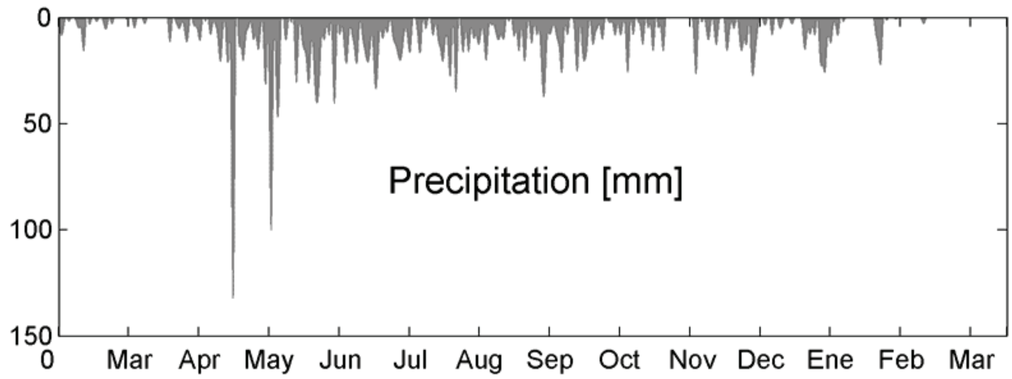

Figure 2. Precipitation from March 2004 to March 2005.

The precipitation regime covers the months from April until December, but precipitation during the so called 'dry season' is frequent. Wind runs mostly from North-Northeast, coming from the Caribbean with speeds from 0.3 to 8 m s^{-1}.

3. Hydrogeological characterisation

In this chapter a literature overview on the hydrogeological role of weathering and fracturing is followed by a description of the extent of weathering in the study area. This description is based on data collected in this research project. The sections on recharge and hydrochemistry are introduced with general concepts preceding some results.

3.1 Hydrogeological importance of weathering and fractures

Groundwater is stored and transmitted by aquifers. These are rock formations that contain sufficient saturated permeable material to yield significant quantities of water to wells and springs (Fetter 2001; Moore 2002). In large aquifers consisting of porous media groundwater travels, is stored and discharged mainly through voids in unconsolidated and coarse-grained sediments. In nonporous media the groundwater will mainly flow through fractures in the rock. In some fractured media water travels along the interstice spaces in rocks that have been altered by the chemical and physical processes caused by weathering.

Weathering is defined as the transformation of primary minerals that were formed at high temperatures and pressure in the inner earth and that become unstable and soluble in water at the surface of the earth (Ollier 1984; Drever 1997). The dissolution of these minerals gives rise to the formation of secondary minerals that are more stable in presence of water. The weathering process acting on the rock sequence gives rise to the formation of a weathered profile with materials of different composition. There is a top zone of leaching from which minerals are removed and only secondary products like iron oxides remain in place. In areas with abundant rainfall the released materials may be transported long distances, and sometimes precipitate in lower parts of the profile or even on the hillsides (Ollier 1984). This situation results in a complex relationship between weathering and the expected permeabilities at different points of the vertical profile. The dissolution of primary minerals and leaching will increase permeability at some points, but the later formation of secondary minerals would lead to the formation of low permeable clay and its accumulation at other points (Wright 1992).

Physical weathering and chemical weathering are not the only processes that transform and remove minerals from the rock; another process called hydrothermal alteration produces changes in rock that lead to the formation of secondary minerals. Hydrothermal alteration is caused by rising waters, steam and other emanations from deep in the earth that move upwards through the rock bringing about some alteration (Ollier 1988).

In areas characterised by the presence of fractured nonporous rock, the formation of groundwater systems is associated with the presence of faults, fractures and joint zones. The natural assumption is then that fault and fracture zones have higher permeability than their host rocks (Forster and Evan 1991; Magowe and Carr 1999; Faybishenko et al. 2000; Barton et al. 1995). There are cases when this is not true, and faults have been known to retard groundwater flow (Rawling et al. 2001). An impermeable fault plane (i.e. a clay filled horizon) would divert flow to other horizons, direct flow along the fracture plane, or force water to emerge as a spring (Seaton and Burbey 2005). In addition, the effects of faults can vary with the structure and texture of the plane surface (Alfaro and Wallace 1994); and the effects of fractures can be controlled by their aperture, connectivity and length (Hatton et al. 1994; Odling 2001). Dip-slip faulting may juxtapose soluble beds against insoluble beds, thereby creating a boundary to groundwater flow. Structurally controlled springs are expected to occur where fault planes intersect the surface (Alfaro and Wallace 1994).

Dykes and veins, which are commonly associated with tectonic displacements, also have a hydrogeological importance similar to fractures. Though quartz gouges themselves are expected to have low hydraulic significance, it is the associated fractures occurring sub parallel to the veins that are permeable (Levens et al. 1994). Recently, Wilkes et al (2004) used piezometric data to illustrate the preferential groundwater flow direction as influenced by dykes and fractured quartz veins.

3.1.1 The extent of weathering

The study area and its surroundings have been exposed to a strong physical and chemical weathering process. It is hard to find fresh rock on the surface. The pyroclastic deposits of the Matagalpa Group present in the south are extremely weathered and it is likely that these deposits were exposed to weathering for a long time before the lava flows were deposited. The basalt and andesite lava flows are less weathered than the pyroclastic rocks. Dykes, veins and other intrusive bodies formed during late Tertiary have been less exposed to the strong weathering than the rocks surrounding them. Earlier studies on the geochemistry of the Nicaraguan volcanism have pointed to hydrothermal alteration as the cause for the removal of primary minerals and formation of secondary minerals in the area (e.g. Levi et al. 1987; Nyström et al. 1988; Darce et al. 1989). In fact, it is difficult to differentiate between products resulting after hydrothermal alteration and products resulting from weathering since both processes produce a common footprint: secondary minerals, including clay minerals (Ollier 1984, 1988). For simplicity in this study, when discussing the local geology, the term weathered rock is used to embrace all kind of altered geological products. The most abundant clay minerals in the study area are kaolinite and illite, which are found from the surface down to 30-40 m (Darce 1990).

In the weathering profile, there is a level beyond which groundwater only penetrates through joints, fractures, faults or near the walls of dykes. This level corresponds to fresh rock interface which is usually a very irregular surface. The change from a saturated and weathered rock to the fresh rock (dry) is commonly sharp. This sharp boundary can be examined and delineated from the resistivity surveys discussed further in chapter 4 and Paper II. Due to the irregularity of the fresh rock surface it is difficult to provide an average depth of weathering in the basin. In general a minimum of 1 m and maximum of 70 m thickness was observed, but along moderately steep terrains a thickness of 3 m to 10 m was common. There were variations in thickness of more than 10 m over distances of less than 100 m in most areas.

3.1.2 Influence of tectonics

Considering the intense fracturing, faulting and quartz veins characterizing the area and their role in the formation of groundwater systems, their mapping was an important task of this research. The more relevant structures are shown in the geological map presented in Figure 1. Rose diagrams presented in Figure 3 suggest a relationship between fracture directions and outflow directions of a group of springs. The bearings of the fractures can be grouped in two directions; east-northeast and north-northwest, and the outflows of springs have a preferential direction towards northeast, indicating that the springs ooze in similar direction to the fractures bearing north-northeast.

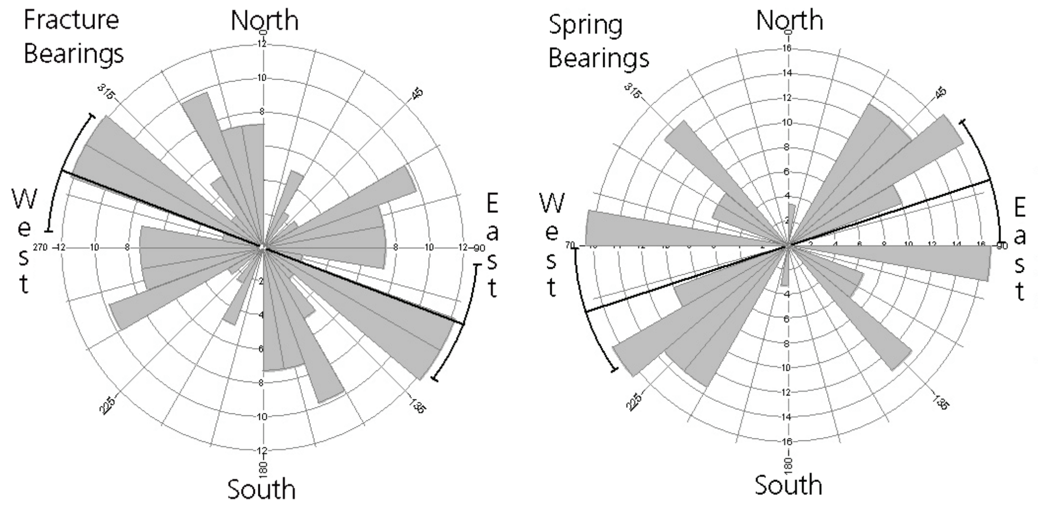

Figure 3. Rose diagrams showing frequency and bearings of 41 fractures (left) and outflow at 30 springs (right) measured in field.

3.2 Hydraulic conductivity tests

Hydraulic conductivity is a key parameter in the characterisation of geological materials. It describes how well the material allows the transport of water. Precisely because hydraulic conductivity is characteristic of every material, it varies as greatly as geology does in a certain area (Neuman 1994; Neuzil 1994). The hydraulic conductivities of rock presented in Figure 4 range through twelve orders of magnitude, constituting one of the physical parameters that present widest range of values (Heath 1983). Currently, significant research is devoted towards understanding the reasons for such high variability in permeability among different materials or arising from the scale of measurements (e.g. Barr 2001; Patriarche et al. 2005; Gierczak et al. 2006).

The lack of wells for water supply in the area prevented estimations of hydraulic conductivities of the saturated zone. This limitation was partially overcome by conducting tests of saturated permeability (Ksat) in the unsaturated zone using a Constant Head Permeameter (Amoozegar 1989). Due to entrapped air during the infiltration process, field saturated hydraulic conductivity could be lower than hydraulic conductivity in completely saturated conditions (Fallico et al. 2005).

These measurements performed in 103 points of the basin are representative of the hydraulic conductivity in the weathering horizon at minimum depths of 0.5 m (Figure 5). The hydraulic conductivity of the weathered horizons and the underlying fractured rock were briefly evaluated by slug tests (Hvorslev 1951) in mini-piezometers located in the Quebrada Alegre site (see location in Figure 1).

The hydraulic conductivity tests in the unsaturated zone delivered a variability of five orders of magnitude throughout the basin. The values ranged from of 8 $\times 10^{-9}$ m s^{-1} in the south to 2 $\times 10^{-5}$ m s^{-1} in the north. In general, higher values were found on the north side and centre of the basin (see Figure 5). In the slug tests performed the hydraulic conductivities ranged from 5.7 10^{-6} m s^{-1} in clay to 2.3 10^{-5} m s^{-1} in areas near a fractured basaltic dyke (see Paper III).

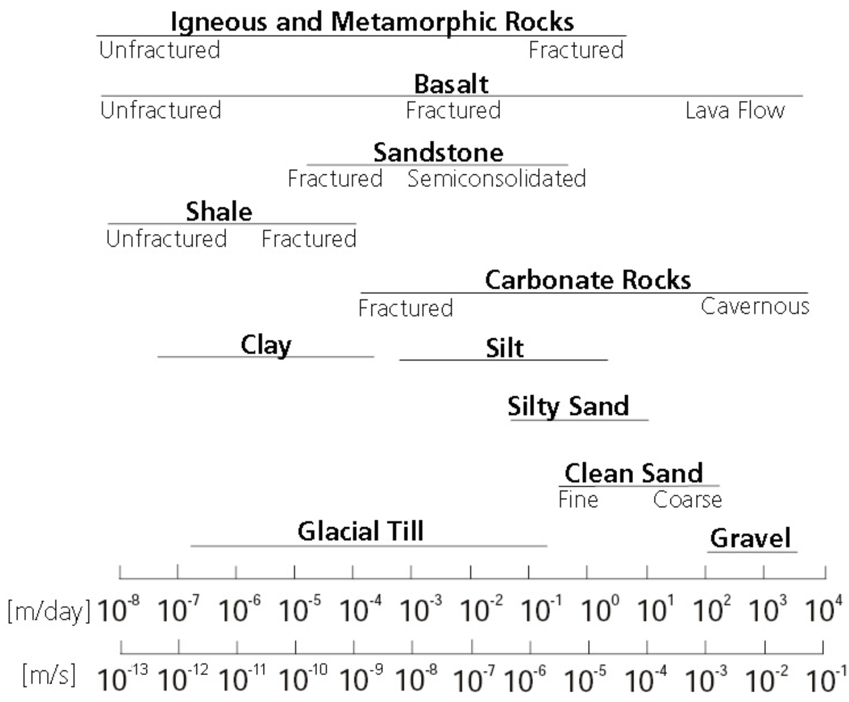

Figure 4. Hydraulic conductivity ranges for different kinds of rocks (Modified from Heath 1983)

3.3 Recharge and occurrence of springs

Recharge is the amount of water that reaches an aquifer from any direction, either laterally or vertically. This implies that recharge does not refer only to that portion of water that reaches the aquifers as an immediate consequence of precipitated water. The difference between recharge and infiltration is that the latter refers to the transport of water from a surface through the soil profile. The surface could be the ground surface or a river bed. Regarding recharge Lerner (1997) distinguishes three different categories described as follows:

- *Direct recharge*, also called *diffuse* recharge, is a disperse process occurring beneath the point of impact of the precipitation.

- *Localised recharge*, resulting from the horizontal movement or concentration of water into joints, rivulets and depressions. These focused points are too frequent to be mappable and measurable, but clearly involve a different mechanism from direct recharge.

- *Indirect recharge*, which involves water that reaches the aquifers from lakes and rivers, whether ephemeral or perennial. The indirect distinction from localised recharge is that the water courses are sufficiently large to be mapped and possibly gauged.

The three kinds of recharge have important hydrological and environmental implications in the study area. Direct recharge and localised recharge are most important for the hydrological cycle locally, while indirect recharge also has environmental importance. As there is percolation to the water table through the beds of surface water courses, pollutants present in the surface waters can also reach the shallow aquifers. This aspect is discussed in more detail in chapter 5 and Paper III.

There are an important number of techniques for studying recharge, most of them based on direct measurements, empirical relationships between recharge and associated processes or relying on water budgets. Scanlon et al (2002) gives a comprehensive review of existing methods to quantify recharge including the water budget approach, base flow discharge (Rorabough 1964), channel water balance (Lerner et al. 1990), water table rise (Healy and Cook 2002) and the chloride method. The chloride balance method was used in this research because it produces point estimations of recharge.

Chloride balance. The use of this method implies some assumptions related to other sources of chloride that could affect the estimations. These assumptions are that (a) the only source of chloride at the land surface is as precipitation or as dryfall (b) there is no contribution from weathering and (c) no fertilizers containing chloride have been used in the region.

The chloride balance method is based on the supposition that on average the flux of chloride through the soil surface is equal to the flux of chloride beneath the root zone, expressed mathematically as (Allison and Hugues 1978; Gaye and Edmunds 1996),

$$PC_p = RC_r$$

where P is the annual rainfall with chloride concentration C_p and R is the recharge flux of chloride concentration C_r .

3.3.1 Recharge estimations and identification of recharge areas

The annual rainfall used for the calculation corresponds to the precipitation gauged in Santo Domingo during 2004 which had a value of 2655 mm yr^{-1} (INETER, unpublished data). The water samples were taken at different sources including former mining galleries, springs, wells and streams. The map in Figure 5 presents graphically the relative values of the recharge obtained at the corresponding sampling locations. The recharge estimation ranged from 780 mm yr^{-1} in a spring located near the water divide to 85 mm yr^{-1} in a mini-piezometer situated near Río Artiguas at El Jabalí (see location in Figure 1).

Although the limitations of the water budget approach have been reviewed and emphasised recently (Bredehoeft 2002; Devlin and Sophocleous 2005), the water budget can provide insights of the recharge/discharge process in the study area. Considering a total basin area of about 28 km^2 and an average recharge based on all Cl- calculations (in 28 analyses), a total recharge of approximately 10^7 m^3 yr^{-1} is obtained. The total discharge estimated from the springs outflow and river gauging approximates the same value of recharge above, which leads to the conclusion that there is a steady water balance in the basin. The water that enters the system roughly equals the amount of water discharged through the springs and streams.

Stable isotope hydrology can also assist on the characterisation of recharge. The composition of stable isotopes in water (i.e. ^{18}O and ^{2}H) varies in relation to the temperature the water had at the moment of precipitation. Water recharged in zones of lower temperatures, often corresponding to higher altitudes, has a lower content of heavy isotopes in relation to water recharged at locations with higher temperatures. This produces an altitude effect that makes it possible to identify recharge areas by analysing the content of stable isotopes in water. By comparing the isotopic composition with the altitudes of the sampling points the possible zones of recharge can be identified. This principle was adopted in this research and water samples were collected from springs and streams to analyse their ^{18}O composition (see Paper I).

The ^{18}O analyses indicate that the water discharged in the springs and along the streams corresponds to water recharged within the basin. It was verified that springs located at higher altitudes, close to the ridges, are formed very close to their average recharge areas. The results of ^{18}O analyses are presented in Paper I as function of the altitude of the springs.

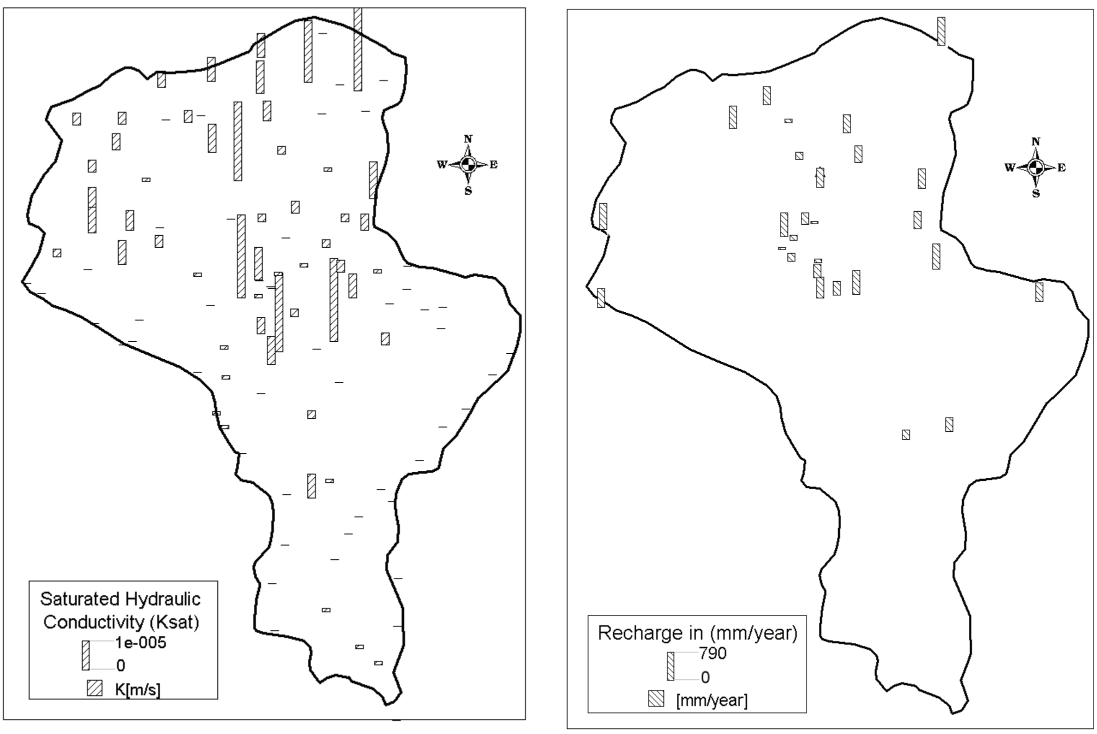

Figure 5. Left, Hydraulic conductivity in the unsaturated zone. The points that do not form a bar correspond to values that are commonly below 10^{-7} m s^{-1}. Right, recharge estimated with the chloride method. Note that the bars are linearly scaled.

3.3.2 Occurrence and classification of springs

Springs are a common feature in some hydrogeological settings like watersheds underlain by fractured rock aquifers (Moore, 2002). The formation of springs is the natural expression of groundwater presence in many regions and is a result of the combination of three conditions a) the water saturation of a certain geological unit b) the existence of a hydraulic gradient along the geological formation and c) the interception of the water saturated units with land surface. There are different mechanisms that can facilitate the formation of springs depending on the local geological setting. Figure 6 presents six classical types of springs. The most common is a simple topographic relief that lowers under a groundwater table, giving place to the formation of a *depression spring*. When a low permeability rock underlies a higher permeability formation another kind of spring, denominated a *contact spring* can be found. Springs can also be formed as result of faults, fracturing and joints in low permeability rocks.

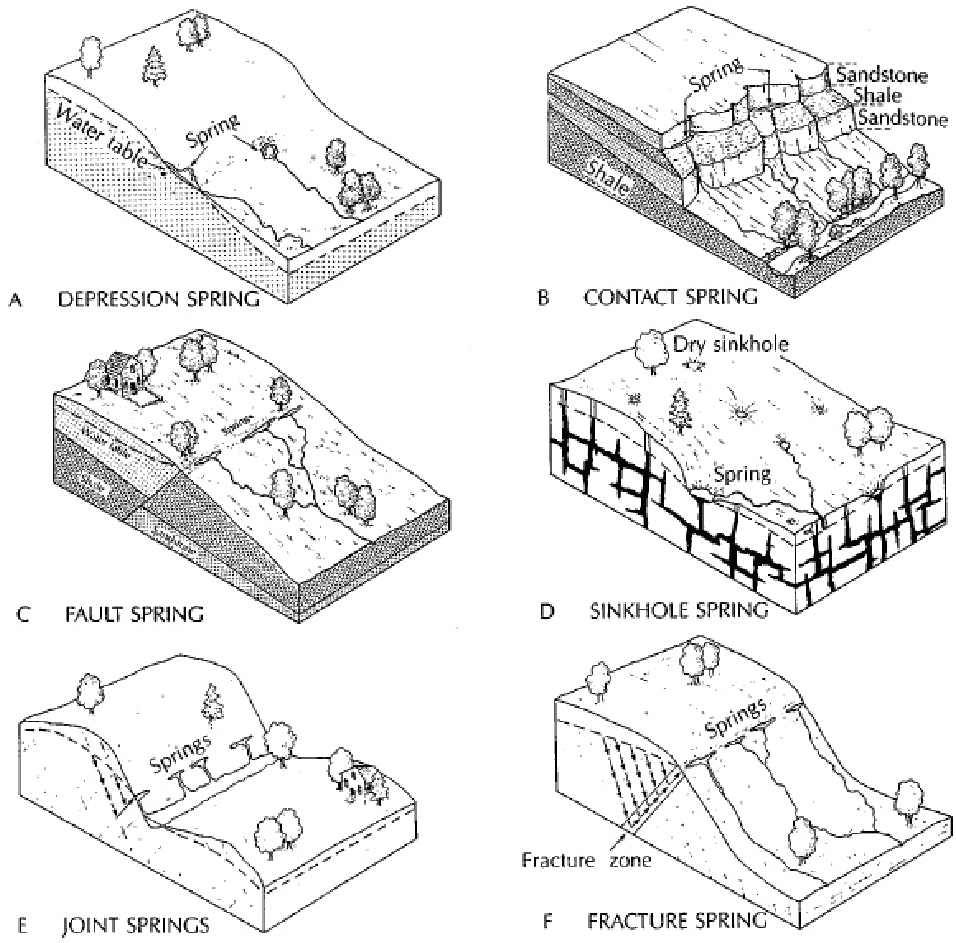

Figure 6. Types of springs. (from Fetter 2001, with permission)

Springs are a valuable source of information for geological and hydrogeological studies. Their position and altitude plus the geomorphology of the areas where they occur can provide relevant insights to the understanding of the processes that govern groundwater occurrence, storage, transport and discharge. Additionally, springs provide a unique opportunity to study a range of sub-surface processes in regions with few boreholes or wells. For instance by using tracers, temperature, and discharge measurements, it is possible to determine the mean-residence time of water, infer the spatial pattern and extent of groundwater flow, and estimate basin-scale hydraulic properties. However, because springs integrate the signal of geological and hydrological processes over large spatial areas and long periods of time, they are an indirect source of information (Manga 2001).

This research used information from springs to study groundwater occurrence in the Río Artiguas basin. First, an inventory of springs was carried out by documenting their position, and characterizing the geological environment and the land use around them. A classification of the springs based on their physiographic features was performed by Aronsson and Wallner (2002) and complemented by Espinosa and Espinosa (2005). A new classification of the springs based on their geological setting is suggested here. Such classification can assist in establishing a hydrogeological framework that explains their origin. There are 99 perennial springs in the basin, which are classified within the following types:

1. *Weathering spring*. This kind of spring is formed at the contact between the weathering profile and either a) the basal clay-rich zone of the weathered profile or b) the fresh rock. A sub classification considering these two kinds of basal layer was impossible due to limited exposures. Figure 7 shows an example of this type of spring. There are 43 of this kind of spring distributed in the area (Figure 8).

2. *Fracture spring*. The spring is classified as a fracture spring when the fracture was visible or when it was situated within 50 m distance from a fracture (or fault) as interpreted from the geological map. In a fracture spring the presence of weathering is secondary in comparison to the fracture or there is no weathering at all. There were 39 cases of fracture spring.

3. *Quartz vein spring*. This is a particular type of fracture spring, which occurs along or very close to the quartz veins (within 50 m outside the vein). There were 17 springs included in this type. Three of these springs are formed at old mining galleries and shafts and are used for water supply due to their high productivity (~0.2 m^3s) (see Figure 7).

The geographic position of all the springs can be found in the Appendix (a).

Figure 7. Above, a typical landscape around a weathering spring, with formation of a wetland. Right, a spring classified as type weathering. Below, a fracture spring near the village of Santo Domingo. Below right, an old mining gallery serves as main source of water for Santo Domingo. The source is located only 100 m from the polluted river. Photo: Marie Aronsson.

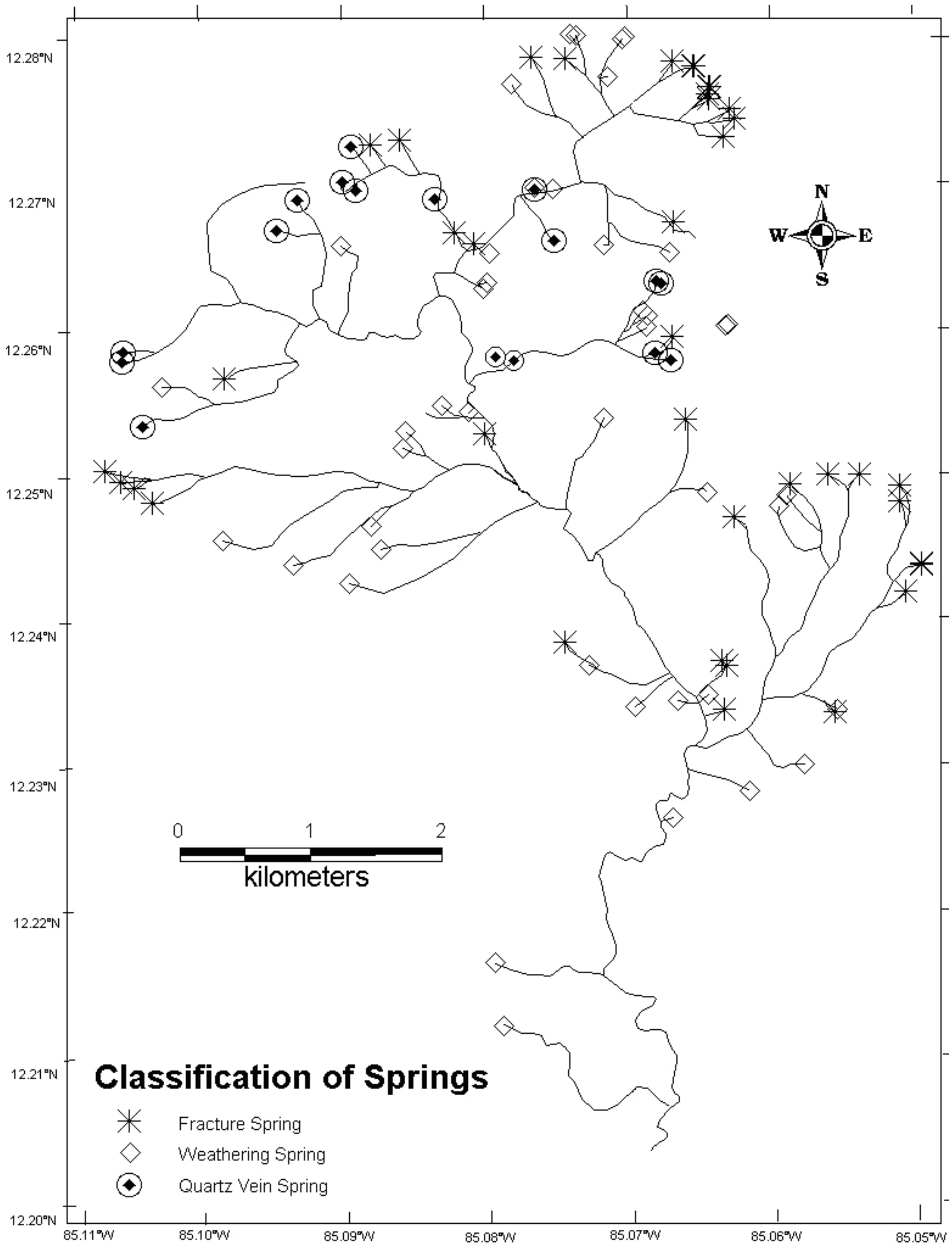

Figure 8. Classification of the 99 springs located in the basin.

Discharges estimated in a selected group of springs indicate differences in discharge between the different types. The selection of the springs to measure discharges was done disregarding their geological settings, but considering their geographic location. Figure 9 shows ranges of discharge for the three kinds of spring measured during three surveys. The quartz vein springs appear to have higher yields than the other two types. It was also found that there are not large differences between the discharges of weathering springs and the discharges in fracture springs.

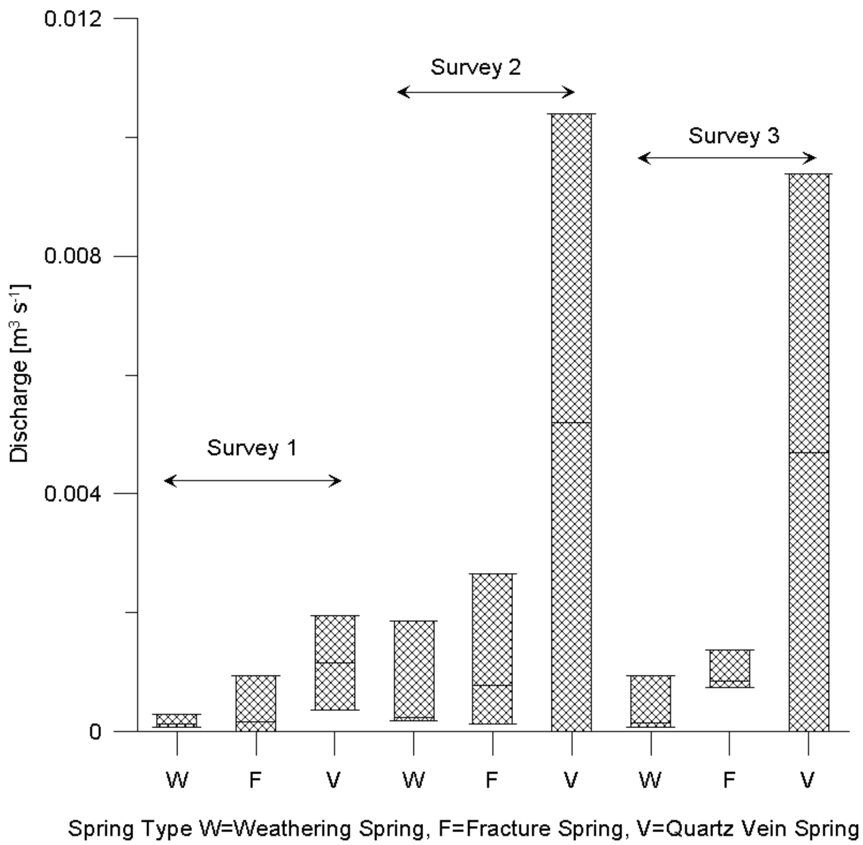

Figure 9. Boxplot of the discharge measured during three surveys at 27 springs. The three surveys were performed during different periods, survey 1 in 2001/08, survey 2 in 2005/07 and survey 3 in 2005/08. Three springs belonging to the vein group were excluded because they are formed in former mining galleries.

3.3.3 Groundwater table

The groundwater table can to some extent be considered as the replica of the topography. This is valid in relatively low-permeability and/or anisotropic aquifers subjected to high recharge rates as compared with their thickness and permeability (Haitjema and Mitchell-Bruker 2005). Since these assumptions can be applied to the study area a groundwater table map was generated using the Digital Elevation Model (DEM) as a drift for kriging of known hydraulic heads (Deutsch and Journel 1992; Goovaerts 1997). The hydraulic heads correspond to 99 springs, 25 piezometers and 15 sections where discharge to the streams was identified.

The groundwater table has a dynamic shape that changes seasonally, and a water table map represents the situation at the time when the hydraulic heads were measured. With an instrumentation error of around +/- 1 m and the fact that the assumptions behind the extrapolation method might not be met at certain locations, the resulting map cannot be regarded as an absolute truth. The normal method to assess the quality of digital groundwater models is to check a sample of groundwater heights from the model against known hydraulic heads, usually derived from a more accurate source of data (Borrough and McDonnell 1998). The degree of agreement between the values from the model and the 'true' data is then reported as the root mean square error (RMSE), calculated as

$$\text{RMSE}=\sqrt{\sum_{i\ 1}^{n} d_i^2 \Big/ n}$$

where *d* is the height difference between the digital groundwater model and test point, and *n* is the number of test points (Wise 2000). This calculation was performed with *n* =133 points, including measurements in mining shafts where the groundwater table is commonly found at ~20 m. The obtained RMSE was 7.29 which is considered a reasonable value for the expected use of the resultant groundwater contour map presented in Figure 10. This groundwater table map can be used for purposes that do not require very high accuracy, such as the vulnerability assessment presented in Paper IV.

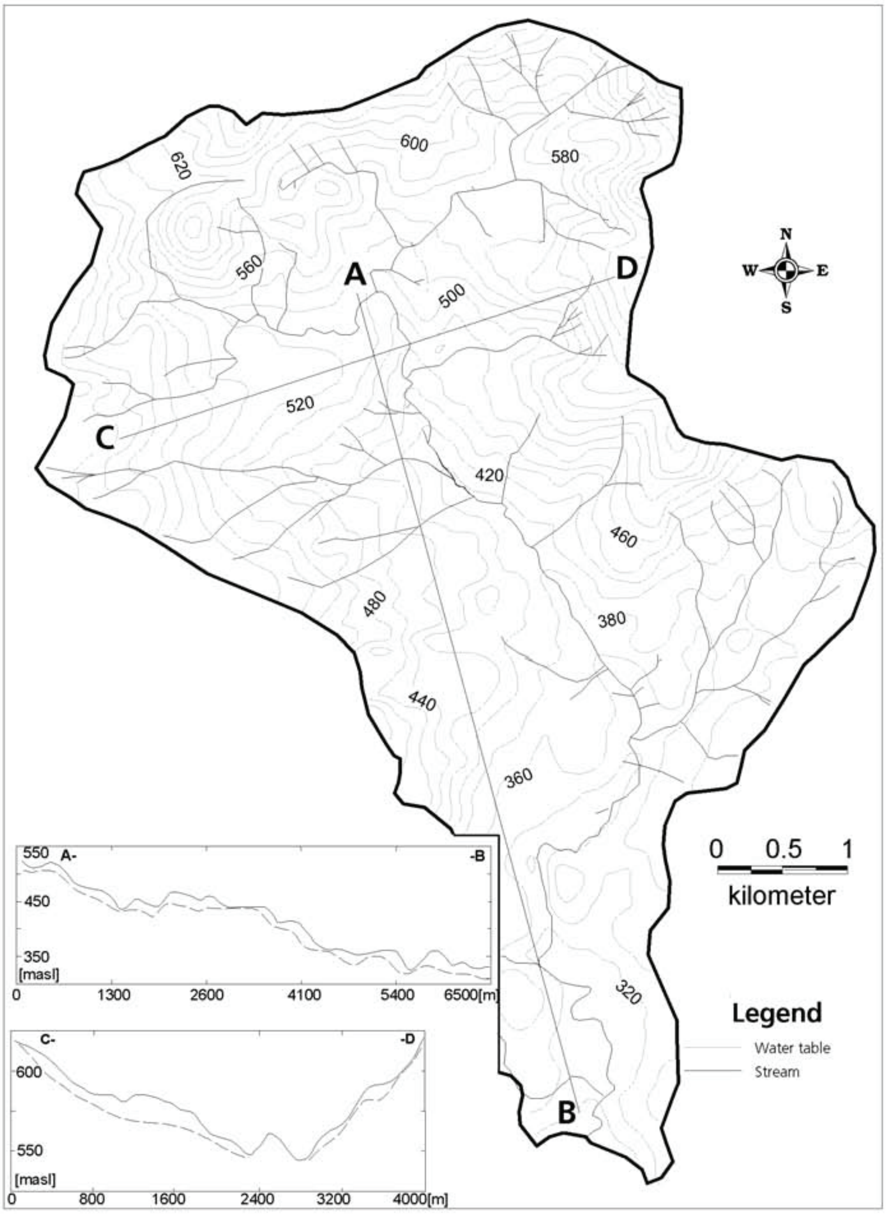

Figure 10. Groundwater table, including two profiles where the estimated position of the water table (dashed line) is compared with the Digital Elevation Model -DEM (continuous line).

3.4 Hydrochemistry

Geochemical methods have improved the interpretation of the hydrochemical processes in groundwater systems, and aided understanding how the structural, geological, mineralogical, and hydrogeological features affect flow and chemistry in these systems (Glynn and Plummer 2005). In the case of a basin, there are two factors that affect the water chemistry; the type of geological materials and the residence time of the water that travels through the system (Winter et al. 1998). The combination of these two factors will define the chemical composition of water when it discharges or immediately after extraction through wells. Therefore, water chemistry analyses can provide insights into different processes occurring in groundwater, including information on the type of rocks where water flows (Garrels and MacKenzie 1975). Water chemistry analyses also have the potential of explaining the origin of groundwater and the stage of its relationship with surface waters.

Normally, the primary constituents of groundwater chemistry are the ions Na^{+}, Ca^{2+}, K^{+}, Mg^{2+}, SO_4^{2-}, Cl^{-}, HCO_3^{-} and CO_3^{2-} (Appelo and Postma 1999; Fetter 2001). The concentration of these ions in groundwater is often indicative of the travel time or path length of water through geological materials and is consequently related to distance to the recharge areas. Thus, low ion concentrations means rapid travel time and short distances from recharge to discharge areas. Low ion concentrations are typical of shallow aquifers while high ion concentrations are found in deeper groundwater flow systems. In deep groundwater the relatively long residence time permits chemical reactions to take place, increasing the ion concentration in water. The ion concentrations found in groundwater will also result from the solubility of the minerals present in the geologic formation.

Most hydrochemical surveys include the determination of pH, temperature, specific electrical conductance (EC) and Total Dissolved Solids (TDS). These chemical-physical parameters offer an important source of information for a preliminary evaluation of the water quality. In particular Total Dissolved Solids (TDS) is important since it gives an estimation of the entire ion concentration in a sample. TDS and pH are conventionally applied parameters in assessment of the quality of drinking water (Moore 2002).

In this study three surveys were conducted to monitor chemical and physical parameters in surface waters and groundwater (springs). A general overview of the results for groundwater chemistry is provided here and more information is provided in Paper I. The temperatures found in the spring water range from 22.1°C to 27.3°C. There were no geographical trends in temperature of the springs. There was a yearly variation of +/- 0.5°C in groundwater temperatures measured in mini-piezometers at Quebrada Alegre (see location in Figure 1).

The majority of water sources have pH values in the interval 5.5 to 7.6, with low values (5.6-5.9) found in wells and springs in Santo Domingo probably influenced by anthropogenic activities. Regarding EC, the highest value was found at the source of the water supply for the village (170 μScm^{-1}). The values are relatively high south of Santo Domingo and decrease to the north, east and west (down to 46 μScm^{-1}).

The general trend is an increase in dissolved solids towards the south and the centre of the area. The TDS concentrations are higher, up to 80 mg l^{-1}, in the centre of the basin, including the water source for the village. The concentrations found in the village are explained by pollution while the value at the water source is related to a higher residence time in the geological formation. The values decrease towards the south to about 40 mg l^{-1}. Towards the basin boundaries the TDS values are much lower, with the lowest value at 22.0 mg l^{-1}. The TDS values were estimated in laboratory by evaporating a known volume of the sample and weighting the remaining solids.

The relative proportions of the major ion species and averaged total dissolved solids found in the area are presented in Figure 11 and discussed further in Paper I. In general there are low ion concentration values. Relatively high values of NO_3^-, SO_4^{2-}, and Cl^- were found in the springs close to the village. Regarding the hydrochemical facies, the groundwater can be classified as calcium - bicarbonate type, which is similar to the hydrochemical facies found in waters of the volcanic terrains in the Pacific plains and other locations in central Nicaragua (Hecht 1995; INETER 2004b).

Heavy metal analyses of spring waters indicate that the springs have no significant concentrations of Hg (values < 0.0006 mg l^{-1}), but elevated values of Pb were found. The highest Pb concentrations 0.011-0.013 mg l^{-1} were found in the springs located towards the basin boundaries (i.e. hilltops), supporting the idea of a natural origin. The Hg concentrations in both groundwater and surface water are discussed in chapter 6.

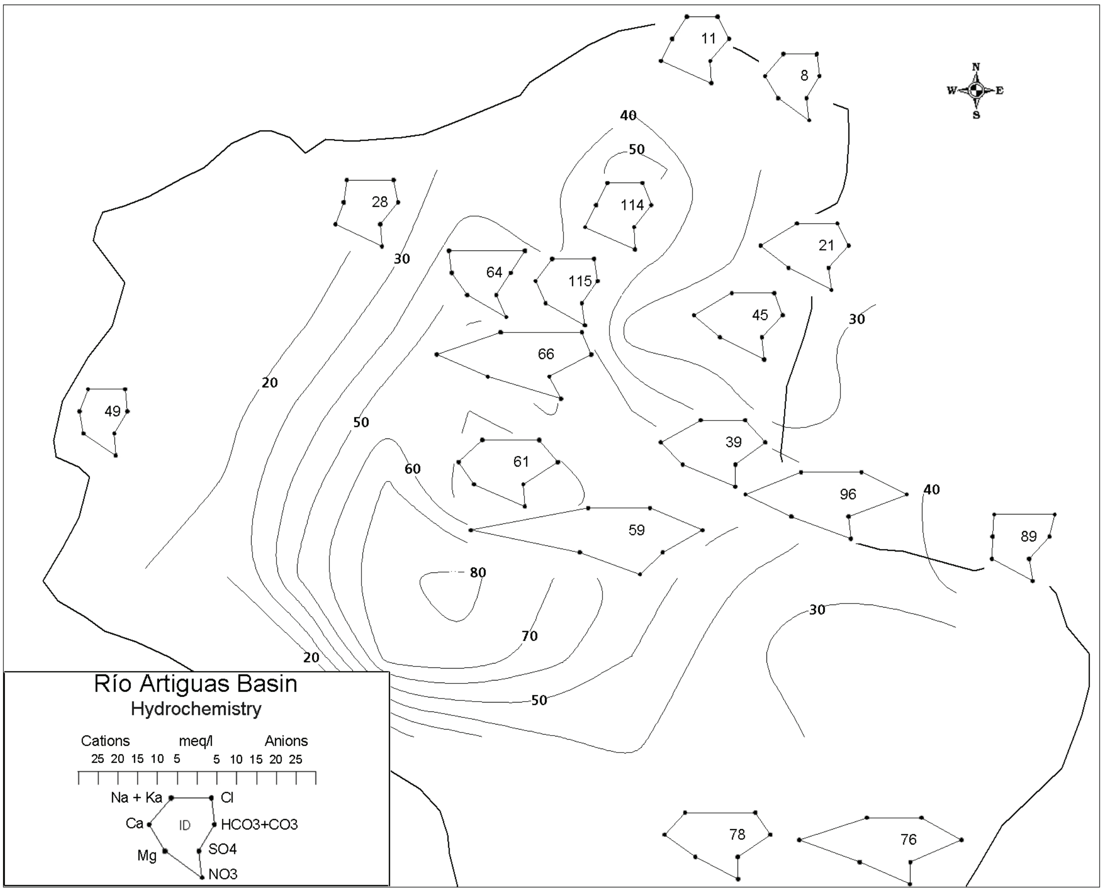

Figure 11. Stiff patterns representing the ion concentrations (meq l^{-1}) in springs, cations are plotted on the left half of the polygons and anions on the right half. The isolines indicate the averaged TDS (mg l^{-1}) measured at 40 springs, most of them located in the north part of the basin.

4. Geophysical investigation

The mapping of geological materials and structures with the geophysical method of electrical resistivity imaging is presented in Chapter 4, including examples from one of the studied sites.

4.1 The resistivity imaging method

The resistivity method was used as a main method for field investigation of the subsurface at diverse sites selected with regards to their hydrogeological importance. Electrical methods have proved to be useful for groundwater exploration studies. The use of geophysical methods in groundwater exploration, prior to drilling projects, saves money and time. In practice, the resistivity method assists in the identification and mapping of geological units that may constitute aquifers. Geological structures which could influence the movement of groundwater can also be delineated with resistivity mapping.

Mapping the extent of weathering in tropical areas is valuable in groundwater exploration since this weathering leads to an increase in porosity, and therefore affects permeability. Resistivity has proved to be an effective method to determine the thickness of weathered layers that overlay unaltered bedrock in equatorial areas (Palacky and Kiyoshi 1979).

The resistivity method is based on the property that geological materials transmit electrical current. The electrical current can be transmitted through the ground by dielectric conduction, electronic conduction (ohmic) and electrolytic conduction. The last occurs by means of pore fluids acting as electrolytes with the actual mineral grains contributing very little to the overall conductivity of the rock, except where those grains are themselves good electronic conductors (Reynolds 1997). Electrolytic conduction is the most common kind of electric conduction and the most important in terms of hydrogeological investigations since rock formations with water content tend to be electrically conductive (Jakosky and Hopper 1937; Zohdy and Jackson 1969).

The resistivity of geological materials has a very wide range of values. Igneous rocks are usually more resistive than sedimentary rocks. Metamorphic rocks have intermediate resistivity values. For example, quartz can give a value of 3×10^{2} Ωm-10^{6} Ωm, while magnetite can have values of 5×10^{-5}Ωm –5.7×10^{3} Ωm.

The resistivity method uses an artificial source of current, which is introduced into the ground through electrodes. The field procedure includes measuring potentials at different points around the current flow. If the geometry in which the current and potential electrodes are arranged is known, the resistivity can be calculated, provided that the current value and potential measured are also known. Several electrode arrays (also termed spreads or geometry) have been designed and used in resistivity surveying (Figure 12). Every array has its advantages and disadvantages which make it more or less suitable for a given investigation. Although the electrodes do not have to be placed in a line, the interpretation may become difficult if not collinear. In this research the arrays used were Wenner, Wenner -Schlumberger, dipole-dipole, pole-dipole and multi gradient. Multiple gradient electrode arrays were preferred during the last field seasons since it has proved to have good resolution capability and be robust in the field (Dahlin and Zhou 2004, 2006).

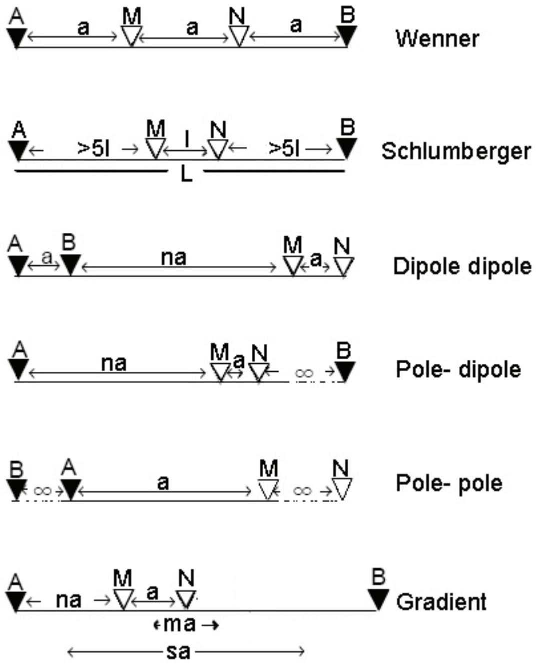

Figure 12. Arrays used in this study, A and B represent electrodes for current transmission and M and N represent electrodes for potential electrodes. The lowercase letters are different geometric factors characteristic in each array.

Since the resistivity values measured in field are intimately related to the electrode geometry used and to the ground changes in homogeneity, these are not average values but values of apparent resistivity. Then, it becomes necessary to use the field data to derive a model that describes the subsurface in consistency with the data. In this way, the so called inversion model represents a solution of the spatial distribution of resistivities which could have been produced by an observed set of measurements.

The ABEM Lund Imaging System (Dahlin 1996) was intensively used for field investigations in the basin. This system is based on the automation of the collection, processing and presentation of resistivity data. The main components of the system used were a robust computer for the system control (optional), a Terrameter SAS4000 with four input channels, an electrode selector unit, four multicore electrode cables (21 take-outs per cable) and steel electrodes. Additionally, GPS receivers and surveying instrumentation were used for precise positioning of the profiles and electrodes. The data collection was performed by using a roll along technique where cables are moved upward or downward along a succession of stations.

4.2 Hydrogeological mapping with electrical resistivity

In total, forty-four (44) resistivity surveys were performed at hydrogeologically relevant locations of the Río Artiguas basin. The main geological targets under investigation were quartz vein areas, fractures, weathered zones and the vicinities of the river channels. The presence of springs in the surroundings was also an important aspect taken in consideration when choosing the locations for the 2D resistivity surveys. The interpretation of resistivity imaging surveys requires additional information on the subsurface geology, as any other geophysical method. Besides surface observation, there were shafts and galleries that served as outcrops to document the subsurface geology for interpretation of the geophysical surveys. The minimum electrode spacing was mostly 1 m, 2 m and 5 m, depending on the target being investigated. Vegetation and anthropogenic activities had to be taken into account in deciding where to put the lines. Most of the resistivity surveys are presented in the papers and related papers (see p. 2). For further reference the geographic coordinates of the lines and electrode arrays used for the surveys are reported in the Appendix (b).

The data processing was performed using the Res2Dinv algorithm (Loke 1997). Interpretation of 2D resistivity data from areas with complex geology, i.e several subsurface regions separated by sharp boundaries, requires use of the robust (L_1-norm) inversion method, which minimizes the absolute differences between measured and calculated apparent resistivity values (Loke et al. 2003). Including the altitude of the electrodes in the data inversion process was imperative for a precise relation of the object position in space along the section. This meant the use of a finite element grid. After processing the data, the final results were prepared for presentation by setting a resistivity scale that suits the expected geological features for each site investigated.

The geophysical surveys indicated that the overall weathering thickness in the area varies from 1 m to 15 m in general, and in some areas up to 70 m. The weathering thickness varies over short distances. These weathered layers consist of heterogeneous material ranging from leached and coarse grained to clay weathered rock (Mendoza et al. 2000). The resistivity surveys allowed the mapping of geological structures such as faults, fractures and veins. Figure 13 shows an example of mapping a quartz vein area that is embedded parallel to a stream in the centre of the basin. The vein, as documented on surface and in nearby shafts, is 1600 m long, has a maximum thickness of 10 m and at least 20 m depth. There is a spring formed along Line 1 at the depression where the quartz vein is intercepted by the topography. In this case groundwater does not discharge directly to the stream but is contained by the vein instead. The spring presumably collects water from the surrounding hillsides and the vein walls but does not discharge in the stream because it is blocked by the thick quartz gouge. Branches of the quartz vein that are not obvious on the surface can be delineated in lines 2 and 3. In all cases there is a layer of high resistivity values on top (>70 Ωm), over a less resistive layer that is in often water saturated (22-70 Ωm). The resistivity lines indicate that the low resistive zone is around 10-15 m thick, becoming more and more resistive at increasing depths. The rock becomes less weathered with depth. The results of Lines 1 and 3 are partially discussed in Paper I.

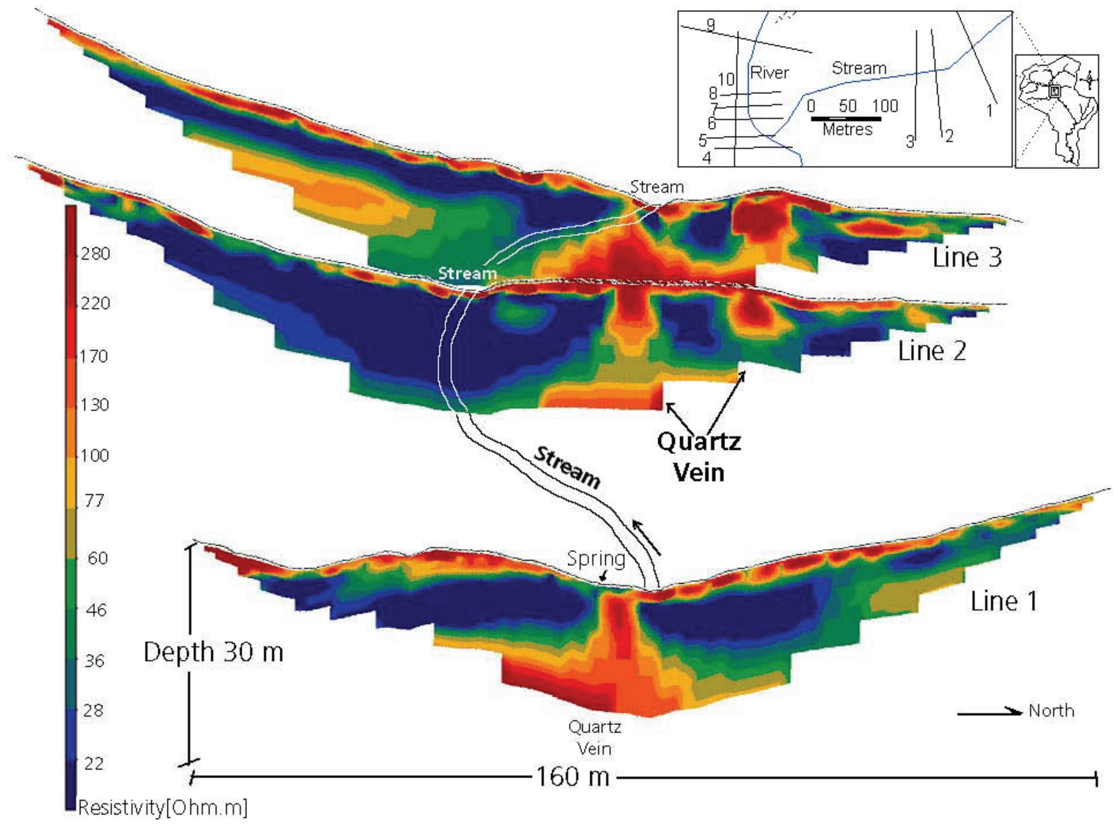

Figure 13. Inverted models of lines 1, 2 and 3. Line 1 was 120 m long and the other two were 160 m long. The minimum electrode spacing was 2 m in all cases and the Wenner array was used. The location of the profiles in the basin is shown in the map inset.

A second set of resistivity surveys, placed across the Río Artiguas channel, are shown in Figure 14. The same quartz vein mapped in Figure 13 is found crossing perpendicularly to the river in the north side of the site with dominant strike oriented east - west and dipping vertically. Groundwater levels were monitored in nine mini-piezometers located at the west side of the river channel. There the water table is found at 0.2-1.9 m depth and the average flow direction indicated discharge to the river. With the exception of one line, all 2D resistivity surveys were performed crossing the river channel. In general, all lines are well correlated. There is a thin conductive layer on top of a resistive layer. The conductive layer is associated with clay, but is interbedded with resistive quartz-rich sediments. The resistive layer consists of a 3-4 m thick leached weathered material and boulders debris derived from mining activities. Below this layer a third layer, interpreted as clay is found, which gives the lowest resistivity values and is commonly water saturated. Less weathered or fresh rock is related to the deeper high resistivity layer. The vertical quartz vein is located at the north end of Line 10. The east half of Line 9 is placed over fresh non-fractured intrusive rock documented in Hodgson (1972) and Darce (1987). The saturated low resistivity layer disappears gradually throughout the lines from south to north as the intrusive body is approached.

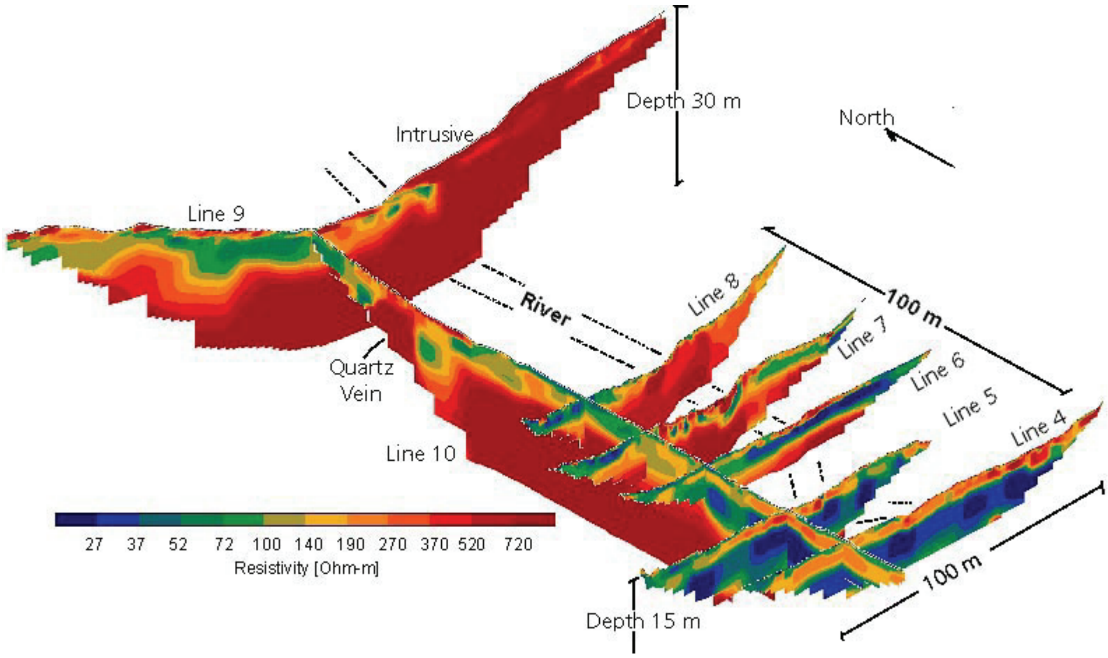

Figure 14. Inverted models of Lines 4-9 crossing Río Artiguas and Line 10 parallel to the channel. Lines 4-8 were 100 m long and had a minimum eletrode spacing of 1 m. Lines 9 and 10 were 200 m long and had a minimum electrode spacing of 2 m. A multiple gradient array was used in all cases.

4.3 Forward modelling

Different electrode arrays can allow the mapping of different areas of the subsurface. They may have higher sensitivity for certain parts of the subsurface or have larger penetration. Moreover, there can be particular geological conditions where some data combinations can be more efficient keeping a good compromise between measuring time and data quality. The advantages and disadvantages of the measuring arrays can be revealed by forward modelling. Though it is infrequently done, it is highly advisable to perform forward modelling in every new field application of a geophysical method, because it can provide criteria for optimising the field procedure and support the interpretation of the results.

In this research, 2D forward modelling of the resistivity response from the studied materials was performed in order to assess the effectiveness of the method, evaluate the electrode geometries used and support the data interpretation. The resistivity model is an idealization of the geological materials and structures in the subsurface. The model is constructed based on the expected resistivity response from those geological entities, upon background information about the area or professional expertise. The subsurface is represented by a network or mesh with blocks of assigned resistivity and nodes where the electrical potentials are measured. In this case, due to the steep topography in the study area, the mesh was adjusted to the form of the surface. Once a resistivity model of the geological subsurface has been built a given array geometry can be tested in terms of its ability to map the chosen geology. This is done by simulating the measurement of apparent resistivity values as it was performed in the fieldwork. Then, the calculated values can be inverted with exactly the same parameters used for real data to obtain the final result of the forward modelling. Figure 15 represents the steps for the forward modelling exercises presented in Paper II.

1. The mesh is designed to include the topography as it was measured in the field.

2. Resistivity values are assigned to the different blocks representing the subsurface. Next the apparent resistivities were calculated with Res2Dmod (Loke and Barker 1996).

3. The calculated resistivity values are inverted using Res2Dinv (Loke 1997).

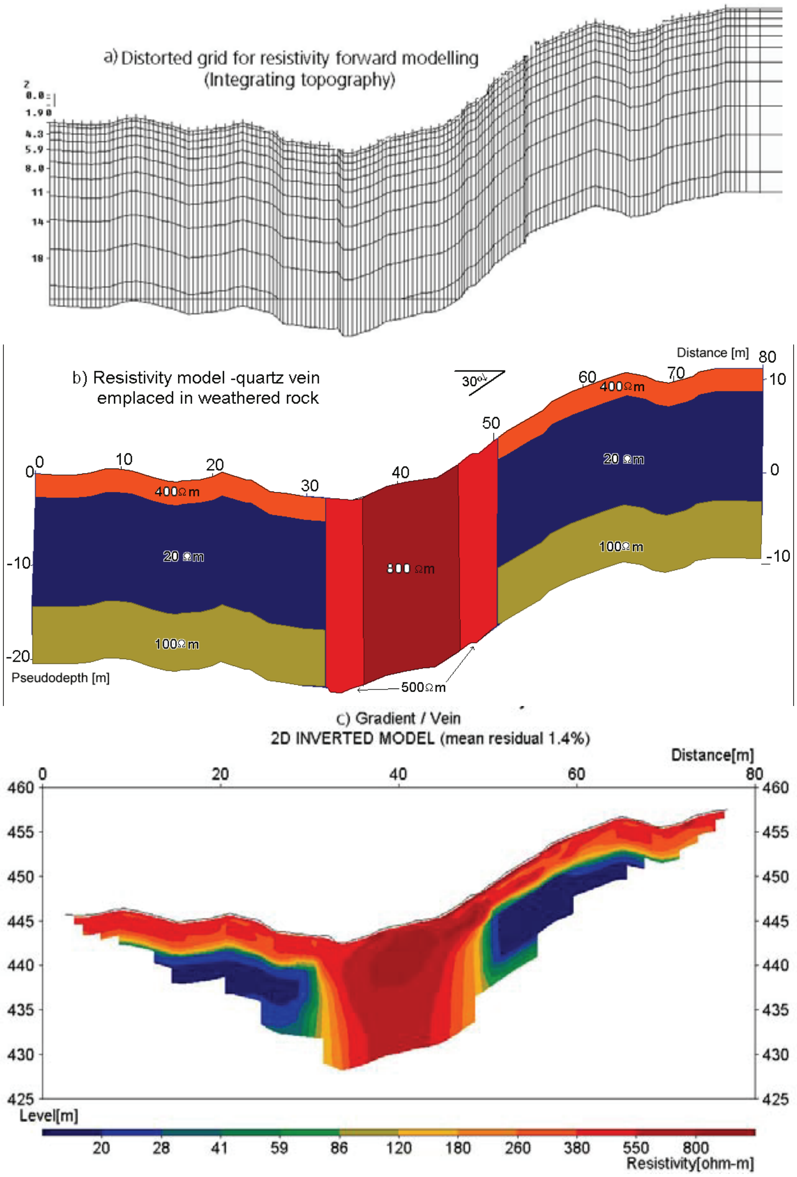

Figure 15. Explanation of the 2D resistivity forward modelling.

5. Groundwater -surface water interactions

This chapter begins by setting the background considerations on the connections between surface water bodies and sub surface water and the methods used for research in the field. Then some achievements in understanding the groundwater-surface water interactions in the basin as investigated at an observation site are discussed.

5.1 Character of the aquifers' relationship with surface water

The discharge of groundwater is not restricted to springs, ponds or lakes; it may also occur directly to streams. There might be ponds, fracturing and finally lowlands along a stream course where water can infiltrate through the subsurface to feed nearby aquifers and perhaps return shortly to the stream (Figure 16). In mountain rivers, with high stream slopes and fresh rock streambeds, there can be sections where contact between surface water and subsurface flow does not occur. Consequently, three different kinds of interactions between groundwater and surface water can be found along a river channel; gaining sections where groundwater feeds the streams, losing sections where streams infiltrate to the groundwater and sections with no contact (Winter 1995; Brunke and Gonser 1997; Winter et al. 1998; Sophocleous 2002).

Winter (1999) pointed out that the relationship between streams and groundwater may be influenced not only by local hydrogeological conditions but also by the climatic regime and ecological constrains. In loosing streams, the annually changing groundwater temperatures can be affected by the daily changing temperatures in surface water (Contantz et al. 1994). Such thermal variations can thus augment or reduce bacterial activity in the streambeds and connected aquifers since bacterial development is temperature dependent (Ward and Stanford 1982; Brunke and Gonser 1997). In human impacted areas these interactions are a critical link that under certain conditions facilitates pollution of either resource. Changes in the hydraulic gradient in sites with groundwater discharge can facilitate infiltration of polluted waters that damage nearby aquifers.

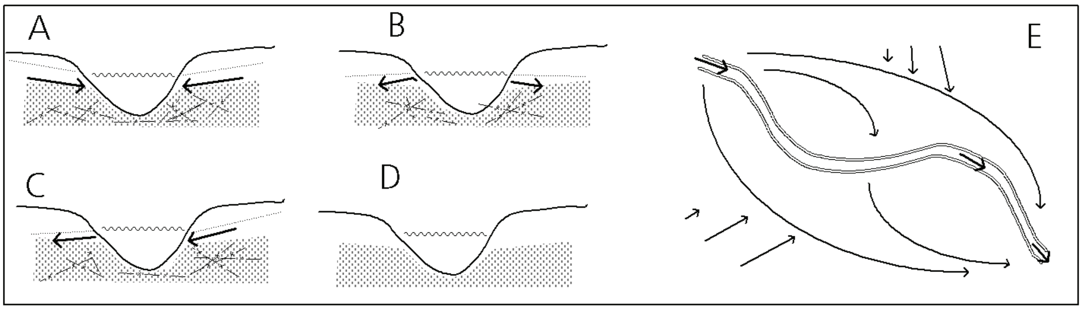

Figure 16. Types of groundwater -surface water interactions. Discharge to the river can occur due to hydraulic gradients from the surroundings (A), but during the dry season it can be the opposite and indirect recharge from the river to the aquifers can occur (B). In some places there can be discharge to the river through one side of the channel, and indirect recharge from the river to the aquifer at the other side of the channel (C). There can also be a lack of connection due to the presence of a fresh rock riverbed or absence of aquifers (D). Hydraulic gradients may differ laterally along the river channel, in such a way that water infiltrating the aquifers at one location may return to be discharged into the river at some point downstream (E).

The study of the connections between streams and groundwater has been the focus of a broad number of investigations in hydrogeological sciences (Sophocleous 2002). Due to the complexity of the interactions these studies frequently include the validation of the employed methodologies. For instance, Sheets et al. (2002) used time series analysis of piezometric data to characterize river infiltration to a well field. Constantz (1998) used periodic temperature measurements to compare variations in stream flow temperatures, stream flow and their connections with groundwater discharge. Genereux (2004) used isotopic data to distinguish between chemically distinct groundwater and stream water in a tropical catchment. From these investigations a conclusion is that large amounts of data and combination of techniques are key conditions to achieve a better understanding of the studied problem.

5.2 Field study of the connections between river and shallow aquifers

Collecting information that could lead to an understanding of the relationship between streams and groundwater was an imperative task in this project. During this research different techniques were used to investigate the discharge-recharge relationships along the streams. First, the gaining-losses method (Lerner 1997), which is based on estimating differences between flow budgets along the streams, was applied along the main channel of the river. The results, summarised in Mendoza (2002) and complemented in Grunander and Nordenberg (2004), suggested that there are alternating periods of discharge to the river and infiltration to the shallow aquifers along the studied channel sections. However, major conclusions could not be drawn due to uncertainties in the collected data in combination with the disputable accuracy of the gaining-losses method for mountain rivers (e.g. Lerner et al. 1990). Next, seepage meters (Lee 1977) were used along the streams without major success due to the rocky bed of the river. Therefore, a closer monitoring of shallow aquifers and river discharge/recharge processes was carried out by installing a group of mini-piezometers and a gauge station.

The monitoring site was selected for its accessibility to a drilling machine due to its gentle topographic roughness. The characteristics of the study site and of the stream are presented in Table 1. Fifteen (15) wells were installed and in nine (9) pressure transducers were set to measure hydraulic heads and temperatures (Figure 17). The monitoring period was from March 2004 to March 2005. The hourly measurements produced a data series that was analysed using auto-correlation and cross-correlation functions. Some results of this time series analyses are presented in Paper III.

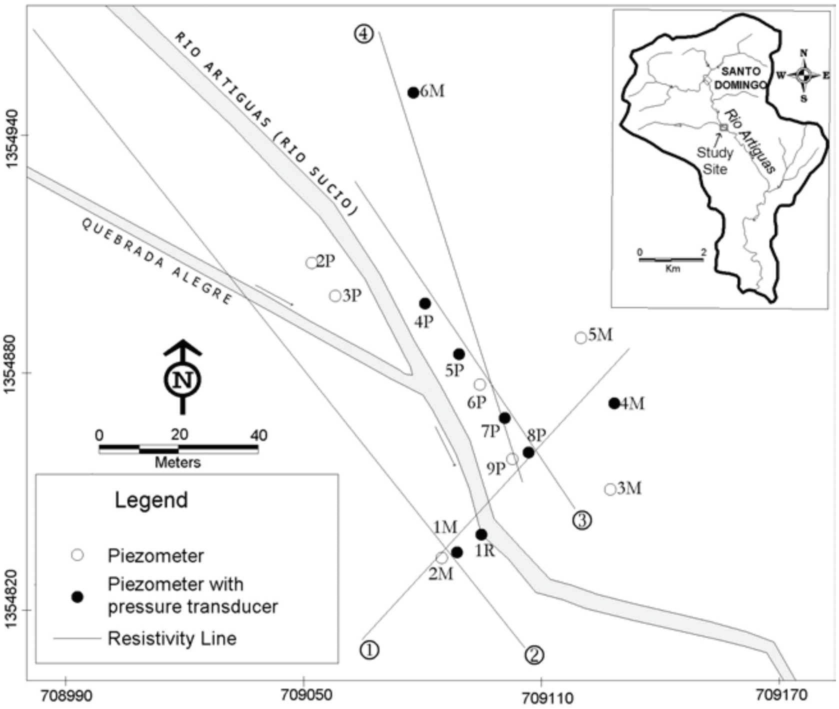

Figure 17. The Quebrada Alegre site

Table 1. Study site and stream characteristics

Catchment Characteristics	
Average Elevation, m	425
Area, ha	1.2
Average stream gradient, m/m	0.04
Sinuosity	1.2
Average stream width, m	5.5
Average width/depth radio	13.75
Study reach length, m	150

The time series analyses required filtering of data to remove outliers, data points affected by sampling, slug tests, and subtraction of the mean values from the signals. The analysis considers two discretized chronological series: the first original data series from a given piezometer, $x_o(x_1, x_2,\ldots,x_n)$, is related to a second original data series from a different point, $y_o(y_1,y_2,\ldots,y_n)$ where n is the total number of data observations present in both observation points (in this case ~8000 hours). The low-pass filtered data to a truncation point, that is the analysed period, m, for k= 0, 1, 2, …,m, are:

$$x_f(n) = [x_o(n-1) + f(x_o(n))]/(1+f) \qquad (1)$$

$$y_f(n) = [y_o(n-1) + f(y_o(n))]/(1+f) \qquad (2)$$

where f is a factor that determines the cut-off frequency of the filter. X_f and Y_f are the low pass filtered data, which is then subtracted from the original data to obtain the high pass version,

$$x_t = x_o - x_f \qquad (3)$$

$$y_t = y_o - y_f \quad (4)$$

After filtering the data the cross-correlation function can be applied to relate the 'input' series x_t and 'output' series y_t. Input and output refers to the convention that one data series is assumed to cause the other. The cross correlation function *r* is not symmetrical (Jenkins and Watts 1968); that is, $r_{+k} \neq r_{-k}$. The expressions for the cross correlation function for the analysed period, *m*, for *k*= 0, 1, 2, …,*m*, are:

$$r_{+k} = r_{xy}(k) = \frac{C_{xy}(k)}{\sqrt{C_x^2(0)C_y^2(0)}} \quad (5)$$

$$r_{-k} = r_{yx}(k) = \frac{C_{yx}(k)}{\sqrt{C_x^2(0)C_y^2(0)}} \quad (6)$$

where

$$C_{xy}(k) = \frac{1}{n}\sum_{t=1}^{n-k}(x_t - \bar{x})(y_{t+k} - \bar{y}) \quad (7)$$

$$C_{yx}(k) = \frac{1}{n}\sum_{t=1}^{n-k}(y_t - \bar{y})(x_{t+k} - \bar{x}) \quad (8)$$

$$C_x(0) = \frac{1}{n}\sum_{t=1}^{n}(x_t - \bar{x})^2 \quad (9)$$

$$C_y(0) = \frac{1}{n}\sum_{t=1}^{n}(y_t - \bar{y})^2 \quad (10)$$

$\bar{x}$ and $\bar{y}$ are the mean values of the series x_t and y_t, respectively. The autocorrelation function is a special case of cross-correlation. In particular cases where strong cross-correlations were found, a coherence function was also applied. The coherence function shows whether variations in the input series respond to the same type of variations in the output series, and thereby indicates the correlation between the periodic variables (Padilla and Pulido-Bosch 1995).

The results of the time series analysis, included in Paper III, indicate that during the dry season the river water infiltrates the near aquifers at the west side of the river and conversely, during the long wet season there is mostly discharge from the shallow aquifers to the river. The temperature variations in the river were larger than in the groundwater (Figure 18). The temperatures in the piezometers close to the river channel are more similar with the temperatures in the river than with the temperatures measured in the wells located away from the stream (see Figure 17 and Figure 18).

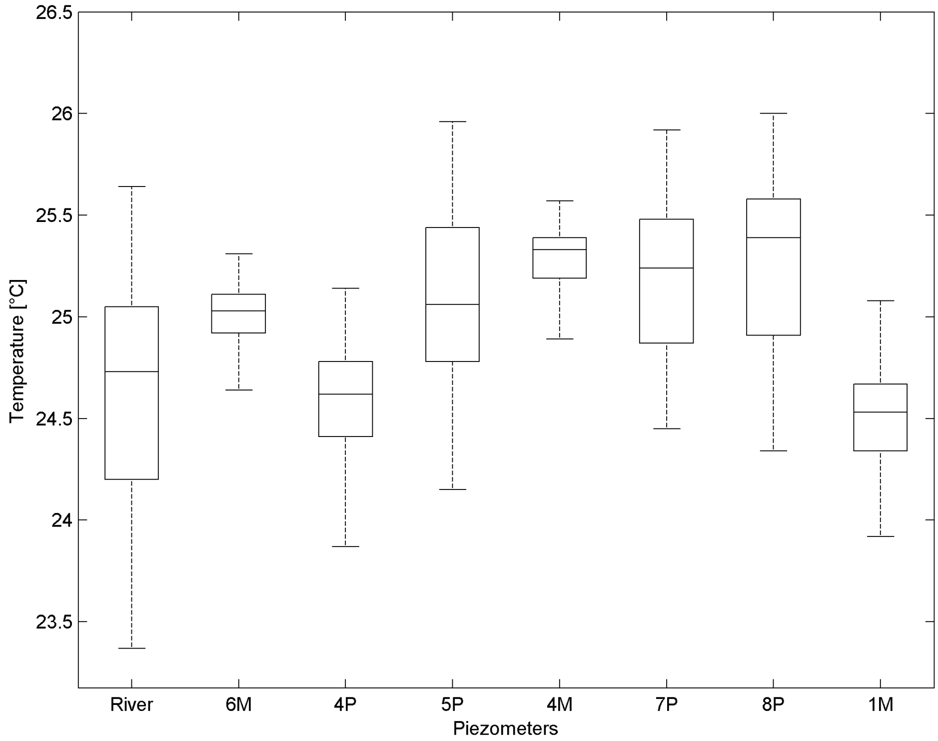

Figure 18. Boxplot showing the variations in temperature in the river and the piezometers at Quebrada Alegre.

There are no significant differences between diurnal variations in the stream temperatures and in the mini-piezometers. This is presumably related to the short residence time of water in both streams and piezometers. The short distance from the discharge areas to the Quebrada Alegre site and the relatively rapid flow in the streams does not give time for the stream water to be affected by the diurnal temperature changes. Then, the measured temperatures are rather an expression of the temperatures present in the aquifers.

Isotope data confirm the close connections between the piezometers and the stream water. Figure 19 shows the ^{18}O and deuterium (^{2}H) signals from the site. The ^{18}O values are within the range of isotopic compositions found in the springs (see Paper I). The isotopic composition between samples 7P, 2P and the river are more similar to each other than the isotopic compositions found at mini-piezometers located away from the stream.

Resistivity imaging and bacteriological analyses were used to map the subsurface and support the interpretation of the piezometers data, respectively. The results are included in Paper III.

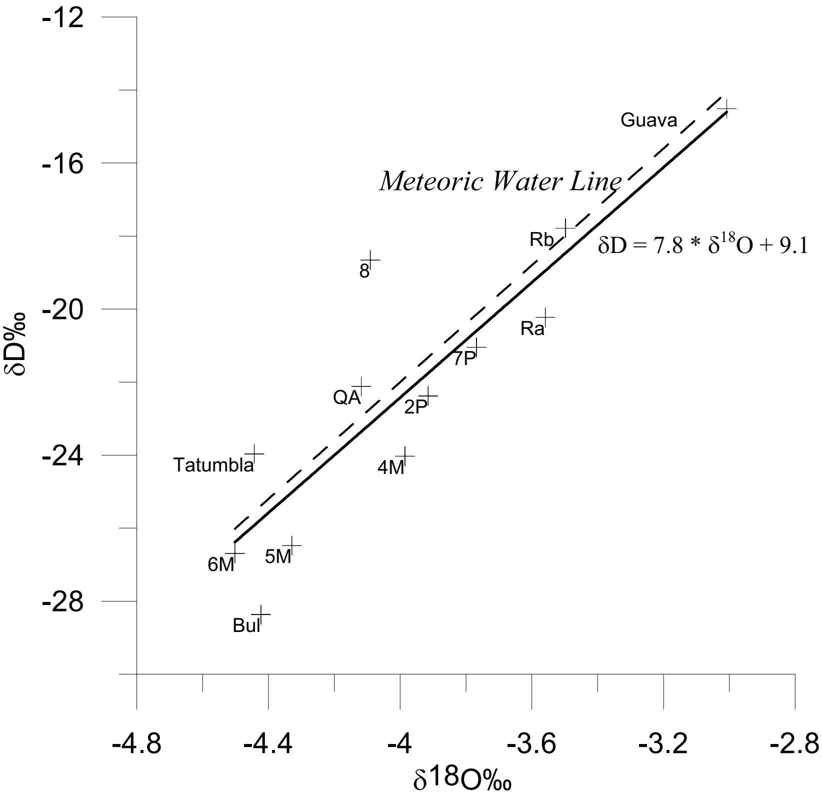

Figure 19. Isotopic composition of the stream at Quebrada Alegre (QA) and the piezometers installed nearby. Tatumbla, Guava and Bul belong to groundwaters sampled at the south extreme of the basin. Rb and Ra are precipitation samples taken at a point located 200 m north from QA.

6. Groundwater Pollution Risk Assessment

The vulnerability and risk associated with the pollution of Río Artiguas are introduced in this chapter and the results are briefly described.

Risk assessment is the practice of gathering and analyzing information in order to predict future risk. In the last couple of decades the concept of risk assessment has been increasingly applied to the problems of predicting human health and ecological effects from exposure to toxic compounds in the environment (Covello and Merkhofer 1993; Asante-Duah 1998; Millard and Neerchal 2001). In this study, groundwater pollution risk is regarded as the combination of exposure to a hazard and the intrinsic vulnerability that a certain area or aquifer possesses. The hazard is related to the probability that a hazardous substance will reach the groundwater in amounts potentially dangerous for human consumption and or ecological damage (Andričević and Cvetković 1996). The vulnerability will represent the degree of weakness that the hydrogeological media inherits regardless of the kind of hazard that the area is exposed to (Foster and Hirata 1995; Belousova 2006).

There are various methods for the vulnerability assessment of groundwater. Commonly, these methods have been designed with the aim of protecting aquifers with certain features and considering the kind of data that is normally available for the assessment. During the last years the most used methods have been DRASTIC, EPIK and SINTATICS. Since DRASTIC was designed in 1987 by Aller et al. (1987), it has been the most used vulnerability assessment tool worldwide. Examples of case studies using DRASTIC include its use for developing groundwater protection criteria in Nigeria (Ibi et al. 2001); selection of an adequate location for waste disposal in South Korea (Lee 2003); and the mapping of karstic aquifer vulnerability in Poland (Witkowski et al. 2003). In Nicaragua, DRASTIC and GOD methods were used to formulate a framework for groundwater protection of the aquifers of Managua (Johansson et al. 1999; Scharp et al. 1997). The GOD method has been recommended for use in areas of Latin America where limitations of available data make it difficult to use vulnerability methods that require several different types of parameters (Foster 1987; Foster et al. 2002).

6.1 Vulnerability evaluation

The vulnerability assessment was carried out using both the DRASTIC method and the GOD method. The DRASTIC method offers a possibility to evaluate the pollution potential based on seven parameters. The seven parameters are depth to groundwater (D), net recharge (R), aquifer media (A), soil media (S), topography (T), influence of the vadose zone (I) and hydraulic conductivity (C) (see Paper IV). These parameters are weighted and combined to produce a potential pollution index. A modification of DRASTIC is included in Paper IV to account for the particular significance that fracturing has in the study area. The modification is an inclusion of an eighth parameter termed 'lineament influence', which represents a combination of connectivity, length and density of fractures, faults and dykes.

The main steps involved in the groundwater vulnerability assessment are presented in Figure 20. The data used was basically the data collected throughout all fieldwork seasons and presented in Papers I, II, and III. Additionally, other sources of data such as geological maps and soil maps were used (see Paper IV and references therein). The digital elevation model (DEM) derived from the 10 m isoaltitude topography map (INETER 1987) was used to compute the slopes needed for the evaluation with DRASTIC. The preparation of data for the vulnerability calculation required conversion from vector data into raster data, which allows matrix operations. The data was then organised to meet the methodology requirements (DRASTIC and GOD). The GOD method was applied for comparison purposes, as a way to appraise the advantages of either index.

The results of the vulnerability assessment show that the areas along the stream valleys and lowlands in the basin exhibit relatively high vulnerability, particularly along the polluted course of Río Artiguas. The modification of DRASTIC to include the lineament influence as an additional parameter allowed a better representation of the pollution potential associated with highly fractured areas. The main parameters influencing the predicted vulnerability were topography and depth to groundwater. In general the limited groundwater resources are susceptible to polluted surface water.

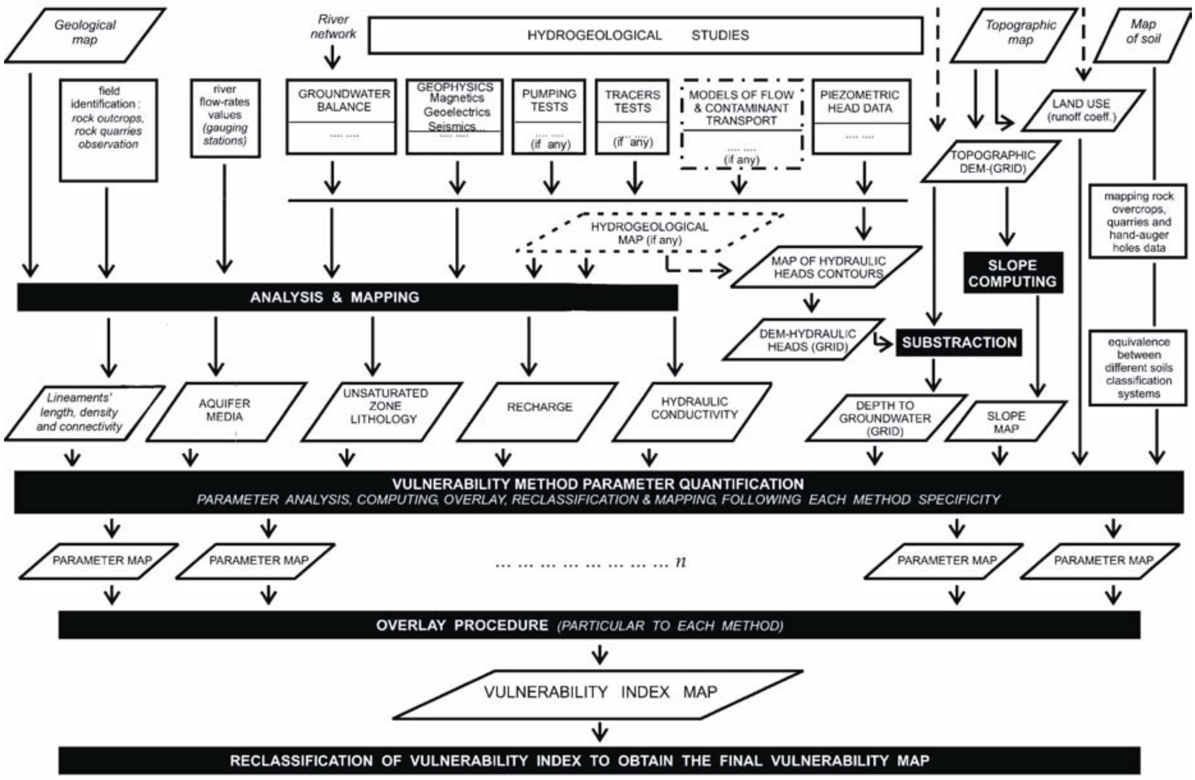

Figure 20. The main steps involved in the groundwater vulnerability assessment (Modified from Gugu et al. 2003, with permission).

6.2 Pollution sources and contaminant load

The classification of potentially polluting activities by their spatial distribution provides a direct evaluation of the type of groundwater contamination threat they pose and the approach to control measures that is likely to be required. Diffuse pollution does not generate clearly defined groundwater pollution plumes but normally impacts a much larger area (and thus volume of aquifer). Point pollution sources normally cause clearly defined and more concentrated plumes, making their identification easier; however when point-source pollution activities are small and multiple, in the end they come to represent an essentially diffuse source, as regards to identification and control (Foster et al. 2002). The Hg pollution sources in the Río Artiguas represent a combination of point and diffuse sources. They are spread in the north side of the basin around the village and near the ore deposits (i.e. along the quartz veins). These sources of pollution are mainly the semi-industrial gold processing plants located in the village and its surroundings, including an electric mill and a few mills moved by rocks. Other pollution sources are the manual mortars and extraction sites, which are spread throughout the basin under even less control from the authorities than the mills in the village.

The gold price fluctuations in the international market have an effect on the intensity of mining and therefore in the regularity of pollution emissions. Increases in gold price are usually followed by new pollution sources appearing; and price depressions result in closing of some refining plants. However, in artisanal and small scale mining the emissions of Hg are also influenced by the availability and price of Hg itself in the local market (Lacerda 2003; Veiga et al. 2006). This implies a wide temporal variation in the mercury emissions to the environment. In addition, the diffuse character of the sources makes it difficult to quantify the amount of Hg released into the streams. An account of the pollution sources and their approximate Hg emissions to the river is given in Table 2.

Table 2. Summary of the sources of Hg in the basin during. Approx. values valid only for the period 2004-2006 (values in Kg).

No.	Pollution source	Hg-usage Hg yr^{-1}	Lost to river Hg yr^{-1}
6	Manual mortars commonly located by a stream	72	36
7	Mills moved by rocks	144	72
1	Electric mill (also known as stamp batteries)	74	37
Total		**290**	**145**

Earlier studies have found mercury concentrations ranging from 1 to 62 µg l^{-1} in surface water around the miner's village Santo Domingo (Silva 1994; Albuquerque 1996; Romero 1996; André et al. 1997). These studies also indicated a quick decrease in mercury content with distance from the village.

During this research a total of 106 water samples were collected in surface waters and springs in the area. The samples were analysed for Hg, Pb and As and a resume of the results is presented in Table 3. Detectable mercury concentrations (0.3- 0.6 µg l^{-1}) were found in wells and springs located within two kilometres from the pollution sources. These concentrations of Hg are attributed to seasonal emissions during intermittent mining campaigns (Grunander and Nordenberg 2004). The springs located at the basin margins are apparently not influenced by pollution as high concentrations of Hg were not found at those locations. In the case of the streams, concentrations above the guideline of 1µg l^{-1} (WHO 1996) were found near the pollution sources.

Table 3 Summary for grouped samples (springs and streams). The table includes only those cases where Hg was detected.

Sample type (number)	As (T) [µg l^{-1}]	Hg (T) [µg l^{-1}]	Pb (T) [µg l^{-1}]
Springs (35)			
Average	0.141	0.039	0.390
Minimum	0.002	0.000	0.013
Maximum	1.060	0.600	1.090
Streams (16)			
Average	0.131	0.982	39.5
Minimum	0.027	0.010	0.3
Maximum	0.253	7.8	179.0

6.3 Method for the assessment of groundwater pollution risk

A groundwater risk assessment can be performed after collecting conclusive information about the intrinsic 'sensibility' of the hydrogeological media to pollution (vulnerability), the magnitude of the pollutant and its areal distribution (hazard) and the relative socioeconomic importance of the groundwater resources.

The method used in this evaluation is adapted from Civita and De Maio (1997) and Ducci (1999) to the particular case of pollutants released from artisanal and small scale mining. In this adaptation, the pollution hazard is assumed to come from the mining mills where Hg is used in the amalgamation process and from the sub-products that are released to the environment. Each plant or mill represents a different magnitude of hazard (see Paper V).

The risk assessment should also include an evaluation of the socioeconomic value of the groundwater resources that could be damaged by pollution. This was done by assigning a socioeconomic value to every catchment that appears to supply water to a given well or spring. This value was designated taking into consideration the size of the population using the water source and whether the source of water (well, spring) is used for economic activities.

The vulnerability, hazard and socioeconomic value maps were converted to grids of 50 X 50 m cells and merged to produce the risk map (see Paper V). The resultant map shows that risk for groundwater pollution from Hg is mainly concentrated around the mining town of Santo Domingo. This is explained by the fact that the vulnerable areas, the larger hazards and the groundwater sources with higher economic values coincide around the centre of the basin. The risk extends from the village along the main river channel. The derived conclusion then is that the pollution can reach the aquifers to the extent that the aquifers are interconnected with the river channel.

It is important to note that the risk of groundwater pollution represents the risk at a point in the timescale. This means that the risk changes as the hazards does with time. Installation or removal of gold processing plants has an effect on increasing or reducing the risk respectively. In the same way, the concentrations of Hg in water of the drainage system are a function of the variability in the emission sources and the changes in flow of the river.

The presence of Hg in the river water affects its quality and threatens to pollute the groundwater resources. Equally important is the fact that the exposure to Hg can produce severe adverse effects in humans and other ecological receptors or entities. This complex scenario needs to be investigated with an integrated approach. This is performed in Paper V, where the risk is assessed from three different disciplines; ecotoxicology, hydrogeology and human health. The risk assessment uses hazard quotients as a common tool to compare and identify the entities at major risk. The hazard quotient (HQ) or hazard index (HI) is defined as the ratio between the estimated chemical exposure level and a reference dose (Covello and Merkhofer 1993; Asante-Duah 1998). In the case of groundwater the reference dose is the guideline for drinking water (1µg l^{-1}). Although hazard quotients are mostly used in environmental and human health risk assessments, they have also been used for evaluations of groundwater pollution risk (e.g. Ehteshami et al. 1991; Peralta et al. 1994; Backman et al. 1998; Sinkevich et al. 2005).

7. Discussion

Reliable measurements of hydrogeological variables in mountain areas are considered difficult to achieve due to extremes in topography, climate, the wide range of magnitude of the variables, uncertainties in the performance of instruments under extreme weather conditions, methods of observation, and difficulties of access (Bandyopadhyay et al. 1997; Wohl 2000; de Jong et al. 2005). The recognition of these limitations motivated the combined use of different methods to investigate the hydrogeological settings in the Río Artiguas watershed. The investigation of different variables (geophysical, geological and hydrogeological) gave an overview of the different natural and anthropogenic factors controlling the occurrence and quality of water resources in the area.

The results of this research, which are presented briefly in this summary and in a more detailed manner in the appended papers, evidence a complex hydrogeological environment characterized by fractured and weathered media. The obtained information requires an integrated interpretation in order to describe the factors that control the formation of groundwater systems in the basin.

The occurrence of springs follows a mechanism where tectonics and weathering are combined to facilitate the transport and discharge of groundwater. This combined mechanism is more obvious in the northern side of the basin where hydrothermal alteration is also present, while a less fractured medium in the south gives rise to a more active role of weathering. The most influential fracture orientation is northeast with regard to the formation of groundwater systems. The quartz veins are also trending northeast and 17% of the springs appear associated to these geological features.

The key hydrochemical feature of the basin is spring-water with low ion content indicative of a short residence time between the zone of recharge and the place of discharge zones. This means that the groundwater is not in contact with minerals in the rock for enough time for chemical reactions to take place. This observation is strengthened by the slightly higher ion content observed in spring waters relatively far from their possible recharge zones.

The isotopic composition of ^{18}O and deuterium found in the groundwater and surface water is similar indicating that both have a common origin (see Chapter 5). The altitude effect allowed identification of the recharge areas as being close to the discharge points at the springs (see Paper I). The values of ^{18}O (min=-5.04‰ max=-3.84‰) found in the groundwater appears enriched in comparison to values of min=-8.5 and max=-5.5 reported by Payne and Yurtsever (1974) from areas located more than 230 km west of this basin. Generoux (2004) reported an averaged ^{18}O=-4.74‰ from an area located 250 km southeast that is subject to recharge water precipitated from the Caribbean.

The resistivity imaging delineated the fractures, faults and quartz veins that cross the strongly weathered Tertiary volcanics. The vertical extension of weathering was also examined at all surveyed locations. The resistivity of zones rich in clay or saturated with water was as low as ~10 Ωm. Layers with coarse grained materials have higher values and the highest resistivities were found in quartz veins and unweathered rock (100-4000 Ωm). The extent of the weathering is highly variable. In areas dominated by lava flows the weathering profile can be between 5 m and 10 m thick on hillslopes. The depth of weathering is as shallow as 1 m at topographic highs that correspond to unweathered rock outcrop, normally intrusives. Generally, the thickness of the weathered layers tends to decrease in the valleys and it is common to find the fresh rock outcropping in the streams channels. This high variability in the depth of weathering is not exclusive to the study area but rather a common feature for other regions characterised by hilly terrain. For instance, Wilkes et al. (2004) reported depth variations of 40 m over distances of 50 m in a basin in South Australia. The variability of weathering depth over short distances has also been observed by Omorinbola (1983) Ollier (1984) and Anand and Paine (2002). Interpretation of the results of the resistivity surveys suggests that the mapped materials are of limited hydrogeological importance and form only small local aquifers.

The shallow aquifers have strong connections to water courses with alternating periods of discharge from the aquifers to the river and indirect recharge from the river to the aquifer. The resistivity surveys performed across the river mapped high resistivity zones at the riverbed which indicates that the interactions between river and aquifers occur through fractured rock. The piezometric data observed at the Quebrada Alegre site represents surface water –groundwater interactions that can be expected at other sections along the river course. This data shows a hydraulic gradient towards the river during most of the monitoring period (March 2004- March 2005, see Paper III), which is supported by the heavy precipitation and localized recharge. However, as the rainy season finishes the hydraulic gradient changed on the west side of the river, allowing indirect recharge from the river to the aquifers. This scenario cannot be extrapolated to the entire basin. Downstream in the basin there are more possibilities for flow from distant locations to meet and thus support a permanent discharge to the river. There are also places where the river flows over unfractured fresh rock and in theses localities no connections between river and aquifers can be expected.

The interpretation of hydraulic data and resistivity imaging collected at Quebrada Alegre is supported with the hydraulic conductivities estimated at different points of the site. Higher permeability was found in areas of fractured rock, where higher cross-correlations were found in the time series analysis (see Paper III). The top layers commonly have lower hydraulic conductivities due to the clay content, but there may be an increase on reaching the fractured rock at depth and in proximity to the fractured dykes.

The information collected allows the formulation of a Hydrogeological Conceptual Model (HCM) for the area (Figure 21). In the north of the basin, after water recharges it concentrates and moves faster through fractured rock located at the base of the weathered layers. Eventually this groundwater meets impermeable clay layers accumulated at the hillsides which forces discharge in a spring or along the streams. In major fractures, tectonic contacts or bed contacts it can travel longer distances and eventually form larger groundwater flows. However, taking into account the large number of springs, the extent of the weathering and the recharge estimations, it is quite clear that most of the water recharged in the basin is discharged locally through the springs and streams. In the north of the basin the influence of tectonics has less effect on the formation of groundwater systems and these are mainly formed in weathered layers. The information collected in this research does not show any indications of regional or trans-basin flow. The hydrogeological setting implies that changes in the precipitation regime can have an immediate effect on the formation of groundwater systems.

The hydrogeological setting with shallow aquifers and steep topography are the most important factors influencing the vulnerability in the area (see Paper IV). The other parameters considered by the DRASTIC index do not have a strong influence as they change smoothly throughout the area. High slopes decrease the DRASTIC index because theoretically a contaminant has less time to infiltrate at steep locations. Conversely the south part of the basin has higher vulnerability as the slopes in these locations are less steep. In the case of GOD, the depth to water was the parameter that had major influence on the overall result. In general, the hydraulic gradient induces groundwater discharge to the polluted river, which supports the relatively high vulnerability values assigned to the river valleys.

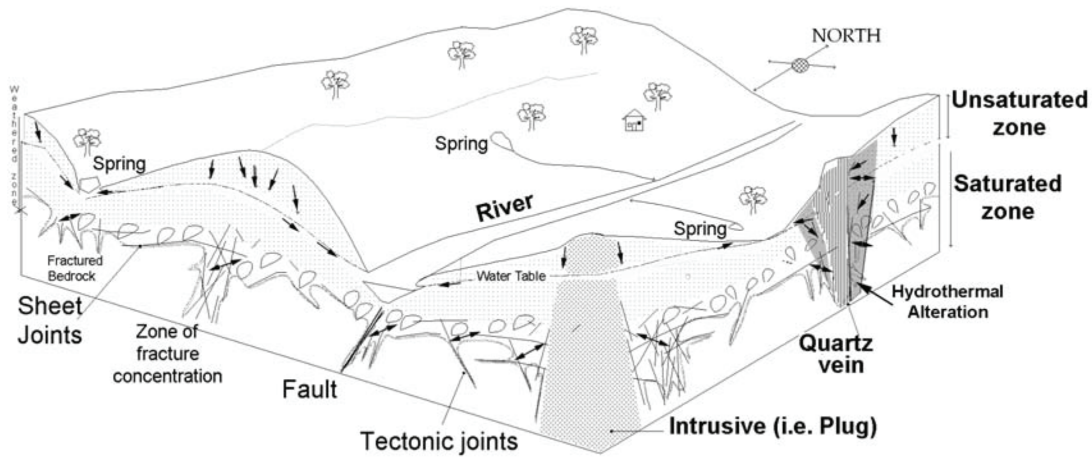

Figure 21. The Hydrogeological Conceptual Model for the Río Artiguas basin.

The risk of groundwater pollution should be considered as an assessment made at a point in the time scale. This means that major changes in the presence of the hazard may increase or decrease the risk of pollution. The diffuse character of the mining, which is not completely restricted to the surroundings of Santo Domingo is a negative factor that increases risk. The precipitation regime is a factor that acts to lower the risk, rapidly diluting the pollutants and spreading them over the large course of the river downstream. The disposal of Hg into Río Artiguas makes this river a vector of pollution to the nearby aquifers. The direct consequence is that the risk of groundwater contamination is concentrated in those sections of the streams where indirect recharge to the aquifers can occur (see Paper III). Considering the high slope of the river channel (0.04 m/m), indirect recharge at one point could reach a location downstream that is not in direct contact with the channel. The small-scale character of the mining and the amounts of Hg used in the process does not represent an extremely high threat to the groundwater resources in its present stage and with the flow regime in the river. However, a change in the river flow due to lowering of precipitation regime can considerable increase the risk of pollution for sources close to the river, such as the main source of water supply for Santo Domingo.

8. Conclusions

The resistivity mapping and hydrogeological surveys with hydrochemical analyses allowed the characterisation of the hydrogeological media in the study area. This included the identification of the geological materials and structures that are related to the formation of groundwater systems and their mechanisms of discharge through the springs.

In general, the formation of groundwater systems in the Río Artiguas basin is controlled by three prime factors;

a) Hydrological, where the high precipitation regime provides permanent recharge to the system.
b) Geological, where tectonics, hydrothermal alteration and weathering are combined to create the aquifers that transport, store and eventually discharge groundwater.
c) Topographical, which combined with geology, facilitates the discharge process.

The hydrological or climatological processes are an immediate source of water to the system, and in conjunction with the geology and steep topography generate a constant and rapid circulation of water from recharge areas to discharge zones. The natural implication of this hydrogeological framework is that the formation of large or regional flows is not evident under the current state of knowledge.

The same factors that influence groundwater occurrence are to some extent responsible for the degree of groundwater vulnerability to pollution. The areas vulnerable to pollution are delineated along the steep valleys of the basin. Since the pollution sources are located near the stream the risk of groundwater pollution is concentrated along the polluted river. The pollutants being disposed near or into the streams are rapidly removed by the river flow and transported far away from the sources.

The vulnerability assessment of fractured media should include the density, length and connectivity of fractures as a new parameter. It is of particular interest to do so in the central regions of the country as fracture density and connectivity are important for groundwater occurrence. Therefore groundwater exploration and vulnerability assessment can be carried out together.

9. Ideas for future research

Based on the results of this research some suggestions are outlined for further research in the central region of Nicaragua or any other geographic location with similar problems and geological environment.

Groundwater systems in mountain or hilly terrains of the tropics are difficult to observe and document, except in their surface expressions (i.e. springs and surface waters where discharge is obvious). Hydrochemical surveys, drillings and other methods are expensive, particularly in developing countries where financial support, wells, laboratories and technical assistance are not abundant. Consequently, it is important to begin a research project by performing a geological reconnaissance with emphasis on the documentation of sources of groundwater. Next, a hydrochemical survey of representative sources could be carried out together with a geophysical investigation.

The geophysical method of resistivity imaging has been a valuable tool in this research and should be considered in further research. It has been used to reliable map the subsurface material and structures likely involved in the development of the groundwater systems. A good start for further research is to carry out resistivity surveys around the springs, aiming to map the geological units related to the occurrence of the springs. Forward modelling to assess electrode geometries and possible responses from the geological units should precede the field investigations.

The electrical method has gained popularity due to its cost-effectiveness, robustness and recent developments in data acquisition preserving data quality. For example, during the last five years the publication of Papers reporting the use of electrical methods on groundwater related studies have increased by 50 % in two peer-reviewed journals (Hydrogeology Journal and Groundwater). The development of joint applications of geostatistical methods with resistivity imaging will probably contribute to further use of resistivity for derivation of hydraulic conductivity.

The hydraulic properties of the streams in this kind of river are difficult to measure, but need to be documented accurately for the characterisation of the surface water – groundwater relationship. This in practice makes installation of a station for periodic observations of hydraulic variables inevitable. Thermography along the river courses can help to identify the discharge sections where the station can be installed. Alternatively, in some cases, evaluation of the interactions might be inferred from the hydrogeological reconnaissance.

The study of the tectonic development of the areas with fractured bedrock can provide valuable information for hydrogeological studies. This should include mapping of fractures and analysis of their geographical relationship with the sources of groundwater.

Most of the cities and towns along the Central American highlands are currently facing water supply deficiencies due partly to the lack of suitable large groundwater reservoirs. In many cases the regional hydrogeological framework is scarcely known or investigations are completely absent. The use of surface waters then becomes an option that is frequently accepted despite the poor quality status of those resources. This situation makes it necessary to integrate local scale research with the regional studies by means of a regional network. There is a lack of comprehensive studies of the isotopic composition of the groundwater in Central America. Such a study could contribute to the qualitative understanding of the recharge process but mainly serve as support to small scale studies.

There are large regions in Nicaragua where hydrogeological data are very limited and groundwater resources are under environmental stress. For those areas, the GOD method is an option that can provide a useful overview of the groundwater vulnerability until further hydrogeological data can be collected to produce more comprehensive vulnerability maps.

The need to stop the pollution of the Río Artiguas is obvious, but the tools to prevent further deterioration overwhelm the hydro geosciences and are located in the socio – political arena. What researchers can do and must do is to communicate the research to make society aware of the availability of water resources and their risk of contamination by anthropogenic activities. In this respect, the research presented in this thesis will gain importance in the extent that it reaches and informs decision makers at the local level.

10. References

Albuquerque N (1996) Estudio de Impacto Ambiental. [Environmental Impact Study] Empresa Asociativa de Pequeños Mineros de SD Chontales 87 pp [in Spanish]

Alfaro C, Wallace M (1994) Origin and classification of springs and historical review with current applications. Environmental geology 24(2):112-124

Aller L, Bennet T, Hehr JH, Petty RJ, Hackett G (1987) DRASTIC: A Standardized System for Evaluation Groundwater Pollution Potential using Hydrogeologic Settings, U.S. Environmental Protection Agency, Ada. Ok, EPA/600/2-87-036, 455 pp

Allison GB, Hugues MW (1978) The Use of environmental Chloride and Tritum to Estimate Total Recharge to an Unconfined Aquifer. Aust. J. Soil Res. 16:181-95

Amoozegar A (1989) A compact constant-head permeameter for measuring saturated hydraulic conductivity of the vadose zone. Soil Sci. Soc. Am. J. 53:1356–1361

Anand RR, Paine M (2002) Regolith geology of the Yilgarn Craton, Western Australia: implications for exploration. Australian Journal of Earth Sciences 49(1): 3-163

André L, Rosén K, Torstendahl J (1997) Minor field study of mercury and lead pollution from gold refining in central Nicaragua. MSc thesis ISBN 1402-1617 Luleå University of Technology, Sweden, 154 pp

Andričević R, Cvetković V (1996) Evaluation of risk from contaminants migrating by groundwater. Water Resources Research 32(3):611–622

Appelo CAJ, Postma D (1999) Geochemistry, groundwater and pollution. Balkema, Rotterdam, 526 pp

Aronsson M, Wallner C (2002) Inventory of springs and hydrochemical investigations of groundwater in the drainage basin of Sucio river, Nicaragua. MSc thesis, ISRN LUTVDG/TVTG—5078—SE. Lund University, Sweden, 105 pp

Asante-Duah K (1998) Risk Assessment in Environmental Management : A Guide for Managing Chemical Contamination Problems. John Wiley and Sons Ltd. West Sussex, England, 515 pp

Backman B, Bodis D, Lahermo P, Rapant S, Tarvainen T (1998) Application of a groundwater contamination index in Finland and Slovakia. Environmental Geology 36(1-2):55-64

Barton CA, Zoback MD, Moos D (1995) Fluid flow along potentially active faults in crystalline rock. Geology 23(8):683–686

Barr DW (2001) Coefficient of permeability determined by measurable parameters. Ground Water 39(3):356– 361

Bandyopadhyay J, Rodda JC, Kattelmann R, Kundzewicz ZW, Kraemer D (1997) Highland water - a resource of global significance. In: Messerli, B. & Ives, J.D. (eds.), Mountains of the world - a global priority. The Parthenon Publishing Group, pp 131-155

Belousova AP (2006) Assessment of groundwater pollution risk as a characteristic of the stability of its quality. Water Resources 33(2):219-232

Bredehoeft JD (2002) The Water Budget Myth revisited: why hydrogeologists model. Ground Water 40(4):340–345

Brunke M, Gonser T (1997) The ecological significance of exchange processes between rivers and groundwater. Freshwater Biology 37(1):1-33

Burrough PA, McDonnell RA (1998) Principles of Geographical Information Systems. Oxford Press, New York, USA

Civita M, De Maio M (1997) Assessing groundwater contamination risk using ARC/INFO via GRID function, Proceedings of ESRI Conference 1997, San Diego, USA, 15 pp

Constantz J (1998) Interaction between stream temperature, streamflow, and groundwater exchanges in alpine streams. Water Resources Research 34(7):1609-1616

Constantz J, Thomas CL, Zellweger G (1994) Influence of diurnal variations in stream temperature on streamflow loss and groundwater recharge. Water Resources Research 30(12):3253–3264

Covello VT, Merkhofer MW (1993) Risk Assessment Methods, Approaches for Assessing Health and Environmental Risks. Plenum Press, New York. 318 pp

Dahlin T (1996) 2D resistivity surveying for environmental and engineering applications. First Break 14(7):275-283

Dahlin T, Zhou B (2004) A numerical comparison of 2D resistivity imaging with 10 electrode arrays. Geophysical Prospecting 52:379-398

Dahlin T, Zhou B (2006) Multiple gradient array measurements for multi-channel 2D resistivity imaging. Near Surface Geophysics, In Press

Darce M (1987) Geology of La Libertad mining district and its surroundings, Nicaragua. Swedish Geological Company (SGAB) report URAP 87002, 18 pp

Darce M (1990) Mineralogic alteration patterns in volcanic rocks of the La Libertad gold mining district and its surroundings, Nicaragua. Economic Geology 85:1059-1071

Darce M, Levi B, Nyström JO & Troëng B (1989) Alteration patterns within an east-west traverse through central Nicaragua. J. South Am. Earth Sci. 2:155-161 de Jong C, Whelan F, Messerli B (2005) The importance of a hydrological research framework for water balance studies in mountain basins. Hydrological Processes 19 (12):2323-2328 DOI: 10.1002/hyp.5886

Deutsch CV, Journel AG, (1992) GSLIB Geostatistical Software Library and User's Guide. Oxford University Press, New York

Devlin JF, Sophocleous M (2005) The persistence of the water budget myth and its relationship to sustainability. Hydrogeology Journal 13(4):549-554

Drever J (1997) Weathering processes. In: Saether OM, de Caritat P (eds) Geochemical processes, weathering and groundwater recharge in catchments. AA Balkema, Rotterdam, pp 109–150

Ducci D (1999) GIS Techniques for Mapping Groundwater Contamination Risk. Natural Hazards 20(2-3):279-294

Ehrenborg (1996) A new stratigraphy for the Tertiary volcanic rocks of Nicaraguan Highlands. Geological Society of America Bulletin, 108(7):830-842

Ehteshami M, Peralta R C., Eisele H, Deer H, Tindall T (1991) Assessing Pesticide Contamination to Ground Water: A Rapid Approach. Ground Water 29(6):862-868

Espinosa L, Espinosa T (2005) Impacto de la minería en la calidad del agua en la microcuenca del Río Antiguas. Énfasis en metales pesados. [Environmental impact of mining in the Río Antiguas basin. Emphasis on heavy metals] Universidad Centroamericana, Managua, Nicaragua 150pp [In Spanish]

Fallico C, Migliari E, Troisi S (2005) Characterization of the field saturated hydraulic conductivity on a hillslope: measurement techniques, data sensitivity analysis and spatial correlation modeling. Hydrol. Earth Sys. Sci. Discuss. 2:1247–1298

Faybishenko B, Doughty C, Steiger M, Long JCS, Wood TR, Jacobsen JS, Lore J, Zawislanski PT (2000) Conceptual model of the geometry and physics of water flow in a fractured basalt vadose zone. Water Resources Research 36(12):3499–3520

Fetter CW (2001) Applied hydrogeology. 4 th Edition. Prentice Hall, New Jersey USA, 598 pp

Feust A (1912) Gold Mines of Chontales, Nicaragua. Mining and Scientific Press, Dewey and Co., San Francisco, USA., 12 pp

Forster CB, Evan JP (1991) Hydrogeology of thrust faults and crystalline thrust sheets: Results of combined field and modeling studies. Geophysical Research Letters 18(5):979–982

Foster SSD (1987) Fundamental concepts in aquifer vulnerability, pollution risk and protection strategy. In: van Duijvenbooden W, van Waegeningh HG (eds) TNO

Committee on hydrological research, The Hague. Vulnerability of soil and groundwater to pollutants, Proc Inf 38, pp 69–86

Foster SSD, Hirata R (1995) Groundwater pollution risk assessment. A methodology using available data. World Health Organisation (WHO), Lima, Peru, 73 pp

Foster SSD, Hirata R, Gomes D, D'Elia M, Paris M (2002) Groundwater Quality Protection; a guide for water utilities, municipal authorities and environment agencies. The World Bank, Washington, D. C. 103 pp

Garrels RM, MacKenzie FT (1975) Origin of the chemical compositions of some springs and lakes. In: Geochemistry of water. Kitano Y (editor) In the collection: Benchmark Papers in Geology 16:247-267

Gaye CB, Edmunds WM (1996) Groundwater recharge estimation using chloride, stable isotopes and tritum profiles in sands of northwestern Senegal. Environmental Geology 27:246-251

Genereux D (2004) Comparison of naturally-occurring chloride and oxygen-18 as tracers of interbasin groundwater transfer in lowland rainforest, Costa Rica. Journal of Hydrology 295(1-4):17-27

Gierczak RFD, Devlin JF, Rudolph DL (2006) Combined use of field and laboratory testing to predict preferred flow paths in an heterogeneous aquifer. Journal of Contaminant Hydrology 82(1-2):75-98

Glynnn FD, Plummer LN (2005) Geochemistry and the understanding of ground-water systems. Hydrogeology Journal 13:263-287

Gogu RC, Hallet V, Dessargues A (2003) Comparison of aquifer vulnerability assessment techniques. Application to the Néblon river basin (Belgium). Environmental Geology 44:881-892

Goovaerts P (1997) Geostatistics for Natural Resources Evaluations. Oxford University Press, New York

Grunander K, Nordenberg L (2004) Investigation of Groundwater – Surface Water Interaction in the Drainage Basin of the River Sucio, Nicaragua, MSc thesis, ISRN LUTVDG/TVTG- -5090- -SE, Lund University, Sweden, 92 pp

Haitjema HM, Mitchell-Bruker S (2005) Are Water Tables a Subdued Replica of the topography? Ground Water 43(6):781–786

Hatton CG, Main IG, Meredith PG (1994) Non universal scaling of fracture length and opening displacement. Nature 367:160-162

Healy RW, Cook PG (2002) Using groundwater levels to estimate recharge. Hydrogeology Journal (1):91-109

Heath RC (1983) Basic groundwater hydrology. U.S. Geological Survey Water Supply Paper, 2220. 84 pp

Hecht G (1995) Hidroquímica de la zona pacífica de Nicaragua In: INETER: Estudio hidrogeológico e hidrogeoquímico de la región del pacífico de Nicaragua [Hydrogeologic and geochemical study of the Pacific region of Nicaragua], Managua, Nicaragua, pp 50-70 [in Spanish]

Hodgson G (1972) Mapa Geológico de la hoja topográfica La Libertad. (Geological map of La Libertad sheet) Catastro e Inventario de Recursos Naturales. Managua, Nicaragua [in Spanish]

Hvorslev MJ (1951) Time Lag and Soil Permeability in Ground Water Observations, Waterways Experimental Station, Corps of Engineers, US Army, Bulletin no. 36, 50 pp

Hurlbut G (1886) The origin of the name "America". Journal of the American Geographical Society of New York 18:301-316

Ibe KM, Nwankwor GI, Onyekuru SO (2001) Assessment of ground water vulnerability and its application to the development of protection strategy for the water supply aquifer in Owerri, Southeastern Nigeria. Environmental Monitoring and Assessment 67:323-360

INETER (1987) Mapa Topográfico Hoja La Libertad 3152-I Escala 1:50000 [Topography map, La Libertad sheet] Instituto Nicaragüense de Estudios Territoriales [in Spanish]

INETER (1991) Anuarios Meteorológicos (1990–1991) [meteorological charts]. Managua, Nicaragua [in Spanish]

INETER (2004a) Mapa Hidrogeológico para la Región Central y Norte de Nicaragua, hoja Juigalpa. Mapa Impreso en Papel a Escala 1: 250,000 [Hydrogeologic map of the Juigalpa Chart] Map [In Spanish]

INETER (2004b) Mapa Hidroquímico para la Región Central y Norte de Nicaragua, hoja Juigalpa. Mapa Impreso en Papel a Escala 1: 250,000 [Hydrochemical map of the Juigalpa Chart] Map [In Spanish]

Jakosky JJ, Hopper RH (1937) The effect of moisture on the direct current resistivities of oil sands and rocks. Geophysics 2:33-55

Jenkins GM, Watts DG (1968) Spectral Analysis and Its Applications, Holden-Day, San Francisco, CA 525 pp

Johansson PO, Scharp C, Alveteg T, Choza A (1999) Framework for Ground Water Protection - the Managua Ground Water System as an Example. Ground Water 37(2):204-213

Krásný J (1998) Hidrogeología de la zona pacífica de Nicaragua. In: INETER: Estudio hidrogeológico e hidrogeoquímico de la región del pacífico de Nicaragua (Hydrogeologic and geochemical study of the Pacific region of Nicaragua), Managua, Nicaragua, pp 19-49 [in Spanish]

Lacerda LD (2003) Updating global Hg emissions from small-scale gold mining and assessing its environmental impacts. Environmental Geology 43:308–314

Lee DR (1977) A device for measuring seepage flux in lakes and estuaries, Limnology and Oceanography 22(1):140-147

Lee S (2003) Evaluation of waste disposal site using the DRASTIC system in Southern Korea. Environmental Geology 44:654-664

Lerner DN (1997) Groundwater recharge. In: Saether OM, de Caritat P (eds) Geochemical processes, weathering and groundwater recharge in catchments. AA Balkema, Rotterdam, pp 109–150

Lerner DN, Issar AS, Simmers I (1990) Groundwater recharge, a guide to understanding and estimating natural recharge. International Association of Hydrogeologists, Kenilworth, Rep 8, 345 pp

Levens RL, Williams RE, Ralston DR, (1994) Hydrogeologic role of geologic structures. Part 1: the paradigm. Journal of Hydrology 156(1-4):227-243

Levi B, Nyström, JO, Darce M, Troëng B (1987) Alteration patterns in volcanic rocks from a geotraverse through Nicaragua—A progress report: SGAB/SAREC/INMINE Report URAP 87004, 13 pp

Loke MH (1997) Rapid 2D resistivity inversion using the least squares method, Manual for RES2DINV. Geolectrical Imaging 2D and 3D, 43 pp

Loke MH, Acworth I, Dahlin T (2003) A comparison of smooth and blocky inversion methods in 2D electrical imaging surveys. Exploration Geophysics 34:182-187

Loke MH, Barker RD (1996) Rapid least-squares inversion of apparent resistivity pseudosections by a quasi-Newton method. Geophysical Prospecting 44 (1):131-152

Magowe M, Carr JR (1999) Relationship Between Lineaments and Ground Water Occurrence in Western Botswana. Ground Water 37(2):282-286

Manga M (2001) Using springs to study groundwater flow and active geologic processes Annu. Rev. Earth Planet. Sci. 29:201–28

Mendoza JA (2002) Geophysical and hydrogeological investigations in the Rio Sucio watershed, Nicaragua. Lic Thesis ISBN 91-972406-0-X, Lund University, Sweden, 60 pp

Mendoza JA, Bjelm L, Dahlin T (2000) Resistivity Imaging as a tool for Groundwater studies at Santo Domingo, central Nicaragua. EEGS Procs. Bochum Germany

Millard SP, Neerchal NK (2001) Environmental statistics with S-Plus. CRC Applied Environmental Statistics Series ISBN 0-0893-7168-6, E-Book. Washington, USA

Moore JE (2002) Field hydrogeology : a guide for site investigations and report preparation. ISBN 1-56670-587-8. Lewis Publishers, E-Book. Washington, USA

Neuman SP (1994) Generalized Scaling of Permeabilities: Validation and Effect of Support Scale. Geophysical Research Letters 21(5):349-352

Neuzil CE (1994) How permeable are clays and shales?. Water Resources Research 30(2):145-150

Nyström JO, Levi B, Troëng B, Ehrenborg J, Carranza G (1988) Geochemistry of volcanic rocks in a traverse through Nicaragua: San José, Costa Rica, Revista Geológica de América Central, v. 8, pp 77–109

Odling NE (2001) The scaling of hydraulic conductivity in rock fractures. Geophysical Research Letters 28(15):3019-3022

Ollier CD (1984) Weathering 2nd Ed. Longman Group Ltd. England, 270 pp

Ollier CD (1988) Deep weathering, groundwater and climate. Geogr. Ann. 70 A (4):285-290

Omorinbola EO (1983) Deep Weathering of Interfluves in the Basement Complex of South-Western Nigeria: Its Geomorphological and Geohydrological Implications. Transactions of the Institute of British Geographers 8(3):342-360

Padilla A, Pulido-Bosch A (1995) Study of hydrographs of karstic aquifers by means of correlation and cross-spectral analysis, Journal of Hydrology 168(1-4):73-89

Palacky GJ, Kiyoshi K (1979) Effect of tropical weathering on electrical and electromagnetic measurements. Geophysics 44 (1):69-88

Patriarche D, Castro MC, Goovaerts P (2005) Estimating regional hydraulic conductivity fields - A comparative study of geostatistical methods Mathematical Geology 37(6):587-613

Payne BR, Yurtsever Y (1974) Environmental isotopes as a hydrogeological tool in Nicaragua, In Proceedings Series: Vienna, International Atomic Energy Agency, pp 193-202

Peralta RC, Hegazy MA, Musharrafieh GR (1994) Preventing pesticide contamination of groundwater while maximizing irrigated crop yield. Water Resources Research 30(11):3183–3194

Rawling GC, Goodwin LB, Wilson JL (2001) Internal architecture, permeability structure, and hydrologic significance of contrasting fault-zone types. Geology 29(1):43–46

Rea J (1964) On the Naming of America. American Speech 1:42-50

Reynolds JM (1997) An introduction to applied and environmental geophysics. John Wiley & Sons, Ltd. England, 796 pp

Romero F (1996) Contaminación de Hg y Pb en fuentes de agua. area de Santo Domingo, Chontales [Hg and Pb contamination in water wells], Centro de Investigaciones Geo-científicas, Managua 21 pp [in Spanish]

Rorabough MI (1964) Estimating changes in bank storage and groundwater contribution to streamflow. Int Assoc Sci Hydro Publ 63:432–441

Scanlon BR, Healy RW, Cook PG (2002) Choosing appropriate techniques for quantifying groundwater recharge: Hydrogeology Journal 10(1):18-39

Scharp C, Alveteg T, Johansson PO, Caldera M (1997) Assigning a groundwater protection value: methodology development. Proceeding of International Association of Hydrogeology Congress: Problems, Processes and Management. Nottingham I pp 659-654

Seaton WJ, Burbey TJ (2005) Influence of Ancient Thrust Faults on the Hydrogeology of the Blue Ridge Province. Ground Water 43(3):301–313

Sheets RA, Darner RA, Whiteberry BL (2002) Lag times of bank infiltration at a well field, Cincinnati, Ohio, USA. Journal of Hydrology 266:162-174

Silva G (1994) Diagnóstico da contaminação ambiental gerada pela actividade minerária sobre los rios Súcio, Mico e Sinecapa, Nicaragua [Diagnose on the contamination caused by the mining activity in the rivers Artiguas, Mico and Sinecapa]. Universidade Federal do parã Centro de Geociências curso de póstgraduação, Belem 123 pp [in Portuguese]

Sinkevich MG, Walter MT, Lembo AJ, Richards BK, Peranginangin N, Aburime SA, Steenhuis TS (2005) A GIS-based ground water contamination risk assessment tool for pesticides. Ground Water Monitoring and Remediation 25(4):82-91

Sophocleous M (2002) Interactions between groundwater and surface water: the state of the science. Hydrogeology Journal 10:52–67

Veiga MM, Maxson PA, Hylander LD (2006) Origin and consumption of mercury in small-scale gold mining. Journal of Cleaner Production 14(3-4):436-447

Ward JV, Stanford JA (1982) Thermal responses in the evolutionary ecology of acuatic insects. Annual Review of Entomotology 27:97-117

Weinberg R (1990) Structural analysis of three gold mining districts of Nicaragua: El Limón, La India and La Libertad. SGAB/INMINE / SAREC Report URAP 90003, 32 pp

Weinberg R (1992) Neotectonic development of western Nicaragua. Tectonics 11(5):1010-1017

Wilkes SM, Clement TP, Otto CJ (2004) Characterisation of the hydrogeology of the Augustus River catchment, Western Australia. Hydrogeology Journal 12:209-223

Winter TC (1995) Recent advances in understanding the interaction of groundwater and surface water, Reviews of Geophysics 33(S1):985–994

Winter TC (1999) Relation of streams, lakes, and wetlands to groundwater flow systems, Hydrogeology Journal, 7:28–45

Winter TC, Harvey JW, Franke OL, Alley W.M. (1998) Ground Water and Surface Water A Single Resource. USGS Circular 1139, 56 pp

Wise S (2000) Assessing the quality for hydrological applications of digital elevation models derived from contours. Hydrological Processes 14(11-12):1909-1929

Witkowski AJ, Rubin K, Kowalczyk A, Rózkowski A, Wróbel J (2003) Groundwater vulnerability map of the Chrzanów karst-fissured Triassic aquifer (Poland). Environmental Geology 41(1):59-67

Wohl E (2000) Mountain Rivers. Water Resources Monograph series, Vol. 14. 320 pp. ISBN 0-86590-318-5

World Health Organization WHO (1996) Guidelines for drinking-water quality, 2nd ed. Vol.2 Geneva, pp 940-949

Wright EP (1992). The hydrogeology of crystalline basement aquifers in Africa. In Wright EP. Burgress WG (eds). Hydrogeology of crystalline basement aquifers. Geological Society Special Publication 66:1–27

Zohdy AAR, Jackson DB (1969) Application of deep electrical soundings for groundwater exploration in Hawaii. Geophysics 34:584-600.

Appendix

(a) Location and classification of the springs

Types of spring; TF: fracture spring, W: weathering spring, TV; quartz vein spring.
(Coordinates System WGS1984)

ID	Easting	Northing	Altitude	Type	ID	Easting	Northing	Altitude	Type
1	710705	1357726	710	TF	54	706844	1354446	614	W
2	710740	1357657	713	TF	55	707380	1354264	583	W
3	710542	1357843	693	TF	56	707808	1354123	565	W
4	710551	1357804	699	TF	57	708042	1354383	525	W
6	710558	1357891	707	TF	58	707970	1354559	524	W
7	710550	1357891	725	TF	59	708845	1355256	435	TF
8	710427	1358050	702	TF	60	708715	1355425	463	W
9	710434	1358055	634	TF	61	708507	1355473	491	W
10	710269	1358092	669	TF	62	708210	1355149	500	W
11	709900	1358280	644	W	63	708234	1355285	509	W
12	709881	1358266	635	W	64	708611	1356784	527	TF
13	709770	1357981	622	W	65	708821	1356367	531	W
14	709530	1358292	636	W	66	708854	1356410	532	W
15	709485	1358299	637	W	68	710271	1352346	336	W
16	709451	1358108	610	TF	69	710858	1352547	365	W
17	709194	1358122	660	TF	70	711271	1352751	383	W
18	709037	1357927	642	W	71	711526	1353169	385	W
20	710663	1357512	660	TF	72	711516	1353141	386	TF
21	710276	1356868	633	TF	73	710687	1353493	370	TF
22	709739	1356696	598	W	74	710654	1353531	375	TF
23	709374	1356740	582	TV	75	710666	1353155	375	TF
24	708760	1356696	523	TF	76	710541	1353281	359	W
25	708195	1357487	597	TF	77	710304	1353234	371	W
26	707971	1357452	600	TF	78	709981	1353188	380	W
27	707820	1357451	615	TV	79	709633	1353503	398	W
28	707760	1357180	587	TV	80	709452	1353669	424	TF
29	707261	1356812	640	TV	84	712054	1354057	403	TF
30	707418	1357038	570	TV	85	712172	1354274	422	TF
31	707737	1356694	573	W	86	712170	1354261	423	TF
32	706854	1355668	615	TF	87	712006	1354740	456	TF
33	706378	1355616	648	W	88	712002	1354859	460	TF
36	710667	1356088	602	W	89	711695	1354951	450	TF
37	710690	1356101	597	W	90	711457	1354950	442	TF
38	710259	1355829	573	TV	91	711174	1354869	474	TF
39	710136	1355887	550	TV	92	711130	1354796	475	W
40	710272	1355990	592	TF	93	711073	1354712	470	W
41	710063	1356074	572	W	94	710739	1354624	496	TF
42	710071	1356160	565	W	95	710528	1354818	499	W
43	710038	1356198	561	W	96	710376	1355368	528	TF
44	710154	1356435	604	TV	97	709746	1355380	520	W
45	710188	1356410	605	TV	108	708980	1350757	403	W
46	710246	1356641	635	W	110	708918	1351237	420	W
47	706234	1355320	662	TV	114	709224	1357124	563	TV
48	706082	1355813	651	TV	115	708874	1356636	503	W
49	706088	1355883	646	TV	201	707857	1357113	590	TV
50	705950	1354966	668	TF	208	708463	1357050	570	TV
51	706066	1354884	657	TF	209	709351	1357126	540	W
52	706171	1354832	658	TF	210	709217	1357133	550	W
53	706307	1354725	649	TF	211	709045	1355811	480	TV
					212	708920	1355840	490	TV

(b): Locations of resistivity surveys

X1, Y1 and X2, Y2 are starting and ending point of a resistivity line, respectively.
Arrays; GR: gradient, W: Wenner, DPDP; dipole dipole, PDP: pole dipole, PP: pole pole

X1	Y1	X2	Y2	Length	Array	Location
707 608.9	1 355 603.9	707 706.5	1 355 738.5	160	W	Across vein
707 823.6	1 355 633.7	707 762.2	1 355 813.1	200	W	Across vein
708 441.3	1 355 275.6	708 445.8	1 355 678.1	400	W	At Jabalí
708 404.8	1 355 482.0	708 603.8	1 355 459.7	200	DPDP	Spring
708 509.4	1 355 385.4	708 498.8	1 355 542.4	160	DPDP	Stream
708 775.6	1 355 773.0	708 583.9	1 355 811.9	200	GR	Near Rastra
708 642.9	1 355 710.3	708 731.7	1 355 715.7	100	GR	Well at 30 m
708 633.8	1 355 691.2	708 734.1	1 355 696.7	100	GR	Well at 40 m
708 636.2	1 355 674.7	708 736.2	1 355 676.5	100	GR	Across well 10
708 623.3	1 355 648.6	708 723.3	1 355 651.3	100	GR	At Jabalí
708 634.2	1 355 631.9	708 748.9	1 355 635.0	100	GR	Crosses Sucio
708 667.9	1 355 803.0	708 662.4	1 355 603.6	200	GR	At Jabalí
708 832.2	1 356 079.1	708 723.1	1 355 090.1	1000	W	At Jabalí
708 508.8	1 355 122.4	708 597.7	1 355 612.1	500	W	At Jabalí
708 539.5	1 355 133.6	708 641.3	1 355 518.6	400	W	At Jabalí
708 733.1	1 355 509.2	708 665.9	1 355 437.4	100	W	At Jabalí
708 754.2	1 355 502.1	708 684.6	1 355 432.8	100	W	At Jabalí
708 694.1	1 355 409.2	708 759.0	1 355 478.5	100	W	At Jabalí
708 568.2	1 355 295.4	708 860.7	1 355 552.4	400	W	Across River
708 601.6	1 355 259.1	709 108.9	1 355 723.4	700	DPDP	Parallel to river
708 862.9	1 355 807.5	709 023.2	1 355 808.7	160	W	Parallel to river
709 046.9	1 355 696.0	708 987.8	1 355 832.3	150	W	Quartz vein
708 966.4	1 355 648.9	708 951.3	1 355 807.2	160	W	Quartz vein
708 926.8	1 355 642.9	708 930.1	1 355 642.9	160	W	Quartz vein
708 735.9	1 355 219.0	709 068.6	1 355 440.7	400	W	Spring
707 708.3	1 357 073.5	707 836.2	1 357 169.4	160	W	Spring
707 834.4	1 357 063.1	707 721.4	1 357 176.0	160	W	Spring
709 883.1	1 356 892.7	709 521.4	1 357 063.6	400	W	Quartz vein
710 114.5	1 356 388.3	710 268.2	1 356 433.3	160	W	Spring
710 217.6	1 356 330.7	710 172.7	1 356 483.4	160	W	Spring
709 473.1	1 357 037.5	709 491.8	1 356 879.5	160	W	Quartz vein
709 513.2	1 357 049.8	709 515.2	1 356 890.6	160	W	Quartz vein
709 542.3	1 357 050.8	709 554.1	1 356 892.0	160	W	Quartz vein
706 267.2	1 354 743.7	706 391.8	1 354 899.4	200	W	Spring
706 392.4	1 354 745.0	706 272.8	1 354 904.6	200	W	Spring
708981.9	1354967	709105.9	1354810	200	GR	Quebrada Alegre
709063	1354928	709118.6	1354845	100	GR	Quebrada Alegre
709064.7	1354813	709132.1	1354886	100	GR	Quebrada Alegre
709069	1354966	709105.2	1354852	120	GR	Quebrada Alegre
708 966.4	1 355 648.9	708 951.3	1 355 807.2	160	PP	El Cuatro
708 966.4	1 355 648.9	708 951.3	1 355 807.2	160	PDP	El Cuatro
709 046.9	1 355 696.0	708 987.8	1 355 832.3	150	GR	El Cuatro
709 080.1	1 354 615.1	709 339.8	1 354 312.2	400	GR	Dyke
708 427.9	1 354 814.5	708 817.7	1 354 360.1	600	GR	Dyke

I

Mendoza JA, Dahlin T, Barmen G (2005) Hydrogeological and hydrochemical features of an area polluted by heavy metals in central Nicaragua. Hydrogeology Journal, DOI: 10.1007/s10040-005-0462-5

Hydrogeological and hydrochemical features of an area polluted by heavy metals in central Nicaragua

Mendoza JA*, Dahlin T**, Barmen G**

(*) Centro de Investigaciones Geocientíficas, Universidad Nacional Autónoma de Nicaragua (CIGEO, UNAN-Managua), Apartado Postal A-131 Managua, Nicaragua,
e-mail: alfredo.mendoza@tg.lth.se, telefax +(505) 277 0613
(**) Department of Engineering Geology, Lund University Box 118, S-221 00 Lund, Sweden

Abstract. This work presents the results of geophysical and hydrochemical surveys used to investigate the hydrogeological conditions in one of the Río Sucio microbasins, in central Nicaragua. Zones of vertical structures (i.e. fractures and quartz veins) and weathering were mapped using Continuous Vertical Electrical Soundings (CVES), as such zones are of major importance for groundwater transport. Water from springs was analysed to determine concentrations of major ions and heavy metals. Low ion concentrations and ^{18}O analyses indicate that the springs occur close to their recharge areas and there is a relatively rapid groundwater circulation. Mercury (Hg) content in the springs was low while comparatively high amounts of lead (Pb) were found. The results presented here demonstrate the important function of weathering and tectonics in the occurrence of groundwater systems in the basin. Hg and Pb found in springs' water reveal the existence of an increase in pollution sources disseminating in the area. More than 100 years of using mercury in the gold mining industry and releasing wastes into rivers has affected water quality and ecosystems. Further investigations are needed in the area to determine the groundwater vulnerability to this pollution as this resource may be needed in the future.

Keywords: Hydrochemistry; geophysical methods; stable isotopes; contamination; Nicaragua

Introduction

In areas where surface waters have been polluted as a result of industrial activity, groundwater has become a main concern, as it constitutes the alternative water supply. However, surface waters may infiltrate and reach aquifers, consequently carrying hazardous substances to the groundwater as well. An important cause of groundwater pollution is associated with mining activities, since toxic substances (i.e. heavy metals), which are typically used throughout the exploitation process, are often released into the environment. For example, artisanal small-scale mining is one of the main sources of mercury (Hg) emissions to the environment worldwide, and particularly in North, Central and South America (Nriagu 1996; Pirrone et al. 1998; Lacerda 2003). Often the high toxicity of such heavy metals leads to the definitive loss of the water resource. The concern about how water pollution affects the environment has triggered several investigations (Barker 1996; Kayabali et al. 1998; Abdul Nassir et al. 2000). As the character of the pollution is complex and the pollution sources may be spread over large areas, these studies combine chemical, geological and geophysical methods, and often include the identification of the groundwater occurrence in order to determine the extent of contamination. However, few studies have been carried out in Latin America, where mining has in fact been extensive in populated areas.

In the central region of Nicaragua, gold mining activities have led to continuous contamination of water basins since the 19th century (Feust 1912). One of those water basins is Río Sucio (formerly named Río Artiguas), where a dispersed cluster of small-scale mills still use mercury (Hg) and cyanide (NaCN) to process ore. The process wastes are then directly released into the water. In addition, the amalgams are frequently burnt by the rivers or in backyards, making it difficult to identify the sources of pollution. Consequently, most of the mercury used to refine gold is released into the environment and there is no possibility to assess responsibility for this pollution (Mendoza 2002).

Earlier analyses of water quality in the Río Sucio watershed indicated that the mercury levels are above the minimum recommended for drinkable water (Romero 1996). Mercury and lead (Pb) have been found in soils, sediments and waters of the basin (André et al. 1997). Further, a study of mercury in miners' hair indicates the need for a continuous monitoring of the effect of water quality on the population living in the area (Silva 1994), since the pollution sources are active, seasonal and mobile, and the population is likely to use surface water for domestic purposes. Unfortunately, there are no previous hydrogeological investigations reported on the Río Sucio area. Geological studies made in the area give a tectonic and lithologic description, but are mainly aimed at assisting ore prospecting, emphasising the gold bearing quartz veins locations in the area (Hodgson 1972; Darce 1990; Carranza 1991). Therefore, increasing knowledge of groundwater systems is needed in the area as a way to assess their vulnerability to pollutants.

This study aims to examine geophysical and hydrochemical information about the Río Sucio watershed, with a focus on the hydrogeological conditions in the study area. This paper includes a geological reconnaissance, a geophysical survey and hydrochemical analyses of springs. A representative group of springs was sampled for chemical analyses, while the geophysical surveys were carried out crossing five springs. Geophysical results for two springs are presented here. The electrical resistivity method was used to map geological materials related to groundwater systems.

Area Description

The study area is located in central Nicaragua. Fig. 1 shows the study area, which is one of the Río Sucio microbasins, covering an area of 28 km^2. The main pollution source is located in the upper part of the microbasin, it is the miners' village of Santo Domingo. The climate is Humid Tropical Montainous, with annual average temperatures between 23ºC and 24ºC. Heavy rains characterise the region making it difficult to set a limit between dry and wet seasons. The steep topography becomes less sharp from north to south.

The young drainage system has developed under a structural control where faults, fractures and joints lead to a rectangular sort of flow pattern regarding surface waters. Streams in the basin sum up a total length of 30 km, which is relatively long considering the basin area. Flow measurements in a centrally located cross-section of the main river indicate an approximate discharge of 1.6 – 8.5 x 10^4 m^3/day.

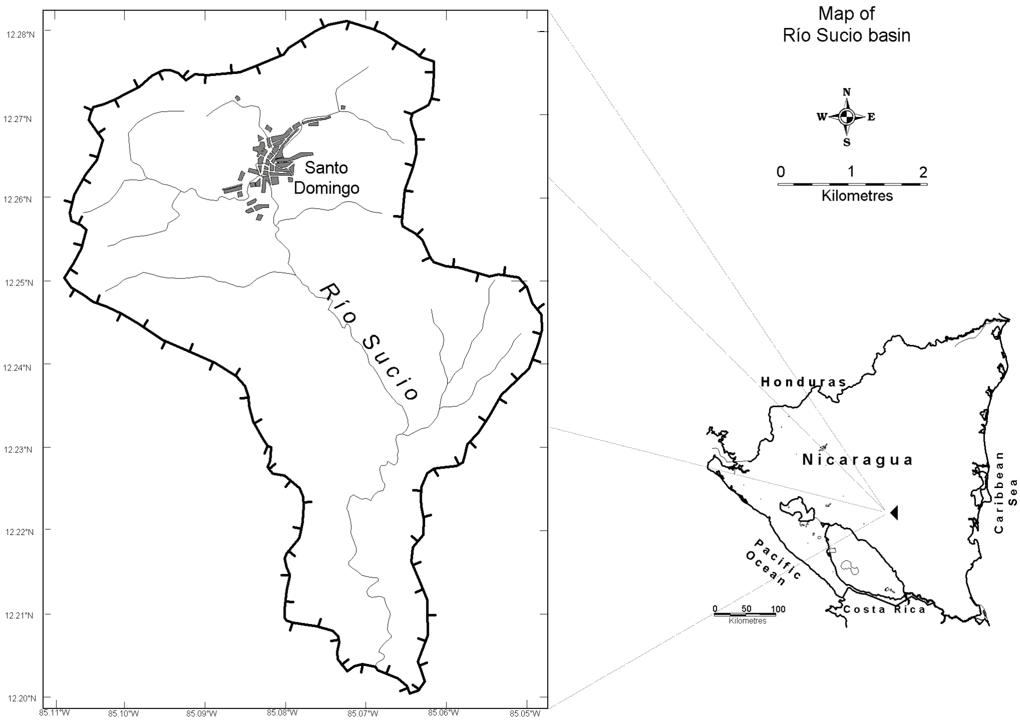

Fig. 1 The study area at Río Sucio basin, in the central mountainous region of Nicaragua.

Fig. 2 shows the two main geological units present in the basin; the old pyroclastic rocks of the Matagalpa group in the south and the basalt to andesite lava flows of the Coyol group in the central and northern part. Several plugs of acid composition have intruded these units (Hodgson 1972; Ehrenborg 1996).

The upstream part of the area is cut by several faults/fractures in an east-west direction. Hydrothermal solutions filled these fractures and formed the gold bearing quartz veins. A second generation of tectonic movements in the south-north direction caused the quartz veins to become segmented and displaced a few meters (Darce 1987).

Methodology

A geological reconnaissance was carried out in the region in order to (a) identify areas with different lithologies (b) get a general, regional grasp of the principal tectonic structures and (c) develop a sense of the orientation of minor faults and fractures. The reconnaissance was carried out together with analysis of aerial photographs to locate major structures like faults, fractures, dikes and quartz veins.

Continuous Vertical Electrical Sounding (CVES), which combines lateral with vertical data acquisition, was the applied resistivity imaging technique. The multi-electrode ABEM Lund Imaging System (Dahlin 1996) was used in varied layouts at diverse locations in the area to locate fractures, zones of quartz veins and to map weathered layers. Examples of five CVES, two using the Wenner array, one using Wenner-Schlumberger array and two using the dipole-dipole array are presented in this work. Documentation of the ground lithology and observations in available mine shafts was done along each line. Three of the CVES lines had a length of 160 m with a 2 m electrode spacing, and two lines had a length of 200 m with 2 m electrode spacing. The CVES were performed at several sites and results from two sites with geological setting representative of the area are presented

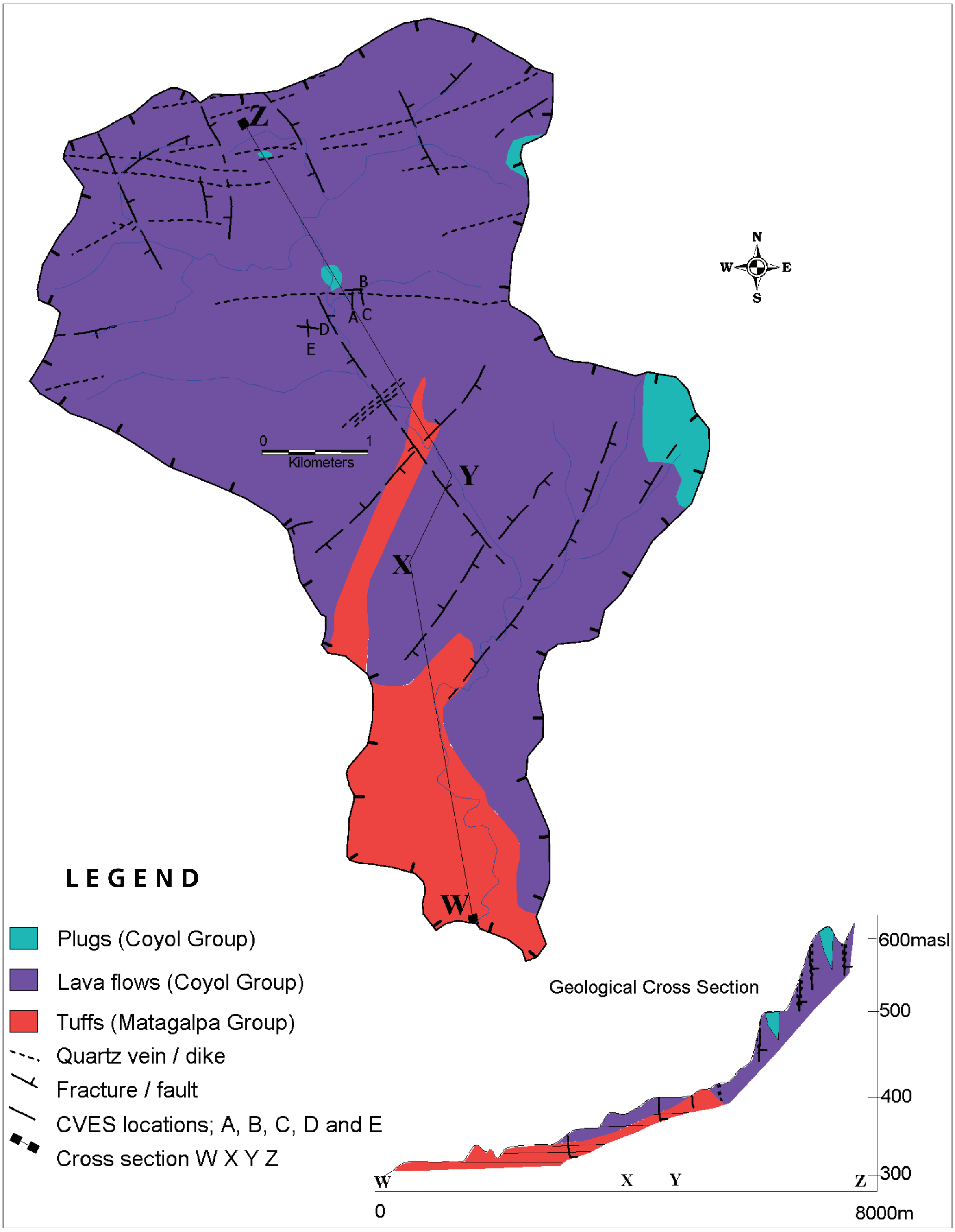

Fig. 2 The lithological and tectonic features of the area and location of CVES surveys (A-E).

here, crossing springs with weathered rock zones and a quartz vein area (Fig. 2).

After data collection, processing was performed using the Res2dinv algorithm, which generates a two-dimensional (2D) model of the subsurface resistivity distribution (Loke 1999). This 2D resistivity model was obtained by applying the robust (L_1-norm) inversion method to the measured data (Loke et al. 2003). Due to the steep topography the inversion had to be based on the generation of a distorted finite element grid of the subsurface. The resistivity model fitness was evaluated by the mean residuals value, which is a comparison between the resistivity values calculated on the model and the measured apparent resistivity. In addition to the multi electrode resistivity survey, punctual resistivity measurements were made using an electrode separation of 0.1 m in different kinds of exposed materials. In this way, reference resistivity for different kinds of materials was compared with the results of the multi electrode surveys.

An inventory of springs in the area was performed which included location with GPS and documentation of each spring site, integrating land use, soil type, geology, seepage site and amount of discharge, when possible. Further, 20 typical springs were sampled for hydrochemical analysis, selected according to the seepage type, geographic location and accessibility. Analysis of ^{18}O was also performed in order to identify recharge areas since the content of this isotope may vary as a function of the average altitude of recharge. The water samples included one from rainwater and two from the polluted main stream of Río Sucio. Analyses of NO_3^-, SO_4^{2-}, S_2^-, Cl^-, and Fe^{2+} were done with a field spectrophotometer Hach DR/2010. Pb and Hg were analysed by a SpectrAA-20 VARIAN atomic absorption spectrophotometer. The laboratory analyses were performed in two laboratories, the National University of Nicaragua (UNAN-Managua) and the Department of Geophysics, University of Copenhagen.

Results

The results of the combined geophysical surveys and geological reconnaissance show that tectonics and weathering processes have dominant influence on the occurrence of groundwater flow systems. Fig. 3 shows the 2D resistivity inversion results for five CVES lines performed in the upper part of the basin. Lines A and B were located at a site where the geology is characterized by a 5 –10 m thick quartz vein intruding weathered andesite– basalt flows (see Fig. 2). Both resistivity lines meet at a spring location and the south-north line (Line A) crosses a stream three times. These two resistivity lines show three layers with different resistivity values. On the top there is a 1 m to 5 m thick layer with values ranging from 60 ohm-m to 220 ohm-m. Below this layer the resistivity drops to 17 ohm-m – 46 ohm-m, becoming at least 10m thick. This area reaches the surface at the spring location at Line B (see Fig. 3). Two vertical patterns, corresponding to quartz vein areas are located at 95 m and 120 m on Line A, giving very high resistivity values (>220 ohm-m). The strong correlation between tectonics and groundwater occurrence is confirmed on Line C, where a spring is found directly on top of a quartz vein. Lines E and D were located so that they crossed one of the analysed springs (#61). Both lines show an upper layer with high resistivity values (>130 ohm-m) in the hilltops and hillsides, which get thinner towards the valley areas. Along Line D at the stream valley the resistivity values are lower (<42 ohm-m).

The resistivity responses of different materials were estimated using punctual resistivity measurements. Fig. 4 shows that the highest resistivity values were observed in massive quartz, followed by unsaturated weathered volcanic rock. Lower values were found in water-saturated weathered rock and surface water.

The inventory of the area reveals 95 springs of three types: wetland springs, punctual springs and shallow wells (probably punctual springs that have been converted to shallow wells by digging). Wetland springs can cover areas of up to 5000 m^2. Punctual springs and wells occur in areas of steeper topography and may be

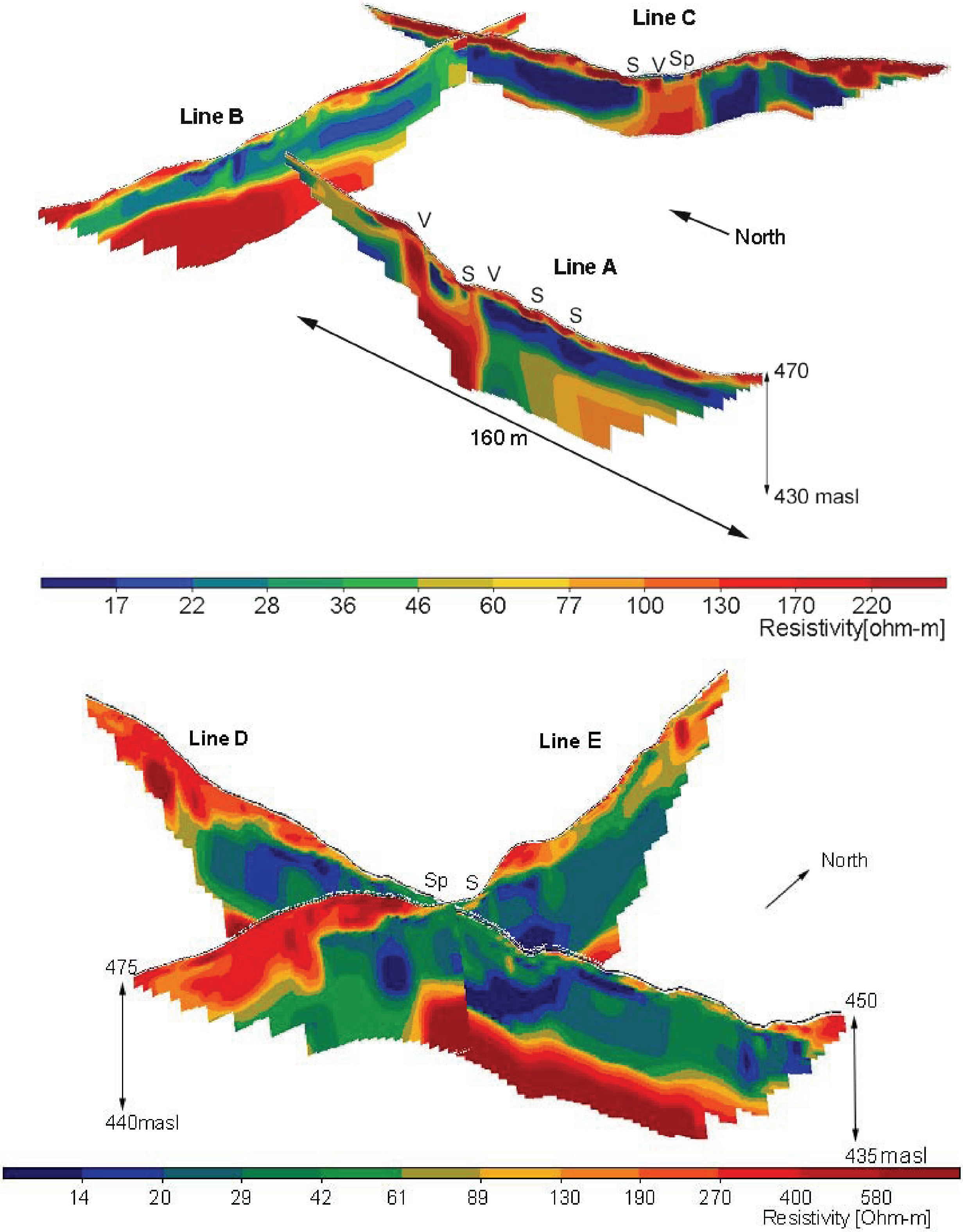

Fig. 3 CVES results. Above, the resistivity inversion models for Line A, Line B and Line C, all 160 m long. Line A shows coarse-grain material on top of a low resistive layer with clay weathered material. Quartz veins (V) stand out as high resistive vertical zones. A spring (Sp) is found on top of a quartz vein (V) on Line C. Below, Lines E and D show the low resistive clay weathered zones reaching the surface at spring 61 along a stream valley (each line is 200 m long). Spring = Sp, Stream = S, Quartz vein = V.

associated with local tectonics. The altitude of the springs varies from 331 m.a.s.l. for those in the south and centre of the region to 731 m.a.s.l. at the northern

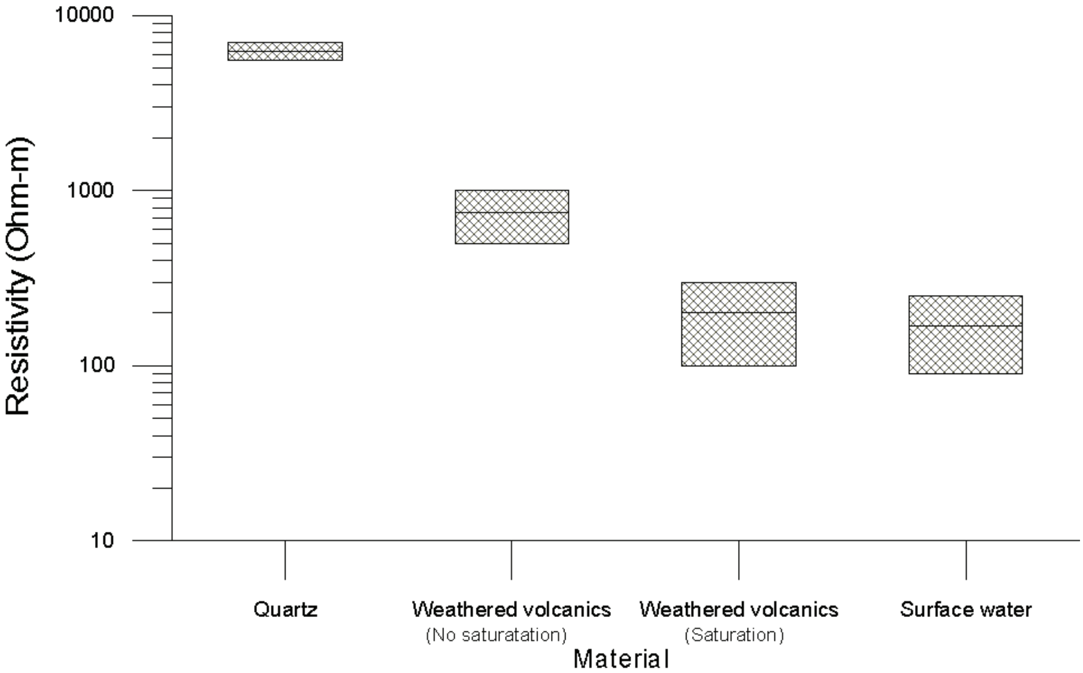

Fig. 4 Ranges of resistivity responses from different materials in the area.

borders of the basin. pH values ranges from 5.81 to 7.47, while conductivity varies from 170 µS/cm to 46 µS/cm. (Aronsson and Wallner 2002) The spring locations are presented in Fig. 5.

The analyses of groundwater from 20 springs generally show low ion concentration values (Fig. 5). Relatively high values of NO_3^-, SO_4^{2-}, and Cl^- were found in the springs close to the village. Analyses of samples from springs 23, 25 and 51 were excluded from the diagrams of figures 5 and 6 since the ion balance error was higher than the accepted error for this study (11%). Fig. 6 presents a Piper diagram indicating that regarding the hydrochemical facies, the spring waters can be classified as calcium type in the cations-triangle, and as bicarbonate type in the anions-triangle. Plots in the central diamond suggest that the spring waters are affected by alkaline lithology. Detectable mercury concentrations were found in locations 39 (0.0003 mg/l) and 89 (0.0006 mg/l), but none of them exceed the health limit of 0.001 mg/l (WHO 1996). Water samples B and C, taken in the main river stream close to the major pollution sources, present higher mercury contents than the water samples from the springs. The highest lead concentrations were found in springs 23 (0.011 mg/l) and 51 (0.013 mg/l). Other high values of Pb were found in springs 8, 28, 39, 49, 89 and 114, all located close to the basin borders.

The ^{18}O analyses indicate that the springs occur at an altitude that ranges from 0 m to 150 m from the average elevation of their recharge areas. The results of ^{18}O are presented in Fig. 7 as function of the altitude of the springs together with an estimation of the average altitude of the recharge areas.

Discussion

Using CVES it was possible to clearly delineate three distinctly different resistivity layers at the investigated locations. For all lines, the results show relatively high resistivity values in the top layer, which is associated with hydraulically permeable coarse-grained material. This might be caused by material

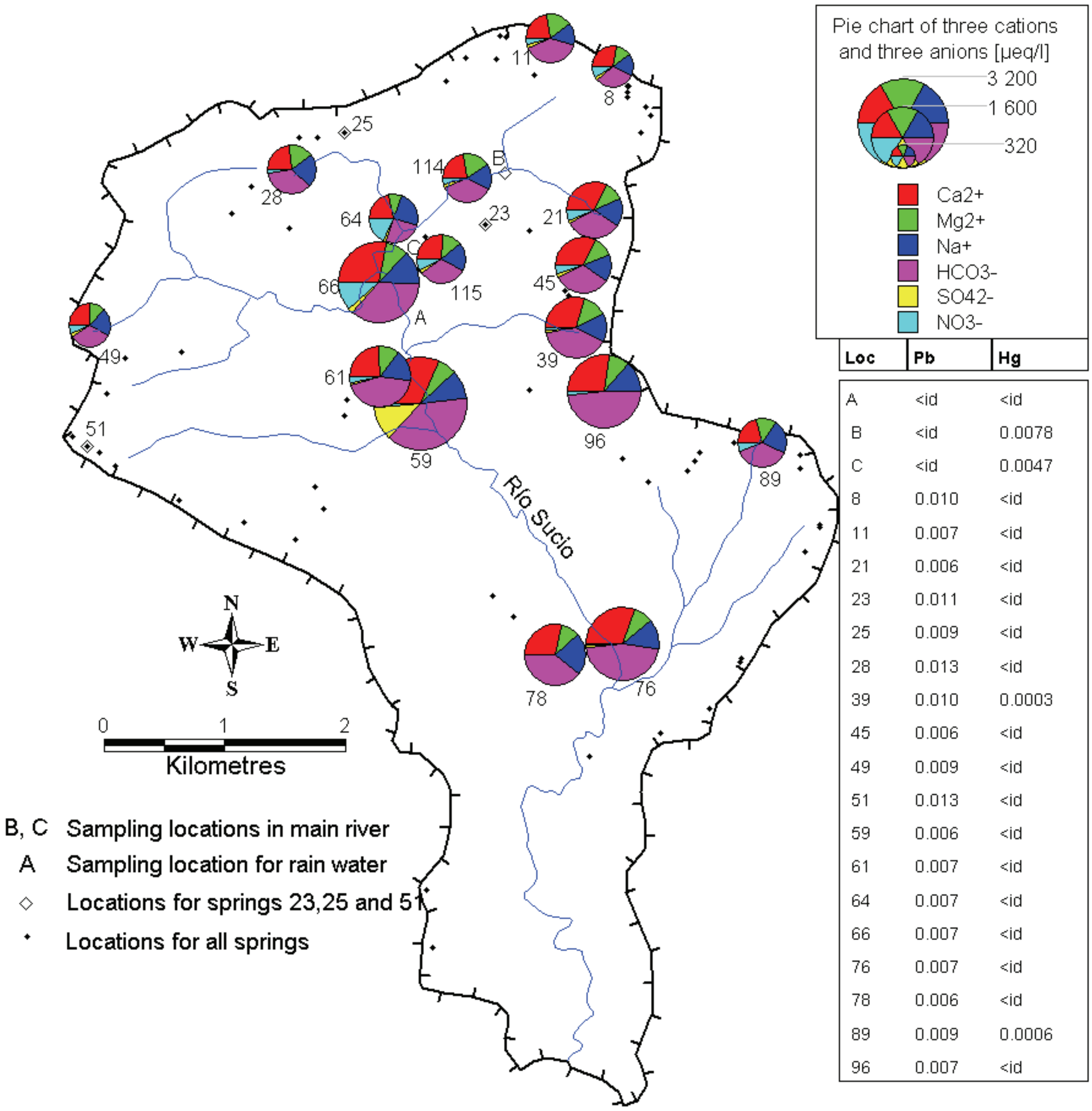

Loc	Pb	Hg
A	<id	<id
B	<id	0.0078
C	<id	0.0047
8	0.010	<id
11	0.007	<id
21	0.006	<id
23	0.011	<id
25	0.009	<id
28	0.013	<id
39	0.010	0.0003
45	0.006	<id
49	0.009	<id
51	0.013	<id
59	0.006	<id
61	0.007	<id
64	0.007	<id
66	0.007	<id
76	0.007	<id
78	0.006	<id
89	0.009	0.0006
96	0.007	<id

Fig. 5 Hydrochemical characteristics of groundwater from springs in the Río Sucio basin. The table presents heavy metals (Hg, Pb) content in the sampled springs (mg/l) (<id = value lower than detection limit).

transported due to natural processes or leached weathered soil, but it might also originate from material removed from mining activities on the surface. The latter is the case for Lines A and B, where mining has been reported around the quartz vein. A second, underlying, layer is then found which appears to be clay weathered material. This clay layer may have low hydraulic conductivity, which explains the fact that a spring is formed where this layer meets the surface on Line E. The bottom resistivity layer is interpreted as less weathered or fresh rock, since very high values were obtained. An intrusive body was visible at the west extreme of Line B (see Fig. 3). As Line E reaches the hillsides and approaches spring 61 and the stream, the low resistive clay layer gets near the surface. This could have implications for discharge, since water infiltrating the uppermost coarse-grained layer can be discharged along the streams. This can also be appreciated on Line D, where the top layer is mostly the low resistive. As the resistive quartz vein appears to have high secondary porosity, it contributes to the spring occurrence on Line C.

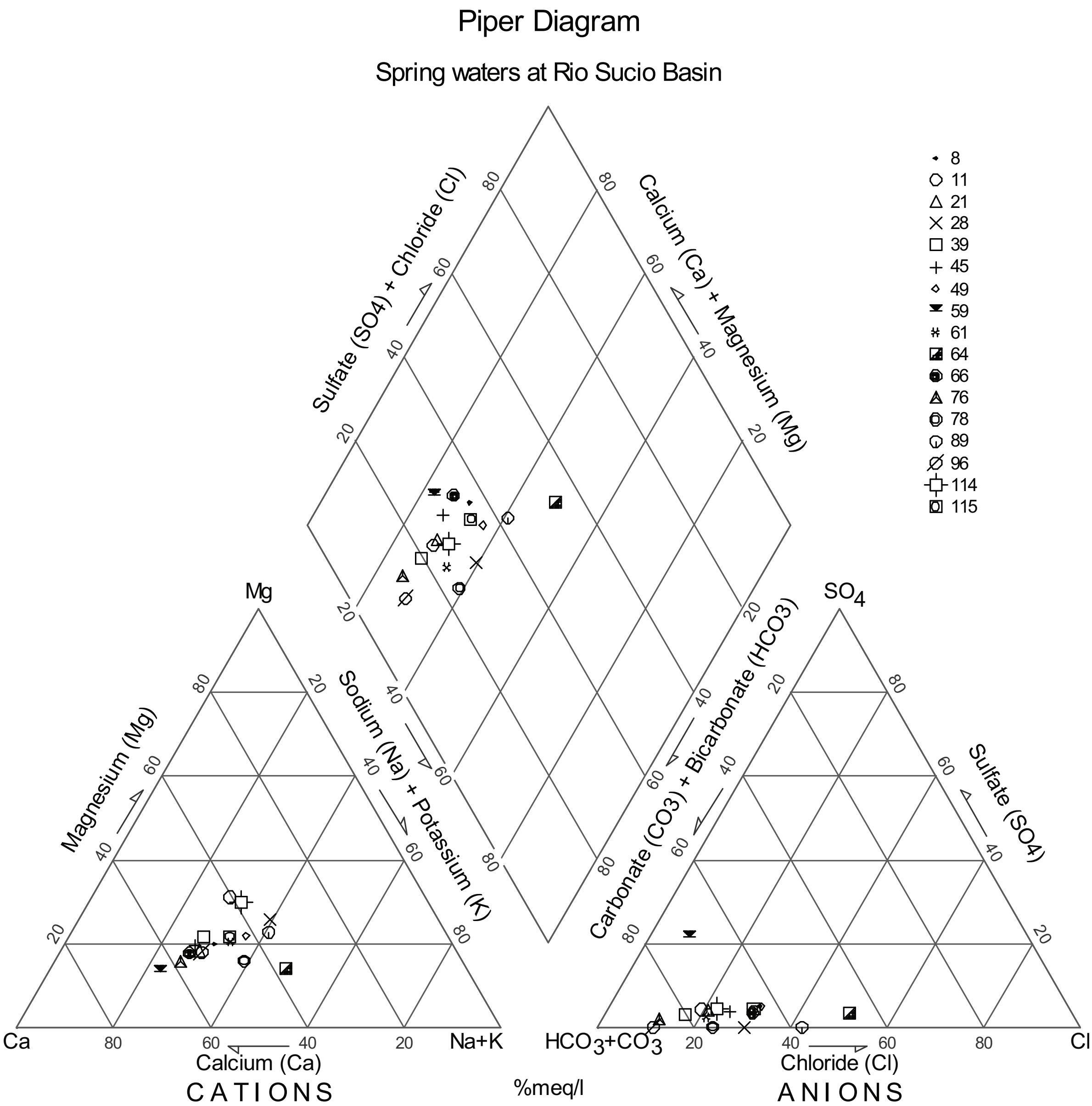

Fig. 6 Piper diagram.

The low ion concentrations in the analysed spring water can probably be explained by infiltrating water that travels very quickly from recharge to discharge areas and consequently, is not in contact with minerals in the rock for enough time for chemical reaction to take place. Relatively higher ion concentrations were observed in spring waters closer to the main river, accordingly the groundwater appears to be in longer contact with weathered materials.

The ^{18}O analyses indicated that 55% of the sampled springs are located very close to their recharge areas, with less than 30 m of difference in altitude, which together with the low ions concentrations, elucidate the relatively rapid groundwater circulation.

Conversely, springs located in the southern part of the basin at lower altitudes seem to be less close to their recharge areas, presumably due to higher hydraulic conductivities in the pyroclastic rocks present in the area. There, the basalt to andesite lava flows of Coyol become

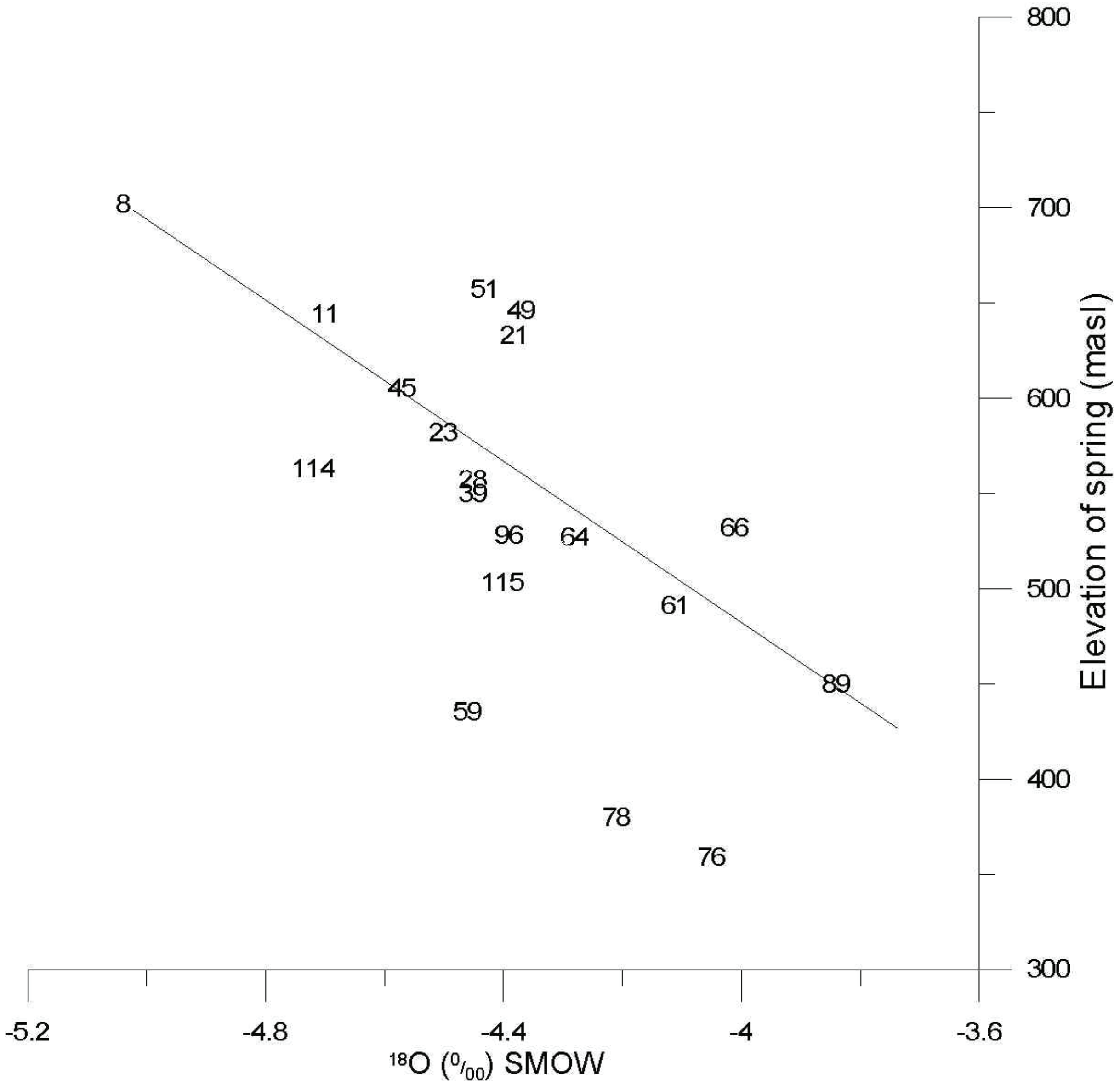

Fig. 7 ^{18}O results plotted against the elevation of the springs. The trend line is adjusted to the elevations of spring 8 and 89, since those springs are judged to be located very close to their recharge area.

thinner southwards, and the very weathered and porous pyroclastic rocks of the Matagalpa unit often appear as 'windows' (Darce 1987; Ehrenborg 1996). Fig. 2 shows a cross section along the river course where a change in lithology can be observed. The high porosity of tuffs is associated with high hydraulic conductivity, permitting water to be transported longer distances before forming springs. Nevertheless, considering the basin area the amount of springs occurring in the Río Sucio basin is high, indicating that most of the groundwater is discharged into the springs, rather than forming large regional aquifers.

The main mercury source was shown to be in the village and its surroundings, where a small-scale semi-industrial plant and several hand-made mills are used for gold processing. Other diffuse sources are spread in the basin, as individual miners looking for new mineral prospects are sometimes processing gold *in situ*. The latter may explain the mercury found at two of the springs (39 and 89).

Conclusions

Vertical structures as faults and quartz veins act as conducts to transport water in the upstream part of the Río Sucio basin. The results of geological reconnaissance and resistivity imaging demonstrate the important function of tectonics and weathering in the groundwater systems. However, more field studies are needed to establish a reliable picture of groundwater flow pattern and groundwater and surface water interaction. Such studies are in progress.

The water chemistry analyses at the selected springs show low ion concentrations, indicating that the groundwater circulation through the basin is rapid. The water chemistry is characteristic of lava flow environments. The ^{18}O analyses indicate that the springs occur very close to the average elevation of their recharge areas, in particular in the upper part of the basin.

As the lithology changes southwards to a more weathered pyroclastic rock, the occurrence of the springs tends to take place at longer distances from their recharge areas. In the downstream part of the basin tectonic features may have less importance for groundwater flow transport, as the porous pyroclastic deposits may take this function instead.

The mercury (Hg) content in the analysed springs was low, while the lead (Pb) amounts found were relatively high. Since no anthropogenic source of pollution has been reported, lead might be of natural origin.

Acknowledgments

This work was conducted as part of a multidisciplinary research program funded by the Swedish International Development Agency (Sida/SAREC). Technical and logistical support was provided by the Department of Engineering Geology at Lund University (Sweden) and Centro de Investigaciones Geocientíficas at UNAN-Managua, respectively. Prof. Leif Bjelm offered valuable guidance and comments. M. Aronsson and C. Wallner devoted time and effort to collect field data for water analyses. Family Duarte is specially acknowledged as their assistance made fieldwork less difficult under the tropical conditions at Río Sucio.

References

Abdul Nassir SS, Loke MH, Lee CY, Nawawi MNM (2000) Salt-water intrusion mapping by geoelectrical imaging surveys. Geophysical Prospecting 47:647-661

André L, Rosén K, Torstendahl J (1997) Minor field study of mercury and lead pollution from gold refining in central Nicaragua. MSc thesis ISBN 1402-1617 Luleå University of Technology, Sweden, 154p

Aronsson M, Wallner C (2002) Inventory of springs and hydrochemical investigations of groundwater in the drainage basin of Sucio river, Nicaragua. MSc thesis Lund University, Sweden, 105p

Barker RD (1996) The application of electrical tomography in groundwater contamination studies. 58th EAGE conference, Amsterdam, The Netherlands, Extended Abstracts, p82

Carranza, G (1991) Lithostratigraphy, tectonics and geochemistry of the Buena Vista-La Libertad area. Lic Thesis no 1991:07L Luleå University, Sweden, 99p.

Dahlin T (1996) 2D resistivity surveying for environmental and engineering applications. First Break 14:275-283

Darce M (1987) Geology of La Libertad mining district and its surroundings, Nicaragua. SGAB/INMINE / SAREC Report URAP 87002, 12p

Darce M (1990) Mineralogic alteration patterns in volcanic rocks of the La Libertad gold mining district and its surroundings, Nicaragua. Economic Geology 85:1059-1071

Ehrenborg (1996) A new stratigraphy for the Tertiary volcanic rocks of Nicaraguan Highlands. Geological Society of America Bulletin 108:830-842

Feust A (1912) Gold mines of Chontales, Nicaragua. Mining and Scientific Press, Dewey and Co., San Francisco, USA., 12p

Hodgson G (1972) Mapa Geológico de la hoja topográfica La Libertad. [Geological map of La Libertad sheet] Catastro e Inventario de Recursos Naturales. Managua, Nicaragua [in Spanish]

Kayabali K, Yüksel F, Yeken T (1998) Integrated use of hydrochemistry and resistivity in groundwater contamination caused by a recently closed solid waste site. Environmental Geology 36:227-234

Lacerda, LD (2003) Updating global Hg emisions from small-scale gold mining and assessing its environmental impacts. Environmental Geology 43:308-314

Loke MH (1999) Rapid 2D resistivity inversion using the least squares method, Manual for RES2DINV, Geolectrical Imaging 2D and 3D, 43 p

Loke MH, Acworth I, Dahlin T (2003) A comparison of smooth and blocky inversion methods in 2-D electrical imaging surveys. Exploration Geophysics 34:183-187.

Mendoza JA (2002) Geophysical and hydrogeological investigations in the Río Sucio watershed, Nicaragua. Lic Thesis ISBN 91-972406-0-X, Lund University, Sweden, 60p

Nriagu JO (1996) A history of global heavy metal pollution. Science 272:223-224

Pirrone N, Allegrini I, Keeler GJ, Nriagu JO, Rossman R, Robbins JA (1998) Hystorical atmosferic mercury emissions and depositions in North America compared to mercury accumulations in sedimentary records. Atmosferic Environment 32:929-940

Romero F (1996) Contaminación de Hg y Pb en fuentes de agua. area de Santo Domingo, Chontales [Hg and Pb contamination in water wells], Centro de Investigaciones Geo-científicas, Managua. [in Spanish], 21p

Silva G (1994) Diagnóstico da contaminação ambiental gerada pela actividade minerária sobre los ríos Súcio, Mico e Sinecapa, Nicaragua [Diagnose on the contamination caused by the mining activity in the rivers Sucio, Mico and Sinecapa]. Universidade Federal do Pará Centro de Geociências curso de postgraduação, Belem [in Portuguese]

World Health Organization WHO (1996) Guidelines for drinking-water quality, 2 nd ed. Vol.2 Geneva, 940-949.

II

Mendoza JA, Dahlin T. Resistiviy imaging in steep and weathered terrains. Journal of Applied Geophysics, submitted

Resistivity Imaging in Steep and Weathered Terrains

J.A. Mendoza[a,b,*], T. Dahlin[b]

[a]*Centro de Investigaciones Geocientíficas, Universidad Nacional Autónoma de Nicaragua Apartado Postal A-131 Managua, Nicaragua*
[b]*Engineering Geology, Lund University, Box 118, S-221 00 Lund, Sweden*

Abstract

In areas where tectonics and weathering have hydrogeological significance electrical methods can assist in mapping the subsurface. In this work, resistivity imaging was used to map fractures, faults and quartz veins emplaced in strongly weathered volcanic rocks. The aim was to map geological units related to formation of groundwater systems in the Río Artiguas basin, Nicaragua. Eight 2D resistivity surveys selected from two sites with characteristic geological features are discussed in this article. The resistivity lines were carried out with a multi-electrode system together with different electrode geometries. The data inversion was done by applying the robust (L_1-norm) method and a finite element grid to accommodate the steep topography. The data interpretation included numerical modelling to assess the suitability of all used electrode arrays in relation to the expected geological settings.
The results indicated a top high resistive layer consisting of colluviums with laterite (>50 Ω m), underlaid by conductive clay weathered layers (10 -50 Ω m). Below the conductive layer less weathered or fresh rock can be found with higher values (50 – 600 Ω m). The quartz veins and dykes stand out as the highest resistive bodies (100 - 4000 Ω m). The results indicated an overall weathering thickness of 10 -70 m or more. In conclusion, the extensive resistivity imaging surveys allowed delineation of geological structures and weathering layers throughout the study area. Furthermore, the vertical extension of weathering was examined at all locations. A finite element grid in the inversion prevented distortions arising from topography regardless of the steep slope observed at the survey locations. The numerical modelling results supported the field data interpretation.

Keywords: Resistivity imaging; dykes; faults; weathering; topography; Nicaragua

Introduction

Resistivity imaging is an effective method for hydrogeological investigations. When applying this method, the target is not groundwater itself but geological materials and structures that can store and transmit groundwater. The reliability of the method has increased since the 1990's due to developments in data acquisition techniques

* Corresponding author. Fax +(46) 46 222 9127
E-mail address: alfredo.mendoza@tg.lth.se

(Dahlin, 2001; Pellerin, 2002), interpretation techniques (Loke and Barker, 1996) and computer technology. As a result, mapping of complex and small-scale geological features has become more precise and efficient (Kemna et al., 2000; Sandberg et al., 2002).

In areas where tectonics and weathering have hydrogeological significance electrical methods can assist in mapping the subsurface. Resistivity soundings and profiling surveys over conductive and resistive intrusive bodies have been reported in several studies (Apparao and Roy, 1973; Verma and Bandyopadhyay, 1983; Batayneh, 2001). Furthermore, automated resistivity surveying have been carried out over dykes and fractures (Dahlin, 1996; Seaton and Burbey, 2002). Electrical methods can also be used to map weathering areas as distinctive contrast should be observed when fresh rock is reached. The weathering response to electrical methods has been examined in previous research (Palacky and Kadekaru, 1979; Doyle and Lindeman, 1985; Timms and Acworth, 2002; Kellett and Bauman, 2004), including the relationship between silica content in weathered rocks and high resistivity responses (Barongo and Palacky, 1991). As there is lateral resistivity heterogeneity commonly associated to weathering layers the use of 2D resistivity imaging has been suggested (Ritz et al., 1999).

For 2D resistivity imaging diverse data collection geometries can be formulated, depending on the aims of investigation, the target's expected dimensions and shape, and logistics constrains. The most used arrays include Wenner, Schlumberger, pole-pole, dipole-dipole and traditional gradient. The applicability of the latter array to different geological structures has been evaluated in earlier studies (Schulz, 1985; Shettigara and Adams, 1989; Furness, 1993). Recently, Dahlin and Zhou (2004) have shown the suitability of the multiple gradient array for multielectrode surveys.

However, in mountainous regions the lateral surface irregularities and high slopes can affect geoelectric surveys regardless the used array. The changes in topography cause distortions of the measured potential field that lead to terrain anomalies (Pous et al., 1996; Tsourlos et al., 1999). These topography effects can be accounted for by integrating altitude data in a finite element grid to be used for the inversion.

The objective of this research was to map geological materials and structures related to formation of groundwater systems in the steep-topography basin of Río Artiguas, in central Nicaragua. Resistivity imaging was used to map fractures, faults and quartz veins emplaced in strongly weathered volcanic rocks.
In total, forty-four (44) 2D resistivity surveys were performed at hydrogeologically relevant locations of the Rio Artiguas (Sucio) basin (Fig. 1). Eight (8) resistivity lines are presented here as they represent typical responses from the geological materials and structures in the area.

For reinforcing the field data interpretation the used electrode arrays were tested against synthetic models of geological units expected to occur in the area. However, carrying out a comprehensive comparison between electrode arrays was not the purpose of this work.

The investigations were carried out within the framework of a multi disciplinary research and training programme, funded by the Swedish International Development Authority (Sida/SAREC), with the aim of mapping groundwater systems in an area contaminated by mining activities.

Hydrogeological setting -area description

Rio Artiguas basin is located eastwards of the central highlands of Nicaragua. This basin has experienced a century of gold mining using the mercury method. A weather station located in the basin reports temperatures between 17°C and 28°C. Historic average precipitations of ca. 2400 mm/yr have been recorded in the area. The young drainage system for surface waters has developed under a structural control where faults, fractures and joints lead to a rectangular flow pattern. The topography is rough with steep hills and valleys: The slopes are more than 10% and up to 45%.

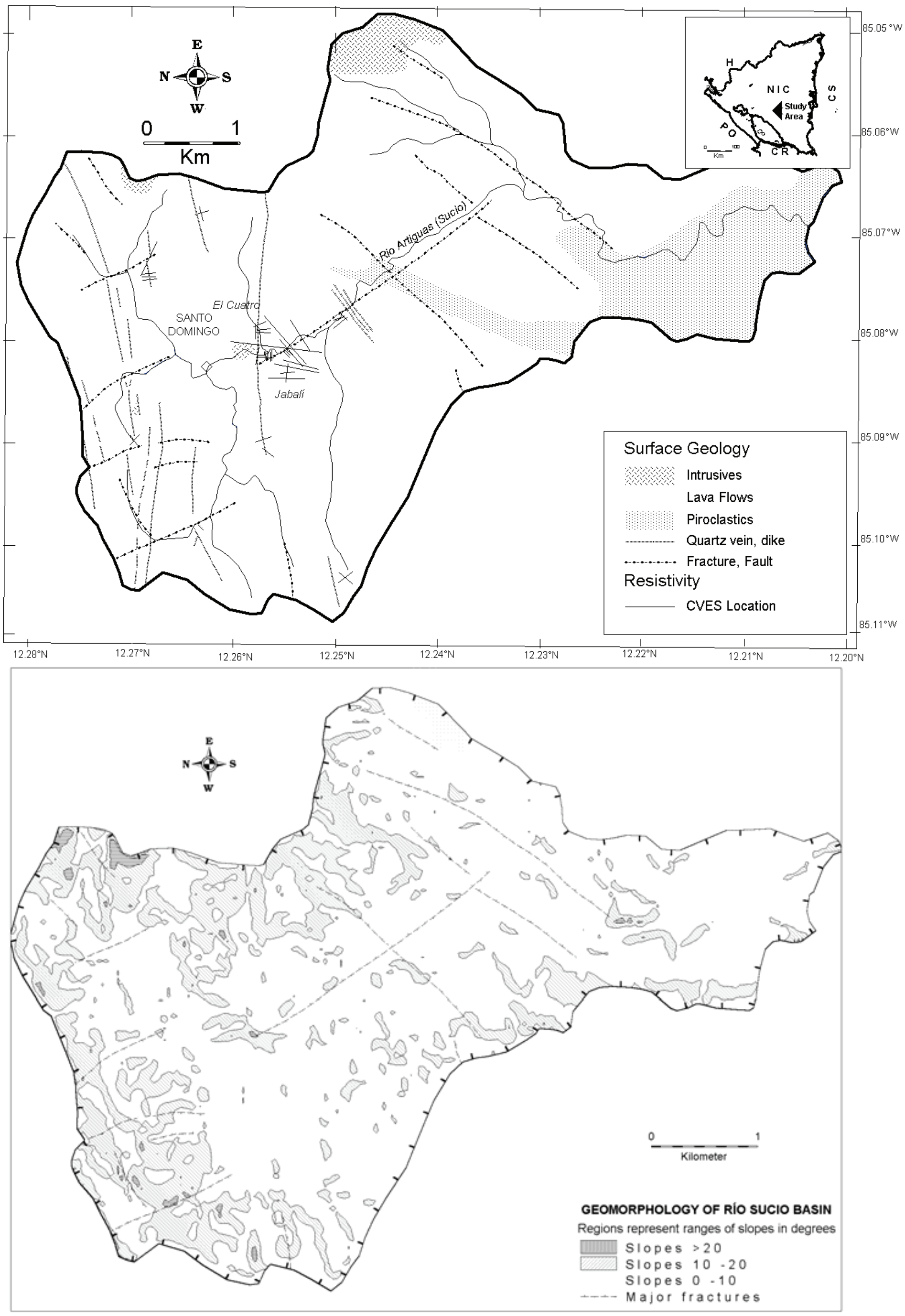

Fig. 1. Top panel, the study area and its surface geology. Bottom panel, the geomorphology indicating the terrain roughness. Inserted location map in Nicaragua. NIC:Nicaragua, H:Honduras, CR:Costa Rica, PO: Pacific Ocean, CS: Caribbean Sea.

Geologically, most of Río Sucio basin is covered by Tertiary volcanic rocks, mainly basalts and andesites lava flows. These lava flows are overlying older rhyolitic-dacitic pyroclastic flows towards the south of the area. There is gold bearing quartz veins embedded in these basalts and andesites lava flows, surrounded by hydrothermal alteration aureoles. More acid rock types are found as plugs intruding the basalts and andesites flows (Hodgson, 1972; Darce, 1990; Ehrenborg, 1996).

The tectonic development and thereby associated fracturing, hydrothermal processes and secondary alteration of veins control groundwater infiltration, occurrence and flow in the area (Mendoza et al., 2005). Complementarily, the weathering processes facilitate infiltration and water transport in the uppermost surface cover (Fig. 2). As regards the hundreds-of-meters thick lava flow covering the area, no major aquifers are expected to occur, but shallow and locally delimitated aquifers in valleys and other depressions (Mendoza, 2002).

a) 

b) 

Fig. 2. a) Coarse grained material above clay at a mining gallery entrance; b) fractured lava flow.

Synthetic modelling

Synthetic models

Numerical modelling was employed to assess the suitability of selected electrode arrays in relation to the expected geological settings. The arrays used were Wenner (electrode spacings a=2 – 48), dipole-dipole (a=2 – 12, n=1 – 6), pole-dipole (a=2 – 20, n=1 – 5) and multiple gradient (a=1 – 8, n=-4 – 4 and s=8). S is the maximum number of potential readings for a current injection as described in Dahlin and Zhou (2006). Two models consisting of 81 electrodes with 1 m electrode spacing were tested. They simulated a) a dyke embedded in low resistive clay and b) a vertical fault displacing low-resistive blocks. The resistivities used for the different geological materials were based on resistivity imaging results over outcropping features in the field, plus direct measurements on the different geological materials in for example cuts and mine shafts using a miniature Wenner array (Mendoza et al., 2005). Fig. 3a shows the model of a 10-m thick dyke emplaced in a top resistive layer (400 Ω m) which overlies a 20 Ω m layer of clay. The dyke is surrounded by zones with hydrothermal alteration (500 Ω m). Fig. 3f shows displaced blocks (20 Ω m) simulating vertical faulting. The low resistive blocks are overlaid by a resistive coarse grained material layer (400 Ω m). In both models, the deeper less weathered rock layer is modelled with a 100 Ω m layer. The apparent resistivities of the models were calculated using electrode configurations identical to those used in field. Moreover, field topography was incorporated into the models before calculation of the apparent resistivity values. The maximum slope along the vein model was 30°, and the maximum slope along the fault model was 17°. Alternatively, in order to illustrate the effects of omitting the topography the apparent resistivities were inverted without including the altitude of the electrodes. The forward response data was computed using the forward modelling program Res2Dmod (Loke and Baker, 1996), and the inversion was performed using the Res2Dinv algorithm (Loke, 1997). The interpretation of the 2D resistivity data was performed by using the robust (L_1-norm) inversion method, which minimizes the absolute differences between measured and calculated apparent resistivity values (Loke et al., 2003). This is an appropriate method for interpreting data from areas were subsurface regions separated by sharp boundaries are expected. Furthermore, a finite element grid was used in the data inversion as including the topography was necessary for precise relation of the object's position in space along the survey lines. After processing the data, the final results were prepared for presentation by setting a resistivity scale that suits the expected geological features for each site investigated.

Modelling results

The four arrays used in the numerical modelling delineated the resistive dyke. The inversion results are shown in Fig. 3. The transition from the high resistive vein (800 Ω m) and its hydrothermal zones (500 Ω m) to the low resistive mid layer (20 Ω m) was sharper with gradient and more gradual with dipole-dipole. However, the actual borders of the quartz dyke cannot be determined from the inversion models. The bottom layer was most clearly detected with the pole-dipole geometry (Fig. 3e).

For the fault modelling the results indicated the lateral changes in resistivities in all cases (see Fig 3g-j). The assigned depth to the uppermost layers was similar in all configurations. The dipole-dipole geometry distinguished the bottom left resistive layer from the right upper resistive layer most clearly.

Fig. 4 shows an example of resistivity inversion without considering the topography. In this case, pole-dipole was more affected by the terrain changes, particularly in the quartz vein case were the maximum observed slope was 30°. For the other arrays Wenner and gradient were less affected, followed by dipole dipole.

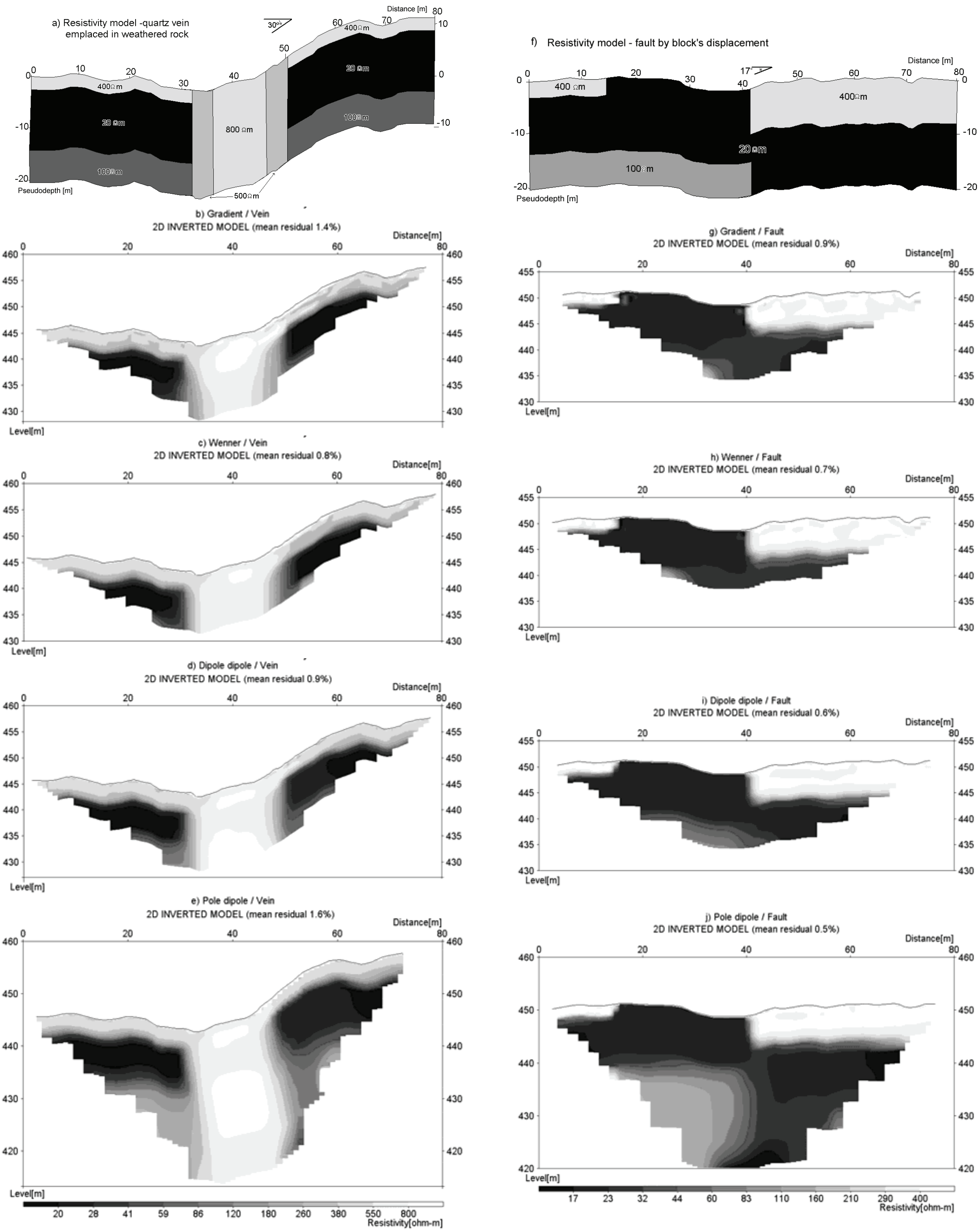

Fig. 3. Numerical modelling inversion results with gradient, Wenner, dipole-dipole and pole dipole arrays. Left column, a quartz vein case; right column a fault case.

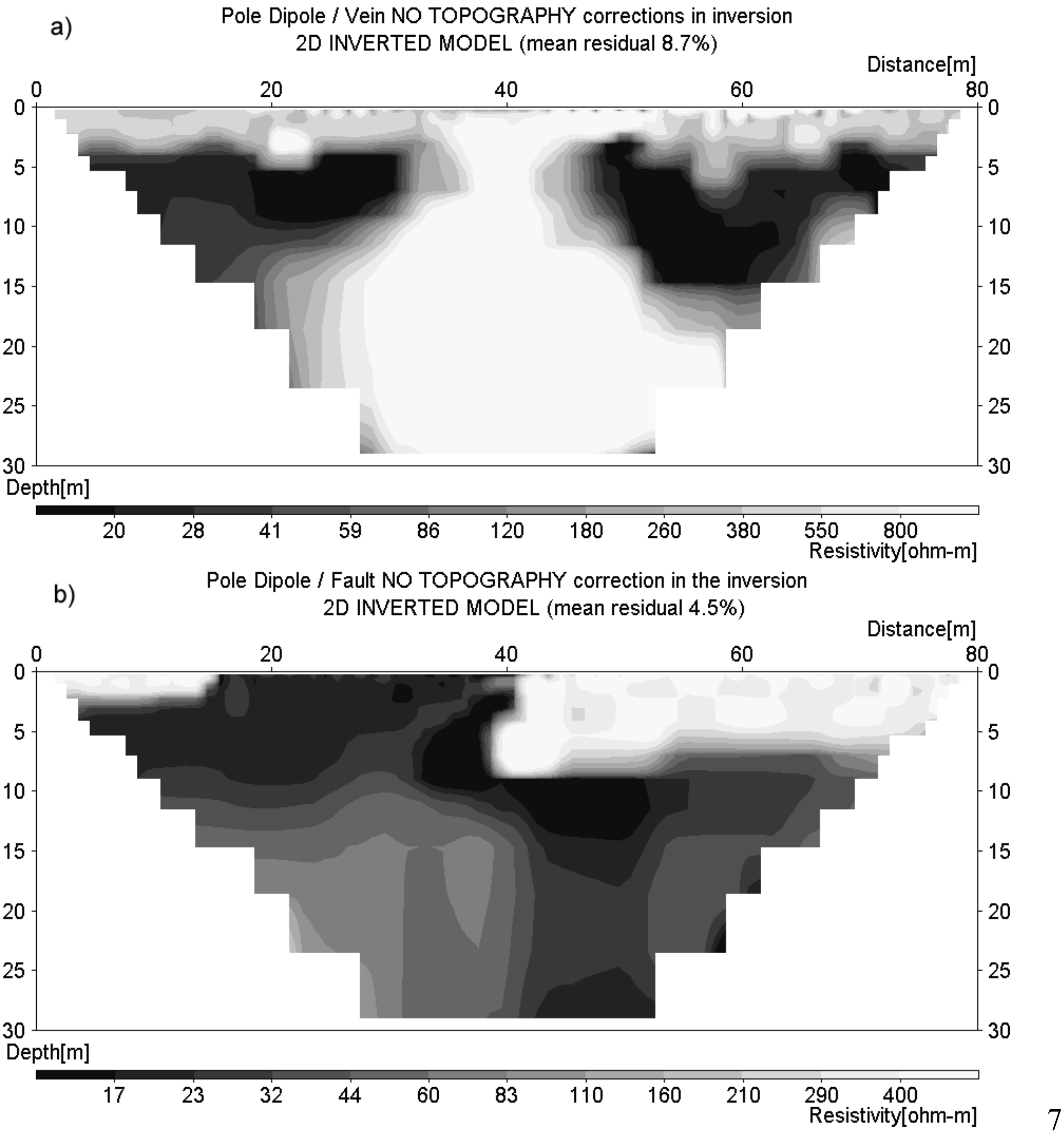

Fig. 4. Numerical modelling inversion *without topography* using pole dipole array for a) the quartz vein case and b) the fault case.

Field data and interpretation

Field procedure

In field, the ABEM Lund Imaging System (Dahlin, 1996) was used with different layouts. The system is based on the automation of the collection, processing and presentation of resistivity data. The data collection was performed by using a roll along technique where cables are moved upward or downward along a succession of stations. Additionally, GPS receivers and surveying instrumentation were used for precise positioning of the profiles and electrodes.

The main geological targets under investigation were those associated with groundwater occurrence in the area. Rock types, fractures, streams or springs in the surroundings were important aspects taken into consideration in selecting the locations for the resistivity lines. It was also important to gather information on the geology in situ, which was made by documenting the ground lithology and observations in shafts, when it was possible. Wenner, dipole-dipole, pole-dipole and gradient electrode arrays were used. As it was important to get information about the resistivity distribution in the near sub surface, the selected electrode spacing was mostly 1 m, 2 m and 5 m, depending on the target being investigated. Vegetation and anthropogenic activities had to be taken into account to decide where to put the lines. The inversion of the resistivity data was performed in the same way as with the synthetic modelling.

Quartz veins

The first case here presented corresponds to a quartz vein area located in the north eastern part of the Rio Artiguas basin, known as El Cuatro. A stream runs parallel to the quartz vein area, which stands up as a positive topographic feature stretched from east to west. Before reaching Rio Sucio the stream crosses the main quartz vein twice revealing an offset in the vein. Some parts of the vein have been explored and exploited, leaving trenches and shafts that were used for geological documentation in this work (Fig. 5). The vein is 1600 m long, has a maximum thickness of 10 m and at least 20 m depth. The site has a steep slope of approximately 30 degrees forming a valley along the stream.

Approximately 30 -50 m west from Line 1 the stream shifts its course to the southern side of the quartz vein. There, lines 2w, 2d, and 2p were located. Laterite soils with colluviums were covering the site along the line, underlayered by clay weathered material. The inversion results for the three arrays used at this location show the high resistivity values at 120 m (>130 Ω m), where the quartz vein position was reported by geological observations (Fig. 6b-d). A non-documented quartz deposit was detected at 120 m on the line and appears to be a short branch of the main body. Quartz was found on the surface during the measurements at this point. The dipole-dipole inversion result shows higher resistivity values in zones with quartz rich boulders accumulated by miners on small caves, i.e. at 80 m. Conversely, the model residuals value was relatively high (11.1%). The inversion result from pole-dipole supports the geological observations that the vertical vein extends deeper (>20 m) than observed with the other arrays. This is due to the measuring parameters used for pole-dipole which allowed for mapping deeper zones as the numerical modelling predicted.

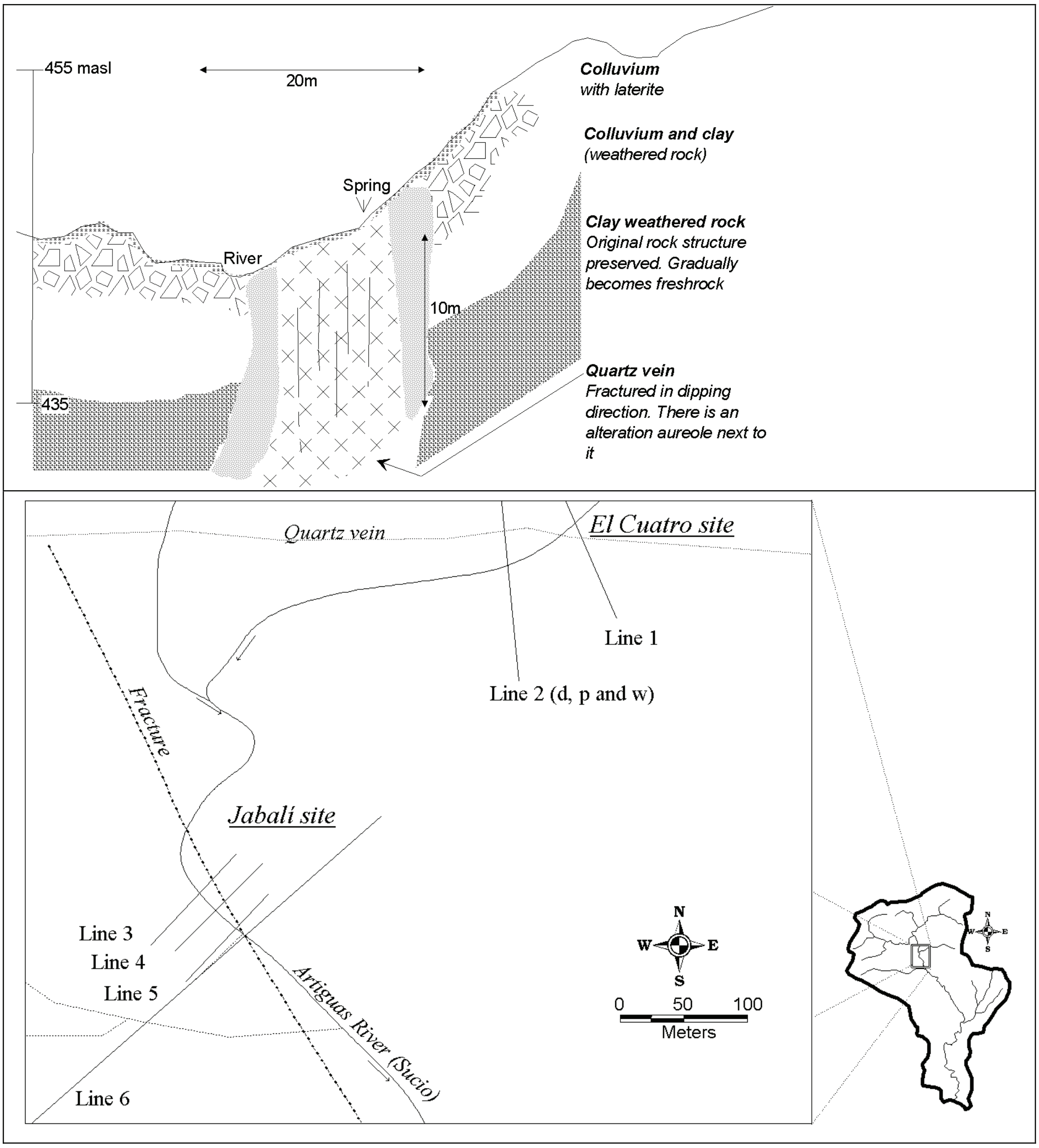

Fig. 5. Top panel, geological situation at location of resistivity Line 1. Bottom panel, map with locations of the resistivity lines presented here.

Fractures

Four resistivity lines were placed perpendicularly to Río Artiguas at El Jabalí site (see Fig. 4). In this case the aim was to investigate the presence of fracturing below the river and understand the subsurface conditions near the river. Gradient array was used for Lines 3 - 5 with 1 m electrode spacing and 100 m length. These lines were set parallel at 10 m distance from each other. For Line 6, the Wenner array was used with 5 m electrode spacing and 400 m total length.

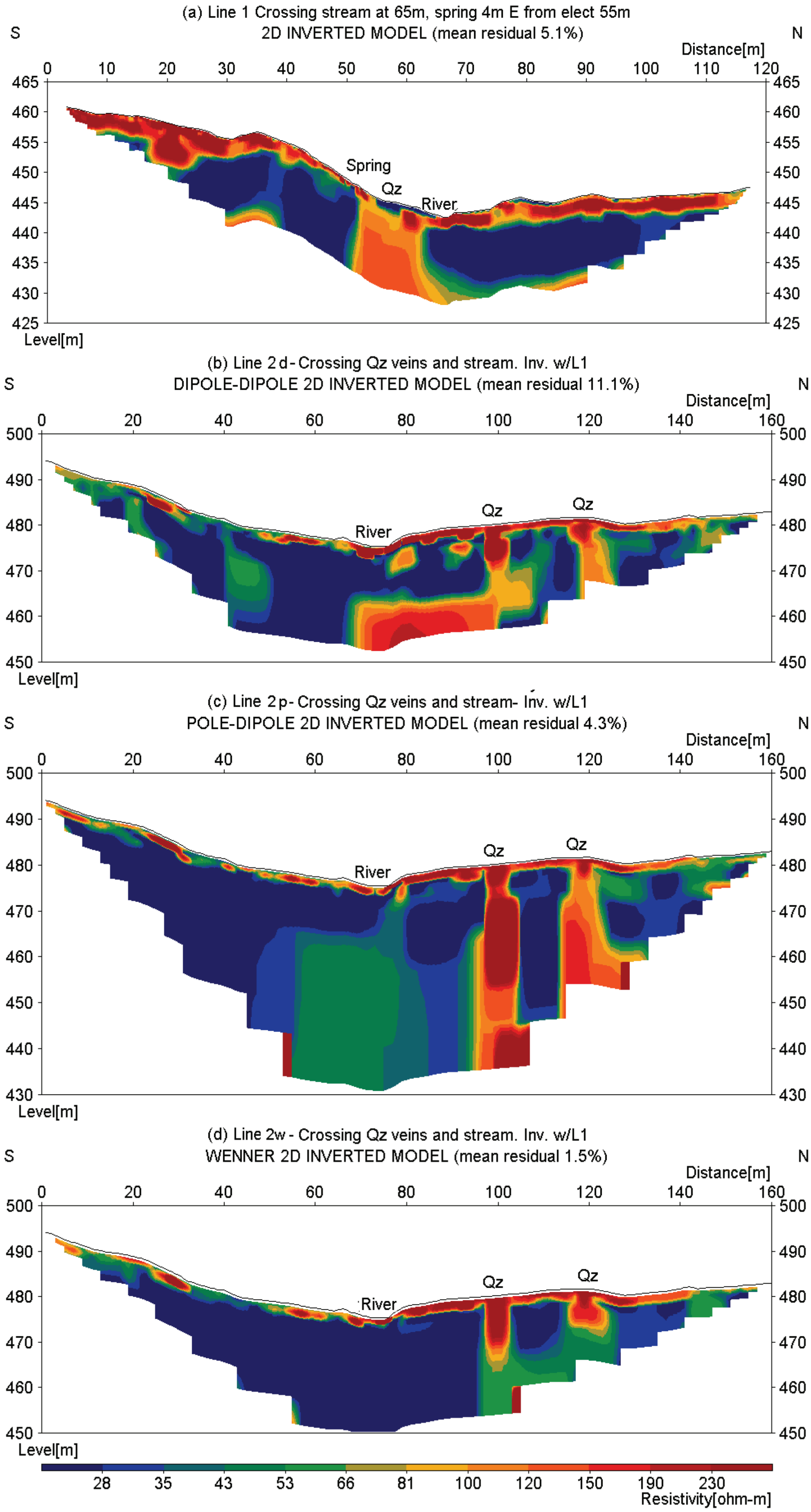

Fig. 6. Resistivity inversion results for surveys at El Cuatro site. On top Line 1, below Lines 2d, 2p and 2w, performed at the same location with three different arrays. Qz = Quartz vein.

The inversion results for Lines 3-6 are presented in Fig. 7. The inversion models indicate the presence of a 3 m -7 m thick high resistive layer on top. Below that layer the resistivity decreases in a 10 m thick layer and increases again after 15 m depth. The clay content in a swamp located next to the river has a clear effect on decreasing the resistivity as shown at 10 m on Line 5 and at 110m on Line 6. The deep high resistive zones cover the entire section after the lines cross the river, where the resistivity increased up to more than 700 Ω m. This strong lateral variation can clearly be seen below the river in the inversion model for Line 6. Further, the conductive layer is associated to clay, while less weathered or fresh rock is related to the deeper high resistive layer.

Discussion and conclusions

The inversion results after the numerical modelling reflected in general the expected features. There were mainly differences in depth of penetration and thicknesses assigned to the different features. The inversion results did not indicate major geometric disturbances in layers or structures due to topography effects when the observed electrodes altitude was taken in consideration during inversion. The numerical modelling of the resistive dyke and the vertical fault predicted that ignoring the topography in the inversion would lead to distortions of the modelled geometry of the subsurface (see Fig. 4).

Regarding the field investigations, Line 1 is a significant example of resistivity imaging effectiveness for mapping vertical structures like the quartz vein (see Fig. 6). Generally there was a high resistive layer on top consisting of colluviums with laterite (>50 Ω m), followed by conductive clay weathered layers (10 -50 Ω m). Below the conductive layer less weathered or fresh rock can be found with higher values (50 – 600 Ω m). The quartz veins and dykes stand as the highest resistive bodies (100 -4000 Ω m). The increasing thickness assigned to the veins at the middle deepest zones in the dipole-dipole and pole-dipole results at El Cuatro site may be an effect of the inversion method. This affirmation is supported by the respective numerical modelling results and the fact that dykes are often thinner downwards in the area. However, compared to Wenner and dipole-dipole, pole-dipole delineated the depth of the vein more in conformity to the numerical modelling results and the observed geology of the site (see Fig. 3 and Fig. 5).

Geomorphology and the aerial photographs interpretation indicate the presence of a fracture zone along the river course at El Jabalí site (see Fig. 5). The tectonic feature has been associated with a Tertiary volcanic caldera (Hodgson, 1972). The inversion results from this site indicated vertical fracturing below the river bed from Lines 3 to 6 (see Fig. 7). The fracture zone was more evident at Line 6 due to higher depth penetration. In lines 3 to 5 the lateral changes in resistivity can be indications of change in the nature of the material or its degree of weathering. These lines also suggest that the fracturing extends along the river at this site.

From these results it can be interpreted that the overall weathering thickness in the area varies from 10 -70 m, or more. The depth to fresh rock varies over short distances as result of the irregular geomorphology. These weathering layers consist of heterogeneous material ranging from leached and coarse grained to clay weathered rock. Since both leached weathered material and fresh rock are high resistive, it was

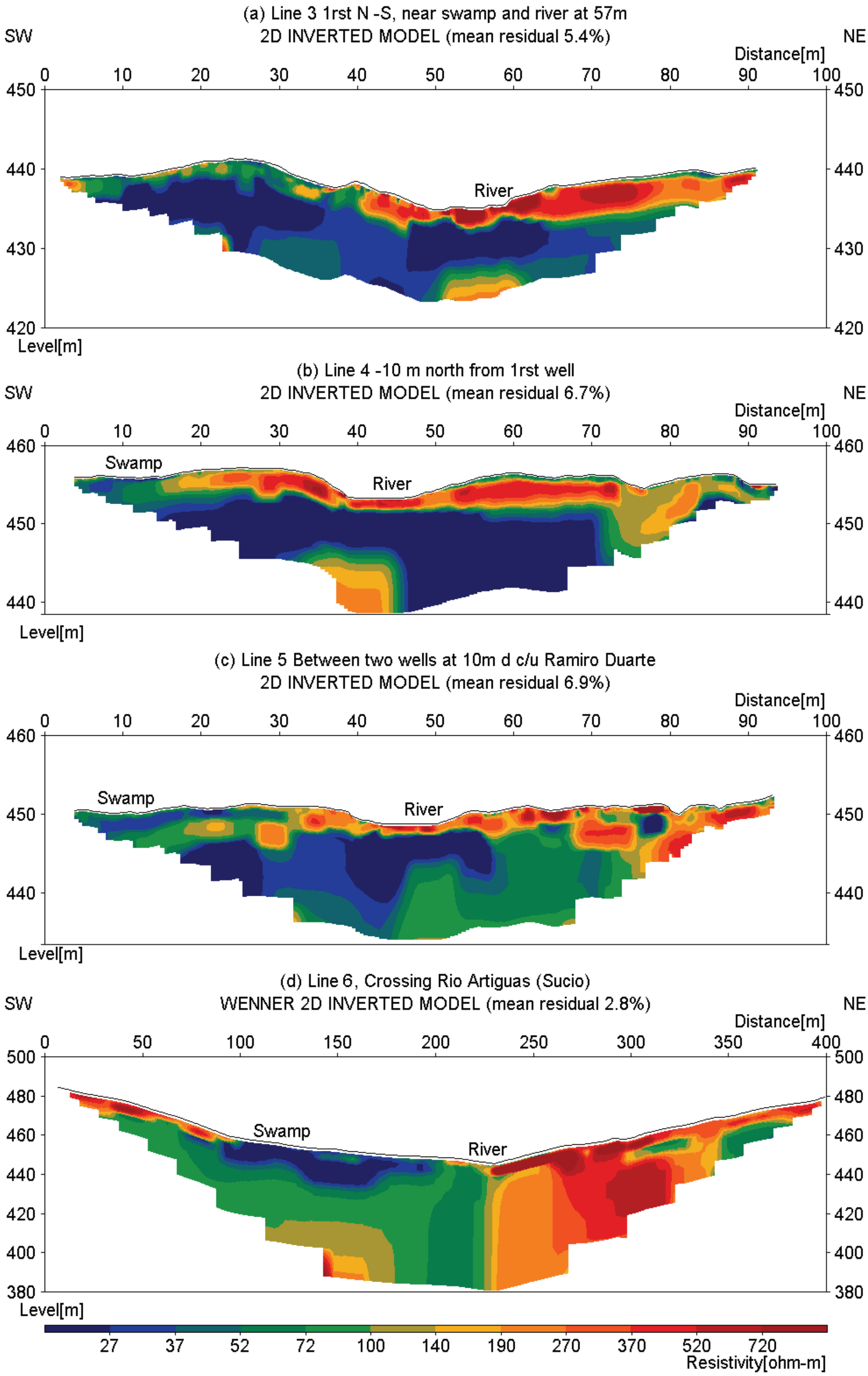

Fig. 7. From top, resistivity lines 3, 4 and 5 with gradient array and 100m length. Bottom panel, Line 6, using Wenner array and 400 m length.

important to document the sites properly. The young dykes, veins and other intrusive bodies have been less exposed to the strong tropical weathering process and therefore electrically contrasting from surrounding rocks as highly resistive. Resistivity contrasts can be particularly marked at the base of weathering, where the transition between deeply weathered materials to fresh rock can occur within a few metres in the inverted models.

Using the resistivity method made it possible to map weathered and hard rock areas as well as vertical structures in the Río Artiguas basin. Fractures, faults and quartz veins crossing the strongly weathered Tertiary volcanics were delineated. Moreover, the vertical extension of weathering was examined at all locations. Using the finite element grid in the inversion prevented distortions arising from topography regardless of the steep slope observed along the lines as shown by the numerical modelling. The examples from the study sites discussed in this paper illustrated the complex geology of the entire basin. Regarding their hydrogeological importance, the mapped materials can only form and host small local aquifers. Resistivity imaging can be used for mapping the subsurface in other areas with similar geological conditions. The numerical modelling results supported the field data interpretation.

Acknowledgements

This work was conducted as part of a multidisciplinary research program funded by the Swedish International Development Agency (Sida/SAREC). Support was provided by the staff at Engineering Geology, Lund University (Sweden) and Centro de Investigaciones Geocientíficas at UNAN-Managua. In particular, Dr. Gerhard Barmen provided valuable ideas to improve the manuscript. Peter Jonsson, Julio Guevara and Roger Wisén assisted along different stages of this work. Families Lazo, Duarte and other local farmers allowed to carry out the surveys despite of their hesitation towards 'mining-like' activities.

References

Apparao, A., Roy, A., 1973. Field results for direct current resistivity profiling with two-electrode array. Geoexploration 11, 21–44.

Batayneh, A.T., 2001. Resistivity imaging for near-surface resistive dyke using two-dimensional DC resistivity techniques. Journal of Applied Geophysics 48, 25-32.

Barongo, J.O., Palacky, G.J., 1991. Investigations of electrical properties of weathered layers in the Yala Area, Western Kenya, using resistivity soundings. Geophysics 56 (1), 133-138.

Dahlin, T., 1996. 2D resistivity surveying for environmental and engineering applications. First Break 14, 275-283.

Dahlin, T., 2001. The development of electrical imaging techniques. Computers and Geosciences 27(9), 1019-1029.

Dahlin, T., Zhou, B., 2004. A numerical comparison of 2D resistivity imaging with 10 electrode arrays. Geophysical Prospecting 52, 379-398.

Dahlin, T., Zhou, B., 2006. Multiple gradient array measurements for multi-channel 2D resistivity imaging. Near Surface Geophysics *In Press*.

Doyle, H. A., Lindeman, F.W., 1985. The effect of deep weathering on geophysical exploration in Australia - a review. Australian Journal of Earth Sciences 32(2), 125-135.

Darce, M., 1990. Mineralogic alteration patterns in volcanic rocks of the La Libertad gold mining district and its surroundings, Nicaragua. Economic Geology 85, 1059-1071.

Ehrenborg, J., 1996. A new stratigraphy for the Tertiary volcanic rocks of Nicaraguan Highlands. Geological Society of America Bulletin 108, 830-842.

Furness, P., 1993. Gradient array profiles over thin resistive veins. Geophysical Prospecting 41 (1), 113-130.

Hodgson, G., 1972. Geological map of La Libertad. Catastro e Inventario de Recursos Naturales. Managua, Nicaragua (in Spanish).

Kemna, A., Binley, A., Ramirez, A., Daily, W., 2000. Complex resistivity tomography for environmental applications. Chemical Engineering Journal 77, 11–18.

Kellett, R., Bauman, P., 2004. Mapping groundwater in regolith and fractured bedrock using ground geophysics: A case study from Malawi, SE Africa. Recorder 29 (2), 24-32.

Loke, M.H., 1997. Rapid 2D resistivity inversion using the least squares method, Manual for RES2DINV, Geolectrical Imaging 2D and 3D, 43 p.

Loke, M.H., Acworth, I., Dahlin, T., 2003. A comparison of smooth and blocky inversion methods in 2D electrical imaging surveys. Exploration Geophysics 34, 182-187.

Loke, M.H., Barker, R. D., 1996. Rapid least-squares inversion of apparent resistivity pseudosections by a quasi-Newton method. Geophysical Prospecting 44 (1) 131-152.

Mendoza, J.A., Dahlin T., Barmen, G., 2005. Hydrogeological and hydrochemical features of an area polluted by heavy metals in central Nicaragua. Hydrogeology Journal, Accepted for publication.

Mendoza, J.A., 2002. Geophysical and hydrogeological investigations in the Rio Sucio watershed, Nicaragua. Lic Thesis ISBN 91-972406-0-X, Lund University, Sweden, 60p.

Palacky, G. J., Kadekaru, K., 1979. Effect of tropical weathering on electrical and electromagnetic measurements. Geophysics 44 (1), 69-88.

Pellerin, L., 2002. Applications of electrical and electromagnetic methods for environmental and geotechnical investigations. Surveys in Geophysics 23, 101-132.

Pous, J., Queralt, P., Chavez, R., 1996. Lateral and topographical effects in geoelectric soundings. Journal of Applied Geophysics 35, 237-248.

Ritz, M., Parisot., J.C., Diouf, S., Beauvais, A., Dione, F., Niang, M., 1999. Electrical imaging of lateritic weathering mantles over granitic and metamorphic basement of eastern Senegal, West Africa. Journal of Applied Geophysics 41, 335–344.

Schulz, R., 1985. Interpretation and Depth of Investigation of Gradient Measurements in Direct Current Geoelectrics. Geophysical Prospecting 33 (8), 1240-1253.

Sandberg, S.K., Slater, L.D., Versteeg, R., 2002. An integrated geophysical investigation of the hydrogeology of an anisotropic unconfined aquifer. Journal of Hydrology 267, 227-243.

Seaton, W.J., Burbey, T.J., 2002. Evaluation of two-dimensional resistivity methods in a fractured crystalline-rock terrain. Journal of Applied Geophysics 51, 21–41.

Shettigara, V.K., Adams, W.M., 1989. Detection of lateral variations in geological structures using electrical-resistivity gradient profiling. Geophysical Prospecting 37 (3), 293-310.

Timms, W., Acworth, I., 2002. Origin, lithology and weathering characteristics of Upper Tertiary – Quaternary clay aquitard units on the Lower Murrumbidgee alluvial fan. Australian Journal of Earth Sciences 49, 525–537.

Tsourlos, P., Szymansky, J., Tsokas, G., 1999. The effect of terrain topography on commonly used resistivity arrays. Geophysics 64 (5), 1357–1363.

Verma, R., Bandyopadhyay, T., 1983. Use of the resistivity methods in geological mapping-case histories from Raniganj Coalfield, India. Geophysical Prospecting 31, 490–507.

III

Mendoza JA, Ulriksen P, Picado F, Dahlin T. Aquifer interaction with a polluted mountain river of Nicaragua. Hydrological Processes, submitted

Aquifer interactions with a polluted mountain river of Nicaragua

José A. Mendoza [1], Peter Ulriksen[2], Francisco Picado[3], Torleif Dahlin[2]

[1] Centro de Investigaciones Geocientíficas, Universidad Nacional Autónoma de Nicaragua (CIGEO, UNAN-Managua), Col. Miguel Bonilla #165 Apartado Postal A-131 Managua, Nicaragua, e-mail: alfredo.mendoza@tg.lth.se, telefax +(505) 277 0613

[2] Department of Engineering Geology, Lund University Box 118, S-221 00 Lund, Sweden

[3] Centro de Investigaciones en Recursos Acuáticos, Universidad Nacional Autónoma de Nicaragua (UNAN-Managua) Apartado Postal 4598, Managua Nicaragua.

Abstract

The interactions between a stream and nearby shallow aquifers were investigated in a mountain basin being polluted by mercury released during mining in central Nicaragua. Hourly data series of water levels and temperatures were analysed for cross correlation. Resistivity imaging was used to map the subsurface and to complement the hydrological data interpretation. The results show the complex hydrogeological conditions that characterise the region, with weathering and fractured rock as main contributors to groundwater transport. The resistivity images suggest the presence of two vertical dykes perpendicular to the stream and zones rich in clay. The data series indicate a rapid response from the aquifers to recharge events, followed by immediate discharge on a yearly basis. Furthermore, alternating periods of stream infiltration and aquifer discharge were identified. This work demonstrates that surface water pollution is a threat to groundwater quality in the area.

Key words: Time series analysis; resistivity imaging; cross correlation; surface water; groundwater; pollution; Nicaragua

---

Introduction

Understanding the relationship between surface waters and groundwater is an important task in hydrological sciences. Characterising this interaction becomes critical as environmental stress on surface waters increases and may be transferred to subsurface waters. Commonly, the interactions occur in the in-stream and near-stream areas where exchange of water and biological processes take place (Sophocleous, 2002). In streams there can be three modes of interactions; gaining flow sections, losing flow sections and steady pressure (Winter *et al.*, 1998). When pollutants are present they may contaminate either resource.

Mining using the mercury method to refine gold have lead to continuous contamination of streams in the central region of Nicaragua since the 19th century. The most polluted river is Río

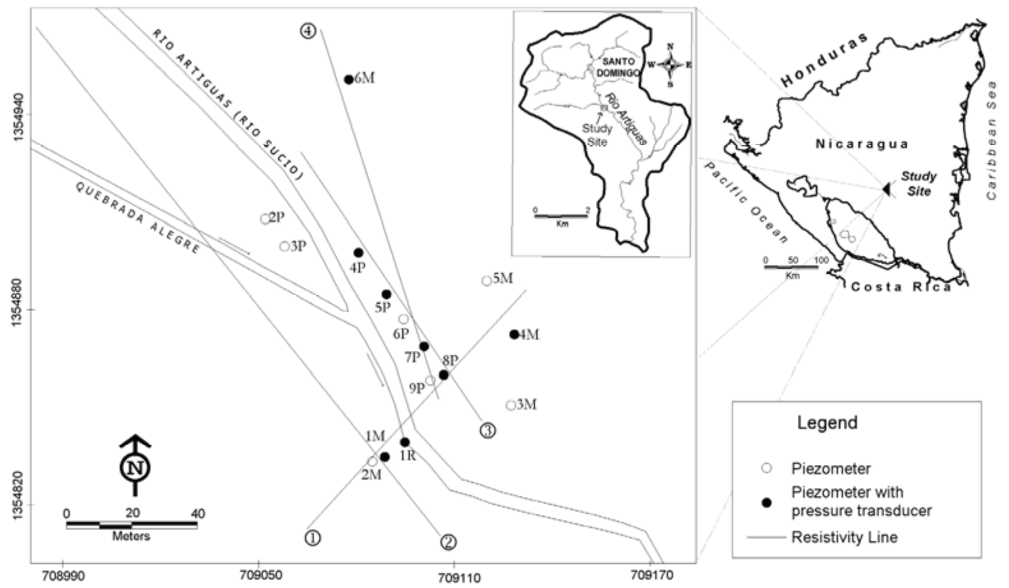

Figure 1. Location of the study site in the Río Artiguas basin (inset), central Nicaragua.

Artiguas (renamed Sucio that means dirty), where a cluster of small-scale mills release mining waste directly into the river water. Thus, the mercury concentrations in the river water are frequently above the guidelines for drinkable water (Silva, 1994; Albuquerque, 1996; Romero, 1996; André *et al.*, 1997). In addition, sewage from the near village of Santo Domingo is disposed to the river (Figure 1). To characterise the connections of the stream waters with the near channel aquifers becomes an urgent task, especially since water supply to the population is provided from sources located in the proximities of the polluted streams.

Among the methods for studying stream-aquifer connections a frequently used approach is the surface water gaining- losses method (Lerner, 1997). This method is based on the identification of gains and losses sections along the river channel by estimating the differences in stream flow budgets. Mendoza (2002) used the gaining-losses method in the Río Artiguas channel but no conclusive results where achieved due to uncertainties derived from measurements error and the rapid changes in velocities of the stream. Additional attempts using seepage meters failed due to the rocky bed of the river (Grunander and Nordenberg, 2004).

The study of time series data can reveal temporal variations and impulse response characteristics in aquifers (Duffy and Gelhar, 1986; Padilla and Pulido-Bosch, 1995). During the last two decades various studies have shown the applicability of time series analyses for understanding hydrological processes. For instance, time series analyses of piezometric data have been used to identify recharge mechanisms (Lee and Lee, 2000), forecast the water level in wells (Bierkens *et al.*, 2001), study of river base flow and estimations of groundwater recharge (Zhang and Schilling, 2004; Crosbie *et al.*, 2005). Generally, the measured parameter used for the time series analyses is hydraulic head but electric conductivity and temperatures have also been used (Laroque *et al.*, 1998; Sheets *et al.*, 2002; Kim *et al.*, 2005).

Geophysical mapping of the subsurface can provide complementary information on the subsurface geology, which can be used for interpretation of the hydrological data. Resistivity imaging is a suitable method for hydrogeological mapping as the electrical resistivity of earth materials is dependent on electrolytic conduction through the pore fluid. The multi-electrode technique permits the acquisition of large amounts of resistivity data (Dahlin, 1996) and fast inversion methods allow to interpret the subsurface resistivity distribution (deGroot-Hedlin and Constable, 1990; Ellis and Oldenburg 1994, Loke and Barker, 1996). Recently, resistivity imaging has been intensively used for hydrogeological mapping in the Río Artiguas basin (Mendoza, 2002; Mendoza *et al.*, 2005).

The objective of this study is to examine time series of hydraulic heads and water temperature data in combination with resistivity imaging to elucidate the factors controlling the shallow groundwater dynamics at the study site. Secondly, verify if the river water infiltrates the near channel aquifers carrying heavy metals to pollute the local groundwater. This information is crucial to promote groundwater protection in the central regions of Nicaragua, where the majority of the population depends on groundwater and also surface water for human consumption. This article presents an application of time series analyses and resistivity imaging to explain a relevant environmental and hydrogeological problem. The work has been developed within the framework of a broad environmental program funded by the Swedish International Development Agency (Sida/SAREC) with the aim to assess the environmental effects of mining activities in Nicaragua.

The Río Artiguas basin and the study site

The study site is located in the Río Artiguas basin, in the eastern part of the central highlands of Nicaragua. The basin has experienced a century of gold mining using the mercury method. A weather station recently installed in the basin reports temperatures with minimum of 15°C and maximum 34°C, for the period November 2004 to March 2005. Historic average precipitations of ca. 2400 mm/yr have been recorded in the area by INETER (1991). The rainy season extends for nine months from April to December having a large influence on the river flow which indicates a discharge from 2×10^4 m^3/day during the dry season to 9×10^4 m^3/day during the wet season. The young drainage system for surface waters has developed under a structural control where faults, fractures and joints lead to a geometrically rectangular flow pattern.

Geologically, most of Río Artiguas basin is covered by Tertiary volcanic rocks, mainly basalts and andesite lava flows. These lava flows are overlying rhyolitic-dacitic pyroclastic flows towards the south of the basin (Hodgson, 1972). The quartz veins and tectonic zones, in combination with fracturing and weathering, are considered the major factors contributing to groundwater occurrence and transport. Consequently, the saturated zone is a composite horizon of both weathered layers and fractured bedrock. Mendoza *et al.* (2005) suggested a hydrogeological model for the basin; water infiltrating the weathered non saturated zone travels through the saturated zone but shortly discharges in a spring or along the streams. If water infiltrates through open fractures, tectonic contacts or bed contacts, it can travel longer distances and eventually form regional groundwater flows. However, such a hydrogeological model is insufficient to explain the interactions between surface waters and groundwater and a smaller area had to be investigated in detail.

The site in the center of the basin is selected for this study because it is regarded as a typical tectonic setting with fracturing along the river (Hodgson, 1972) and a smooth valley that allowed accessibility and drilling in the otherwise rough relief of the basin. Aerial photographs indicate fracturing perpendicular to the river and field documentation verified that the fractured bedrock underlies on average 3 m thick soils. The groundwater table is usually found within 3 m and much of the shallow groundwater is expected to discharge into the river (Mendoza *et al.*, 2004). The Río Artiguas is joined by the generally clean Quebrada Alegre tributary at the site. The area is used for grazing and grass covers a wetland on the east side of the river (Figure 1).

Methodology

Fourteen (14) piezometers were installed at the site and one level gauge in the river (1R). The piezometers are cased with 6 cm diameter PVC pipe and in the uppermost part 1-m metal tubes with lock to prevent from robbery. The piezometers were also packed with a mixture of gravel and clay and the upper part sealed with cement to prevent direct infiltration along the casing. The maximum depth to the fractured bedrock in the piezometers is 2.35 m occurring at piezometer 6M. The piezometers located closer to the river channel have shallower depth as they reach the bedrock. Most piezometers are located in a rather even terrain but piezometers 6M, 5M and 4M are located at the hillsides. The soil at the outer piezometers had more clay loam content, while higher sand content was found in the piezometers closer to the river. The elevations of the piezometers were determined by differential-GPS measurements. In cases were the GPS observation error were high, traditional leveling was carried out.

Continuous hydraulic head and temperature measurements were taken hourly in eight piezometers, including the gage height at the river (1R), with pressure transducers from March 2004 until March 2005. Furthermore, piezometer 4M was equipped with an additional barometric pressure transducer for post processing correction. The pressure transducers were all Van Essen Instruments Divers with 2 mm and 0.01°C resolution for hydraulic head and temperature, respectively. Daily precipitation data was measured with a standard rain gage located 800 m from the site and since November 2004 an automatic weather station located 300 m from the site records hourly precipitation. Data was retrieved from the data loggers every three months and occasionally manual measurements were done for data quality checks.

Preparation of the data series for analysis included a) removing values from occasional perturbations in water levels following slug tests and water sampling and b) applying a high-pass filter to remove the seasonal trends and DC components from the original data. The analysis of the hydrological data was performed using the cross-correlation function as described by Jenkins and Watts (1968), Padilla and

Pulido-Bosch (1995) and Laroque *et al.*, (1998). The cross-correlation function establishes an interrelationship between an input and an output signal. In this study the river data are considered input signals and the water level fluctuation in the piezometers as output signals. A particular case of cross-correlation is the autocorrelation. The autocorrelation function quantifies the linear dependency of successive values over a time period. Thus, the autocorrelation function checks the data suitability before a cross-correlation analysis is carried out. The main result of the correlation is the correlation coefficient (*C*), which ranges from -1.0 to +1.0. The time at maximum *C* is the lag time between the input and output signal. A coherence function was applied in cases where relevant cross-correlation was found. The coherence function expresses the linear contribution of an input signal to an output signal and is analogous to the cross-correlation in the frequency domain (Padilla and Pulido-Bosch, 1995).

For the geophysical survey, the ABEM Lund Imaging System (Dahlin, 1996) was used to explore the electrical resistivity distribution in the subsurface of the site. The system is based on the automation of collection, processing and presentation of resistivity data. The data collection was performed as 2D resistivity imaging by using a roll along technique where cables are moved upward or downward along a succession of stations. As it was important to get information about the resistivity distribution in the upper subsurface, the minimum electrode spacing was 1 m. Multiple gradient electrode array was used for the measurements, since it has proved to have good resolution capability and be robust in the field (Dahlin and Zhou, 2004, 2006). Four resistivity lines were performed, line 1 was 100 m, line 2 was 160 m long, line 3 was 100 m and line 4 was 120 m long (see Figure 1).

Once the resistivity survey was carried out the data processing was performed using the Res2Dinv algorithm (Loke, 1997). Interpretation of the 2D resistivity data was performed by using the robust (L_1-norm) inversion method, which minimizes the absolute differences between measured and calculated apparent resistivity values (Loke *et al.*, 2003). This is an appropriate method for interpreting data from areas were subsurface regions separated by sharp boundaries are expected. Furthermore, a finite element grid was used in the data inversion as including the topography was necessary for precise relation of the object's position in space along the survey lines.

The hydraulic conductivities of the unsaturated and saturated zones were investigated at a few points of the site by using a Constant Head Permeameter (Amoozegar, 1989) and slug tests (Hvorslev, 1951), respectively. The permeability can contribute to the interpretation of the cross-correlation analyses.

Complementarily to the time series data and geophysical survey, chemical analyses of hazardous substances were carried out. Four water samples for bacterial analyses were collected from 1M, Río Artiguas, the river at Quebrada Alegre and from an old mining gallery that serves as water supply for the village and is located just upstream from the site. It is assumed that high presence of coliform bacteria in groundwater would originate from Río Artiguas as this river is highly contaminated with sewage. The bacterial analyses were carried out at the National University in Managua (UNAN-Managua). Later, 1M, 3P, 8P and river were sampled for Hg analyses, which were performed with an ICP Mass Spectrometer instrument from Perkin Elmer model Elan 6000 at the Department of Ecology, Lund University, Sweden.

Results

The water levels of the river indicate a rapid response to precipitation during most of the monitoring period (March 2004-March 2005) (Figure 2). In general, the hydraulic heads in 5P, 7P, 8P and 1M have a tendency to change together with the river levels (1R). Less or small response is observed at 6M, 4P and 4M. The temperatures are also having a similar trend among the piezometers during the studied period, except of 4M and 6M that present a rather straight curve (see Figure 2).

The autocorrelation functions show that the changes in water levels at 6M, 4M and 4P occur gradually along the studied period (Figure 3). Conversely, the changes in water levels in all the other piezometers and the river take place rapidly, within a lag time of maximum 24 hours.

The cross-correlation analyses between the river data and each piezometer are presented in Figure 4. The strongest correlation between hydraulic heads is observed at 8P, which has a correlation coefficient (C) of 0.62, followed by 1M (C=0.57), 7P (C=0.50) and 5P (C=0.32). In contrast, low or weak correlation is found with 6M (C=0.06), 4P (C=0.22) and 4M (C=0.09). In the case of the temperatures, the cross-correlation is strong in all cases, being the highest at 8P (C=0.93) and the lowest at 6M (C=0.70). The lag times in level fluctuations at the piezometers located near the river channel are short and positive, except for 4P which precedes the river signal by 64 days (see Figure 4). The temperature in 7P, 4P, 8P, 4M and 1M lag the temperature in the river, while a negative lag is found for 6M and 5P.

Since the higher cross-correlations were found between the river level and the piezometers situated near the channel, a coherence function was applied to explore the linear connection between those points. The coherence functions shown in Figure 5 indicate that in general there is a strong connection between the river levels and piezometers 7P, 9P and 1M already at periods of 12 hours. Similarly high coherences are found between 7P and 5P, 8P and 1M. However, poor or no coherence were found between the river and 5P and 4M.

Based on the time series data, two scenarios were interpreted for the periods with lowest groundwater level and the periods with higher groundwater level. During the long wet season a clear gradient towards the river is observed (Figures 6a and 6c). During the dry season (January- March 2004) groundwater levels were lower and infiltration from the river to 1M and 2M occurred (Figures 6b and 6c). At the east side of the river, the groundwater gradient does not indicate river intrusion during the dry season.

The inversion results of electrical resistivity surveys are presented in Figure 7. Line 1 was placed crossing Río Artiguas perpendicularly, while lines 2 and 3 were located parallel to the river. Line 2 crosses the tributary stream and line 4 crosses the wetland until the hillsides. The inversion models indicate the presence of a 3 m -

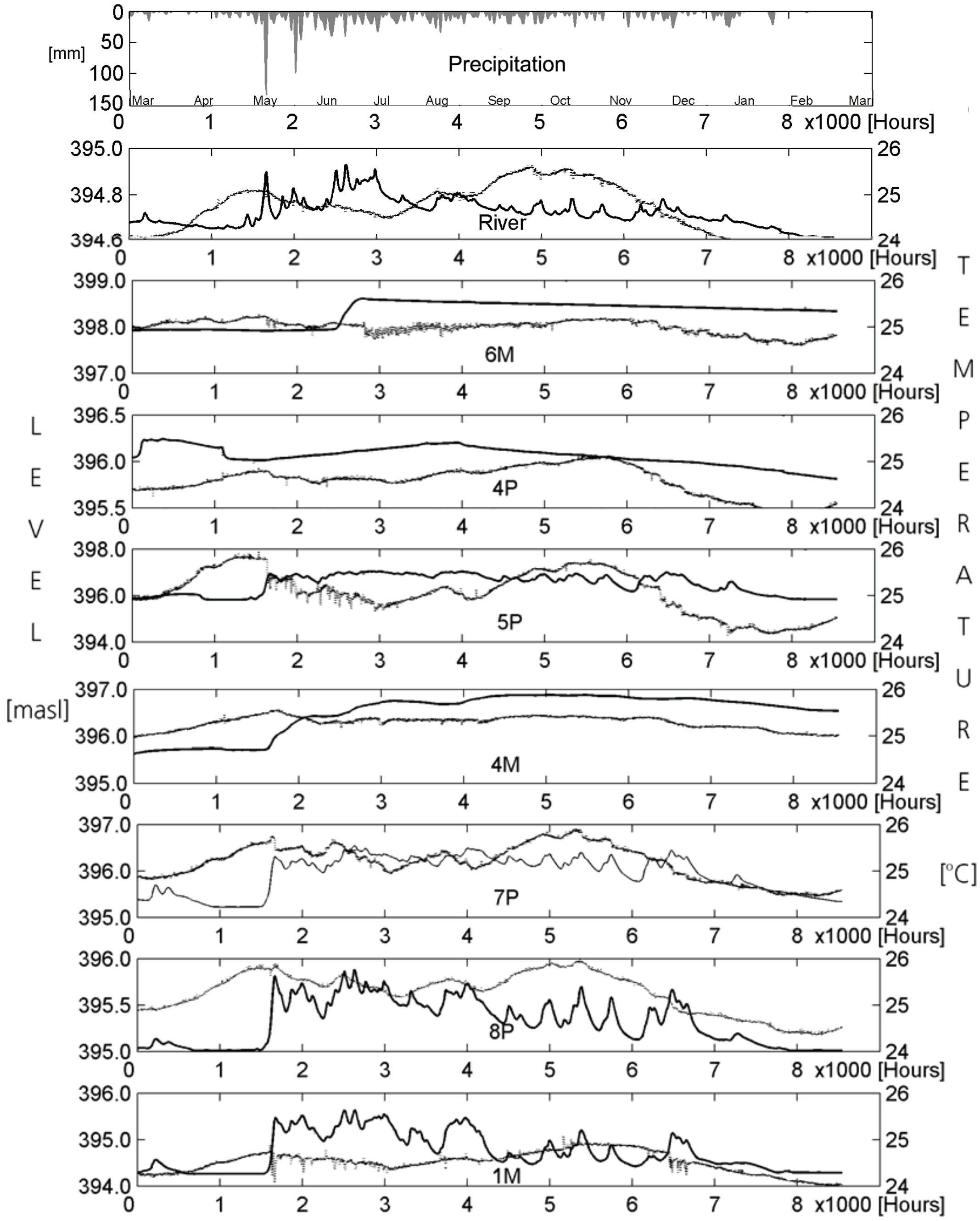

Figure 2. Rainfall, river water and groundwater levels and temperatures measured from March 2004 to March 2005. Continuous lines represent levels and dashed lines represent temperatures.

7 m thick high resistive top layer (>160 Ω m) at lines 2 and 1, particularly at the sections where the lines cross the streams. Similarly, high resistive zones extending vertically are found at the north ends of lines 2 and 4, and at the south side of line 2. Other highly resistive zones appear at the south extreme of lines 2, 3 and 4. The clay content in a swamp located next to the river has a clear effect on decreasing the resistivity as shown along the upper zones of line 4 and at the east side of line 1. Deeper low resistive zones are located below the areas where the lines

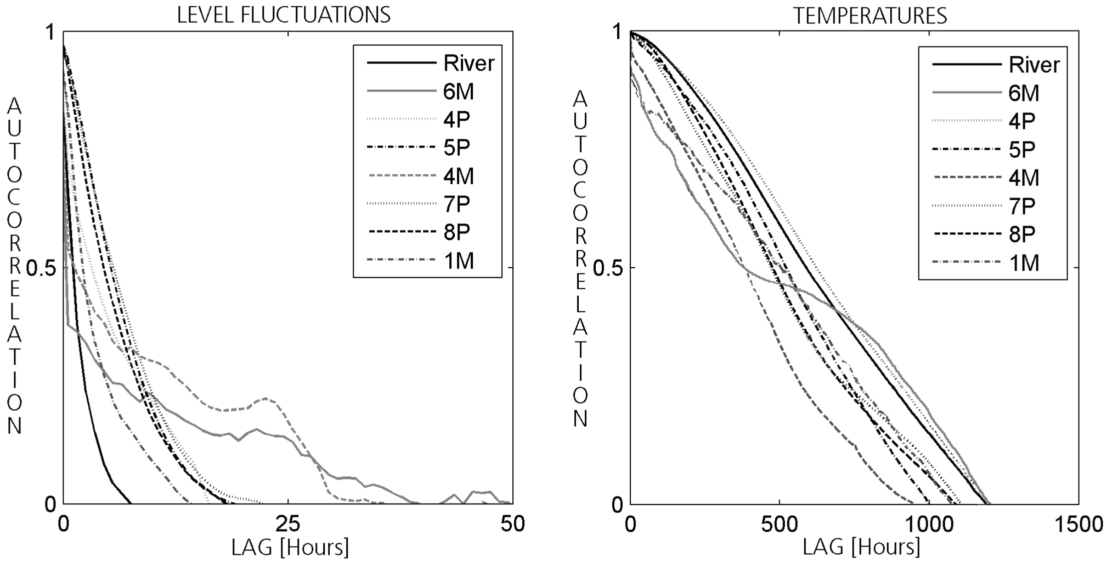

Figure 3. Autocorrelation functions for the groundwater levels (left) and for temperatures (right).

intersects and at deeper zones below the river beds (<40 Ω m).

The permeabilities at the site are generally low at the clay rich vadose zone (upper 1 m), but show an increase at the saturated zone near the river channel (5P, 7P, 8P and 1M). In contrast, permeability tests at the hillsides indicate very low or no measurable permeability (4M, 5M and 6M). Figure 8 presents the hydraulic conductivities performed at different points along resistivity line 3. Higher permeabilities are found in areas of high electrical resistivity values. The hydraulic conductivities of the vadose zone, as estimated with the Constant Head Permeameter, indicate a permeability ranging from of 8 $x10^{-8}$ m s^{-1} in the proximity of 5P to 10^{-5} m s^{-1} at the south extreme of resistivity line 3. A test performed next to 5M show a permeability of 10^{-6} m s^{-1} at that side of the wetland. The slug tests performed in the piezometers indicate permeabilities ranging from 2 $x10^{-5}$ m s^{-1} at 5P to 10^{-4} m s^{-1} at 8P. The estimated permeability at 1M was 5 $x10^{-6}$ m s^{-1}.

The bacterial analyses show a low number of *Escherichia coli* in the main source of drinking water for Santo Domingo (300 bacterial number/100mL), which it is not of health concern. However, in the Río Artiguas river a high concentration of bacteria was found (10^4-10^5 bacterial number/100mL). Moreover, an important concentration of *Escherichia coli* was detected at 2M (~10^3 bacterial number/100mL). Detectable mercury concentrations were found in water samples from the piezometers and the river, the highest value was found at 1M (0.11μg/L), followed by the river (0.04μg/L), 8P (0.03μg/L) and 3P (0.01μg/L).

Discussion

The river water level is strongly influenced by the heavy precipitation regime that characterises the basin. Additionally, the groundwater level fluctuations appear to be controlled by rapid infiltration following rainfall. This strong link between changes in the river level and groundwater table fluctuation suggests a seasonal character of the shallow aquifers. In

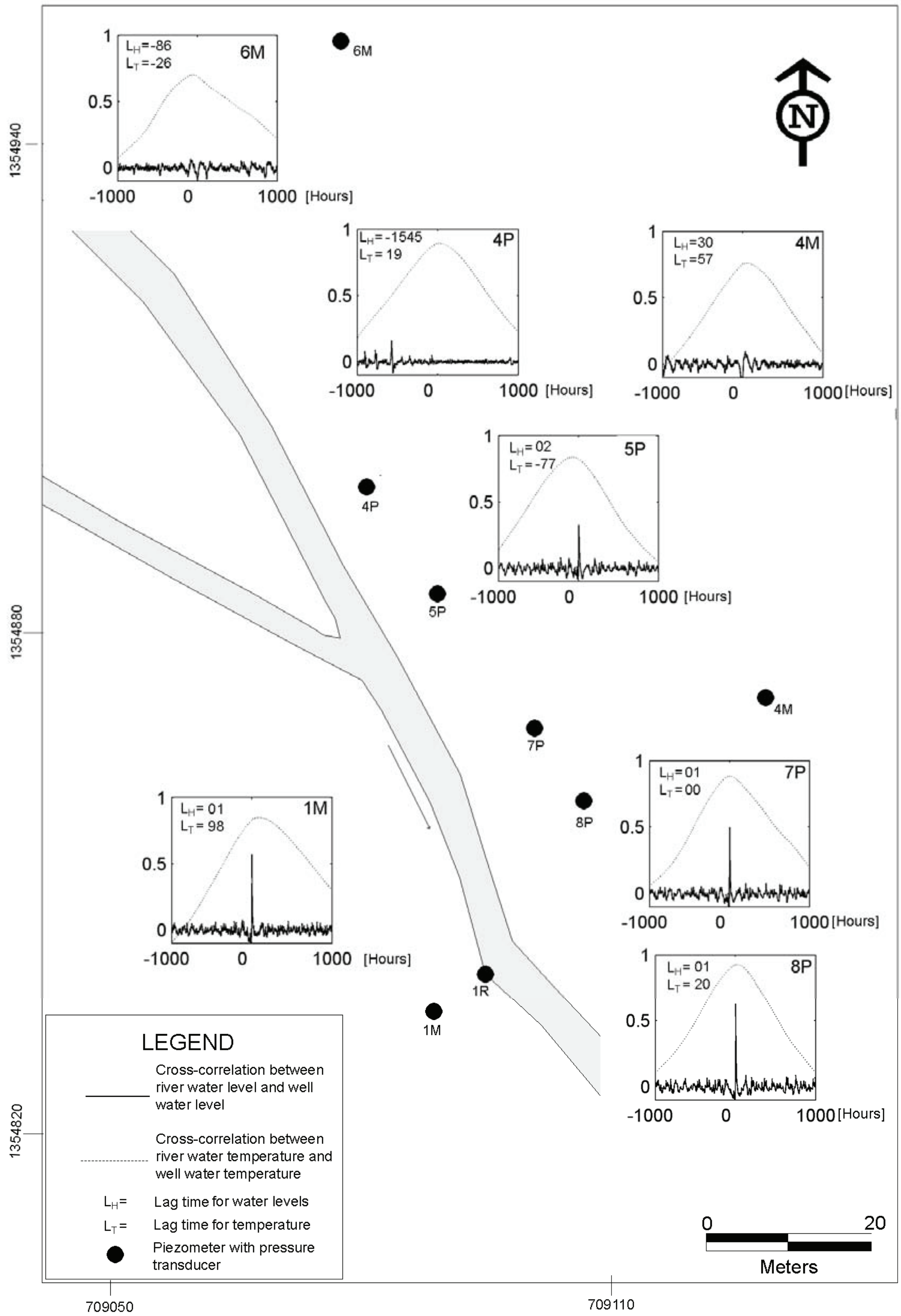

Figure 4. Cross-correlation between river level and each of the monitored piezometers at the site.

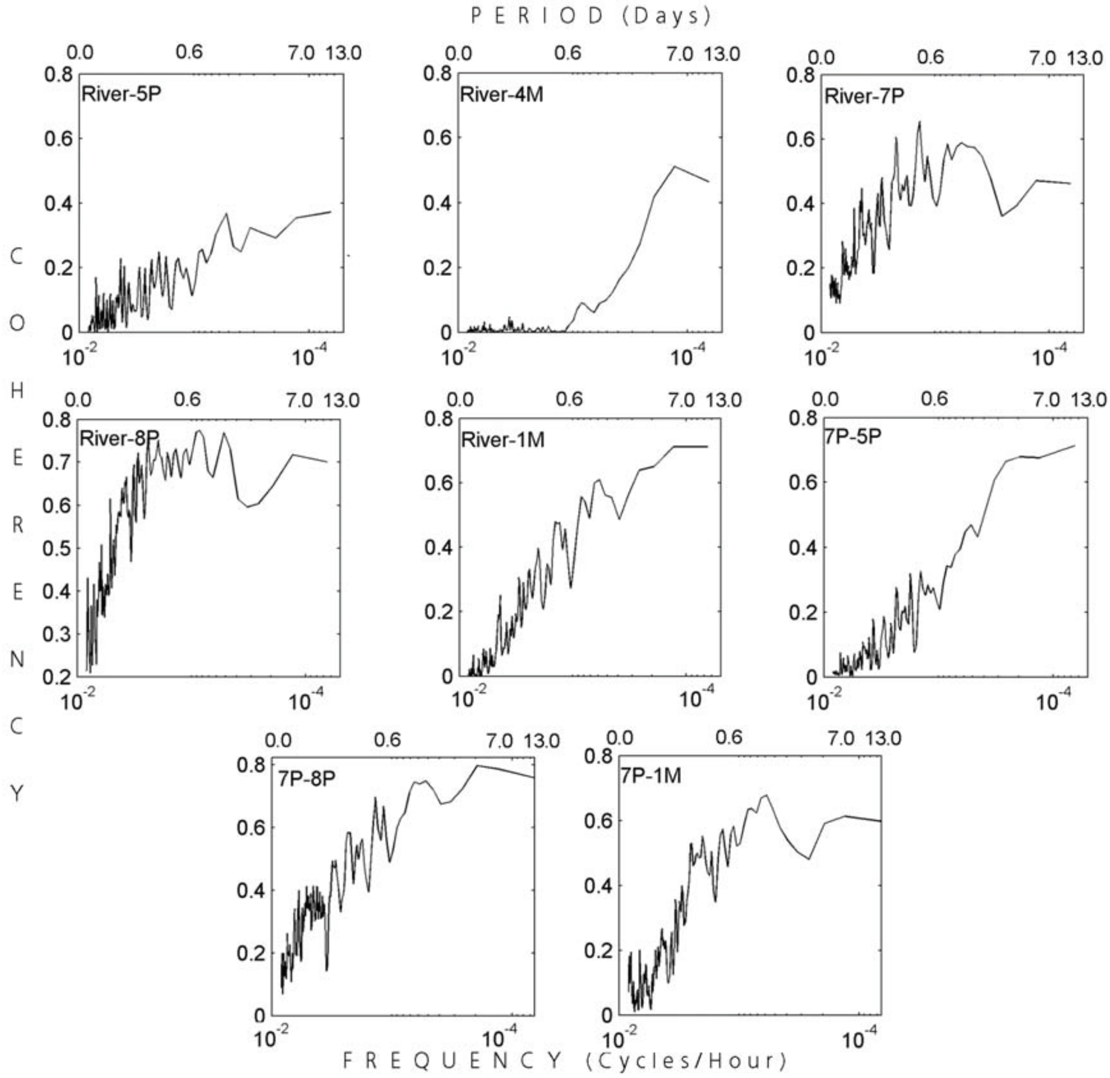

Figure 5. Coherence functions between river and nearest piezometers and between 7P and nearest piezometers.

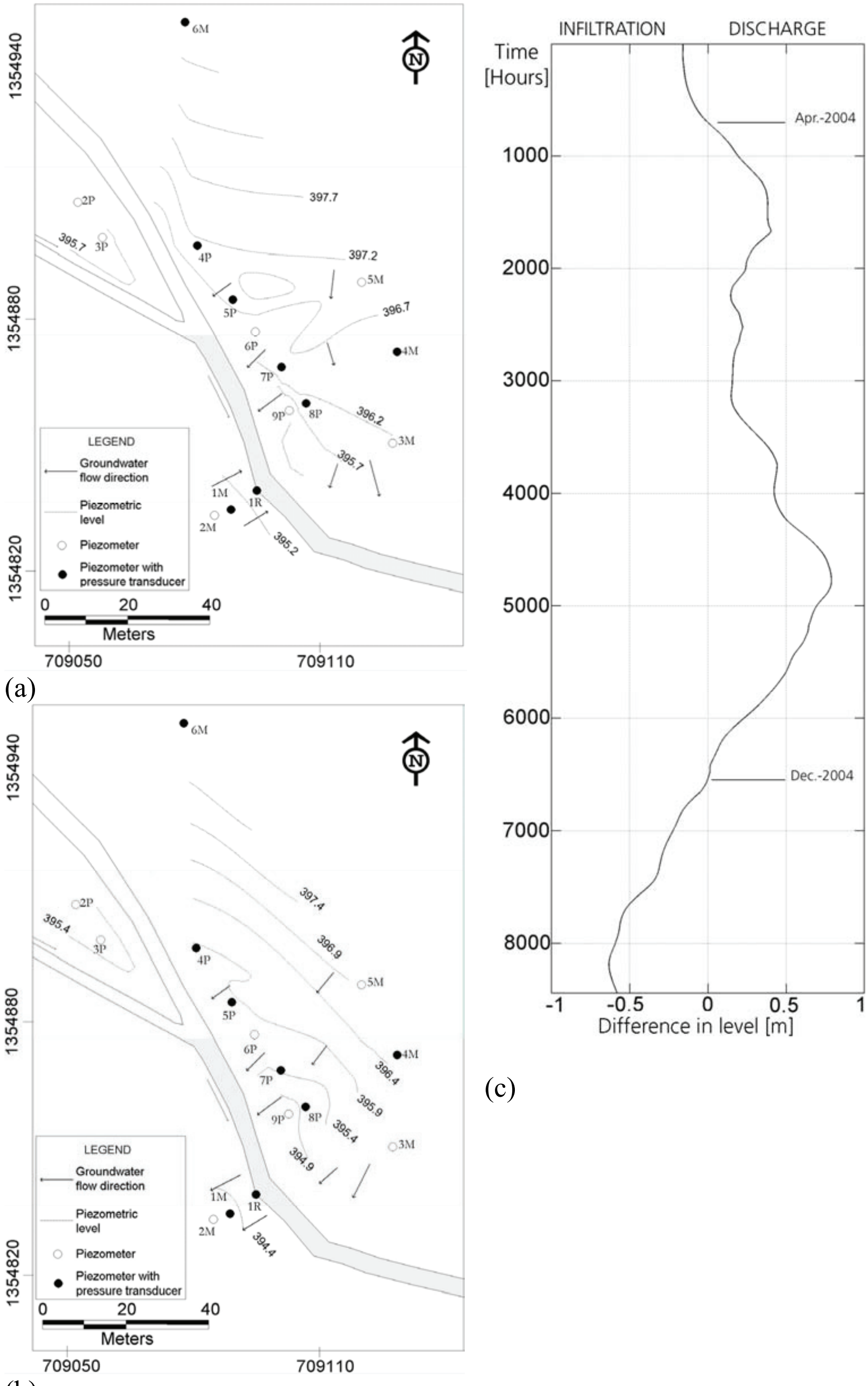

Figure 6. Groundwater table (a) period of highest hydraulic heads and (b) period of lowest hydraulic heads and (c) periods of infiltration from the river and discharge to the river as observed at 1M.

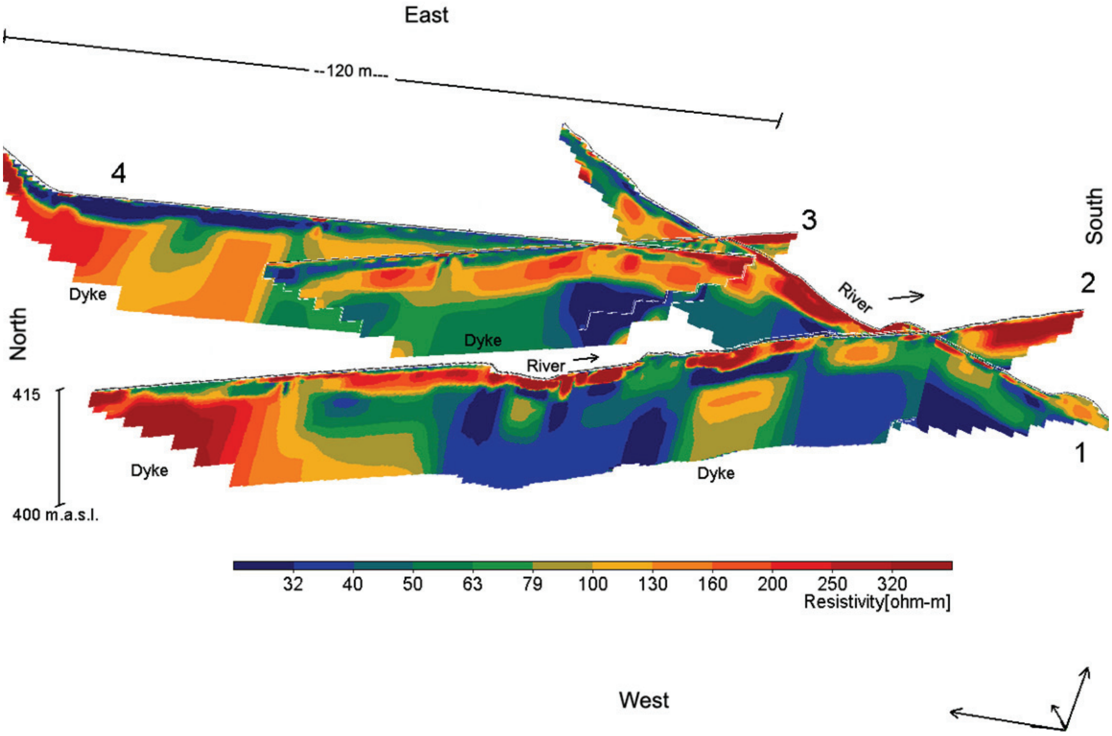

Figure 7. Electrical resistivity images.

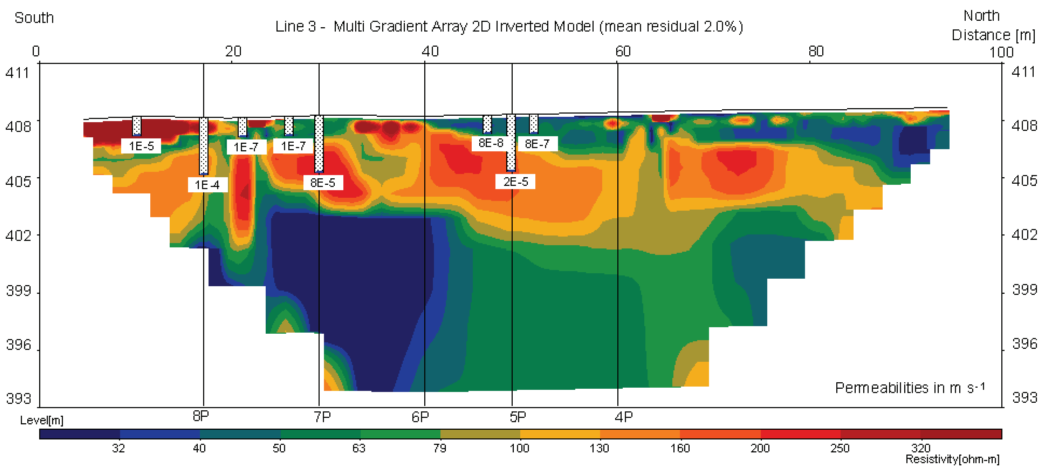

Figure 8. Electrical resistivity image of line 3 including values of permeability tests.

the areas near the hillsides (6M and 4M) groundwater fluctuations are less influenced by infiltration, probably due to a high clay content, which also contributes to the formation of the wetland. In opposition, the relatively high cross-correlation (> C=0.32) found in all piezometers located next to the river channel denotes a faster infiltration and transport of water through the fractured rock. However, considering the short distance between piezometers and the low cross-correlation found at 4P (C=0.22), a high spatial variability of the hydraulic properties should be expected in the area. Moreover, the coherence functions indicate a marked connection in frequency domain between the fluctuations at the south side of site (1R-7P-8P-1M), but this strong relationship is not present between the piezometers elsewhere. The strong cross correlation of temperatures found in all cases reflects the similar origin of both river water and groundwater.

The high variability of hydraulic properties at the site is also supported by the electrical resistivity surveys. The resistivity response from the top areas varies from high resistive zones (>160 Ω m) associated to coarse grain material and hard rock to the low resistive zones rich in clay content (<40 Ω m) (see Figures 7 and 8). There are strong lateral variations in the resistivity over short distances, which indicate an intense vertical fracturing. Furthermore, previous aerial photointerpretation, field documentation and geophysical surveys in the basin (Mendoza, 2002) suggest that the vertical zones of high resistivity present in the resistivity images of lines 2, 3 and 4 might be associated to two basaltic dykes located perpendicular to the river.

Zones of discharge near the channel of the river cannot be interpreted from the resistivity images. Nevertheless, areas with high resistivity values associated with bedrock were observed near the channel in line 1. This may be an indicator that discharge to the river does not occur through sediments but through fractures in the bedrock.

Regarding the groundwater table, there was a hydraulic gradient towards the river most of the monitoring period. This gradient is maintained by the heavy precipitation and expected high infiltration rate. However, as the rain season finished the hydraulic gradient changed on the west side of the river, allowing river water infiltration (See Figure 6). The topographically controlled hydraulic gradient on the northeast side of the river permitted a continuous flow to southwest during the short dry season. This situation explains the bacterial concentrations in 2M, similar to the concentration found in the river water. The Hg concentrations found in 1M are higher than in 3P and the piezometers located on the other side of the river channel.

The interpretation of hydraulic data and resistivity imaging is supported with the hydraulic conductivities estimated at different points of the site. Higher permeability was found at 8P, which also presents higher cross-correlation (see Figure 4). The top layers are commonly having lower hydraulic conductivities due to the clay content, but there may be an increase when reaching the fractured rock in depth and in the proximities of the fractured dykes.

In general, these results are in agreement with the findings of Mendoza *et al.*, (2005), who suggested that there is a rapid groundwater circulation through the basin. From these local groundwater systems water travels relatively fast when moving through joints and fractures until discharging into the river. When precipitation lowers, the situation could be the inverse, with channel water infiltrating the near shallow aquifers.

Conclusions

This paper has shown that rainfall infiltration is the main factor controlling the shallow groundwater dynamics in the near channel aquifers along the Río Artiguas river. Cross-correlation analyses of river levels against hydraulic heads revealed a rapid response of the groundwater table to river infiltration and direct recharge. The piezometers located far from the river channel exposed poor correlation to the river, indicating a lack of contact with the nearby groundwater. This may be caused by the high clay content found at those areas, as interpreted from the electrical resistivity images. Less weathered or fresh rock is related to the deeper high resistive zones, where flow through fractures may be of major hydrogeological significance.

The high bacteria concentrations found in the river and in the groundwater at 2M confirm that there is a connection between the river and the shallow aquifers in the proximities. This is also supported by the hydraulic heads, which suggests that most of the river infiltration to aquifers occur during the dry season. However, the frequent river floods can also spread the pollutants to the nearby aquifers.

The results presented here demand major concern on the exposure of groundwater systems to pollution in basins characterised by fractured media, like the highlands of Nicaragua. In this case, waste disposal in surface water can also mean direct pollution of groundwater. The seasonal character of the aquifers evidence limited availability of groundwater resources, as they seem to depend on recent recharge. Further research could be addressed to characterise the recharge and discharge processes throughout the river basin, which can increase the understanding of the groundwater - surface water relationship.

Acknowledgments

This work was conducted as part of a multidisciplinary research program funded by the Swedish International Development Agency (Sida/SAREC). Technical and logistical support was provided by the Department of Engineering Geology at Lund University (Sweden) and Centro de Investigaciones Geocientíficas at UNAN-Managua, respectively. Prof. Göran Bengtsson suggested valuable ideas for the study. Kjell Andersson assisted in the piezometers installation and Tommy Olsson made the mercury analyses. Jonas Hedberg installed the meteorological station and Marvin Corriols retrieved divers' data. Family Duarte is specially acknowledged as their assistance made fieldwork less difficult under the tropical conditions at Río Artiguas.

References

Albuquerque N. 1996. Estudio de Impacto Ambiental. [Environmental Impact Study] Empresa Asociativa de Pequeños Mineros de SD Chontales; 87.

Amoozegar A. 1989. A compact constant-head permeameter for measuring saturated hydraulic conductivity of the vadose zone. *Soil Science Society of America Journal* **53**: 1356–1361.

André L, Rosén K, Torstendahl J. 1997. Minor Field Study of Mercury and Lead Pollution from Gold Refining in Central Nicaragua. MSc thesis, ISBN 1402-1617. Luleå University of Technology: Sweden; 154.

Aronsson M, Wallner C. 2002. Inventory of springs and hydrochemical investigations of groundwater in the drainage basin of

Sucio river, Nicaragua. MSc thesis, ISRN LUTVDG/TVTG—5078—SE. Lund University: Sweden; 105.

Bierkens MFP, Knotters M, Hoogland T. 2001. Space-time modeling of water table depth using a regionalized time series model and the Kalman filter. *Water Resources Research* **37**:1277–1290.

Crosbie RS, Binning P, Kalma JD. 2005. A time series approach to inferring groundwater recharge using the water table fluctuation method. *Water Resources Research* 41: W01008. DOI:10.1029/2004WR003077.

Dahlin T. 1996. 2D resistivity surveying for environmental and engineering applications. *First Break* **14**(7): 275–283.

Dahlin T, Zhou B. 2004. A numerical comparison of 2D resistivity imaging with 10 electrode arrays. *Geophysical Prospecting* **52**: 379-398.

Dahlin T, Zhou B. 2006. Multiple gradient array measurements for multi-channel 2D resistivity imaging. *Near Surface Geophysics*. In Press.

deGroot-Hedlin C, Constable S. 1990. Occam's inversion to generate smooth, two-dimensional models from magnetotelluric data. *Geophysics* **55**: 1613-1624.

Duffy CJ, Gelhar LW. 1986. A Frequency Domain Analysis of Groundwater Quality Fluctuations: Interpretation of Field Data. *Water Resources Research* **22**(7): 1115–1128.

Ellis RG, Oldenburg DW. 1994. Applied geophysical inversion. *Geophysical Journal International* **116**: 5-11.

Grunander K, Nordenberg L. 2004. Investigation of Groundwater – Surface Water Interaction in the Drainage Basin of the River Sucio, Nicaragua. MSc thesis, ISRN LUTVDG/TVTG- -5090- -SE. Lund University: Sweden; 92.

Hodgson G. 1972. Geological map of La Libertad, Catastro e Inventario de Recursos Naturales: Nicaragua.

Hvorslev MJ. 1951. Time Lag and Soil Permeability in Ground Water Observations, Waterways Experimental Station, Corps of Engineers, US Army, Bulletin no. 36; 50.

INETER. 1991. Anuarios Meteorológicos (1990, 1991) [meteorological charts] Catastro e Inventatio de Recursos Naturales: Nicaragua.

Jenkins GM, Watts DG. 1968. Spectral analysis and its applications. Holden-Day series in time series analysis: San Francisco; 487.

Kim JH, Lee J, Cheong TJ, Kim RH, Koh DC, Ryu JS, Chang HW. 2005. Use of time series analysis for the identification of tidal effect on groundwater in the coastal area of Kimje, Korea**.** *Journal of Hydrology* **300(**1-4): 188-198.

Larocque M, Mangin A, Razack M, Banton O. (1998). Contribution of correlation and spectral analyses to the regional study of a large karst aquifer (Charente, France). *Journal of Hydrology* **205(**3-4): 217-231.

Lee JY, Lee KK. (2000). Use of hydrologic time series data for identification of recharge mechanism in a fractured bedrock aquifer system. *Journal of Hydrology* **229**: 190–201.

Lerner DN. (1997). Groundwater recharge. In *Geochemical processes, weathering and groundwater recharge in catchments*, Saether OM, deCaritat P (eds) AA Balkema: Rotterdam, Holland;109–150.

Loke MH, Barker RD. (1996). Rapid least-squares inversion of apparent resistivity pseudosections by a quasi-Newton method. *Geophysical Prospecting,* **44**(1): 131-152.

Loke MH. (1997). Rapid 2D resistivity inversion using the least squares method, Manual for RES2DINV, Geolectrical Imaging 2D and 3D; 43

Mendoza JA. (2002). Geophysical and hydrogeological investigations in the Rio Sucio watershed, Nicaragua. Lic Thesis, ISBN 91-972406-0-X. Lund University, Sweden; 60.

Mendoza JA, Dahlin T, Barmen G. (2004). Use of resistivity imaging in a surface water –groundwater interactions study, Procc. XXXIII Congress IAH - 7º ALHSUD 11-15 October, 2004, Zacatecas City, Mexico.

Mendoza JA, Dahlin T, Barmen G. (2005), Hydrogeological and hydrochemical features of an area polluted by heavy metals in central Nicaragua. *Hydrogeology Journal.* DOI: 10.1007/s10040-005-0462-5.

Padilla A, Pulido-Bosch A. (1995). Study of hydrographs of karstic aquifers by means of correlation and cross-spectral analysis. *Journal of Hydrology* **168**(1-4): 73-89.

Romero F. (1996). Contaminación de Hg y Pb en fuentes de agua. area de Santo Domingo, Chontales [Hg and Pb contamination in water wells], Centro de Investigaciones Geocientíficas: Managua, Nicaragua; 21.

Sheets RA, Darner RA, Whiteberry BL. (2002). Lag times of bank infiltration at a well field, Cincinnati, Ohio, USA. *Journal of Hydrology* **266**: 162-174.

Silva G. (1994), Diagnóstico da contaminação ambiental gerada pela actividade minerária sobre los rios Súcio, Mico e Sinecapa, Nicaragua [Diagnose on the contamination caused by the mining activity in the rivers Sucio, Mico and Sinecapa]. Universidade Federal do parã Centro de Geociências curso de póstgraduação: Belem, Brasil; 150.

Sophocleous M. (2002). Interactions between groundwater and surface water: the state of the science. *Hydrogeology Journal* **10**: 52–67.

Winter TC. (1999). Relation of streams, lakes, and wetlands to groundwater flow systems, *Hydrogeology Journal* **7**: 28–45.

Winter TC, Harvey JW, Franke OL, Alley WM. (1998). Ground water and surface water – a single resource. US Geological Survey Circular 1139: Denver, USA; 79.

Zhang, YK, Schilling K. (2004). Temporal scaling of hydraulic head and river base flow and its implication for groundwater recharge. *Water Resources Research* **40**: W03504. DOI:10.1029/2003WR002094.

IV

Mendoza JA, Barmen G. (2006) Assessment of groundwater vulnerability in the Río Artiguas basin, Nicaragua. Environmental Geology, DOI 10.1007/s00254-006-0233-1

Environ Geol (2006)
DOI 10.1007/s00254-006-0233-1

ORIGINAL ARTICLE

J. A. Mendoza
G. Barmen

Assessment of groundwater vulnerability in the Río Artiguas basin, Nicaragua

Received: 14 December 2005
Accepted: 16 February 2006

J. A. Mendoza (✉)
Centro de Investigaciones Geocientíficas,
Universidad Nacional Autónoma
de Nicaragua (CIGEO, UNAN-Managua),
Col. Miguel Bonilla #165 Apartado
Postal A-131, Managua, Nicaragua
E-mail: alfredo.mendoza@tg.lth.se
Tel.: +505-2-770621
Fax: +505-2-770613

G. Barmen
Department of Engineering Geology,
Lund University, Box 118,
221 00 Lund, Sweden

Abstract The Río Artiguas basin in central Nicaragua shows a distinctive case of environmental deterioration due to anthropogenic activities. Heavy metals used in gold mining and other wastes are continuously released into the rivers, representing a threat to the water quality. This article aims to evaluate the groundwater intrinsic vulnerability in the Río Artiguas basin and to provide information for sustainable use of water resources. The DRASTIC and GOD methods were used to analyse the relative pollution potential within the basin. DRASTIC was modified to include the degree of influence that geological structures have on the vulnerability. Moderate vulnerability areas cover most of the basin along stream valleys and lowlands, increasing downstream in the basin. The resulting vulnerability maps show that the limited groundwater resources are susceptible to surface water pollution as high vulnerability areas converge along the river valleys.

Keywords Vulnerability · DRASTIC · GOD · Nicaragua · Río Artiguas

Introduction

Groundwater vulnerability assessment is an important process for understanding the intrinsic fragility that a certain region opposes to a given threat, whether this hazard has a natural or anthropogenic origin. Frequently, the vulnerability assessments are carried out in areas with water resources under stress originated from industrial activities. Therefore, the vulnerability studies can provide valuable information for stakeholders working on preventing further deterioration of the environment.

One of the activities that often represent a threat to groundwater quality is mining. In the Río Artiguas basin (Fig. 1), in the central mountainous region of Nicaragua, the sewage mismanagement and use of mercury in gold mining with consequent release to the environment demands groundwater protection. Prior to a water protection plan, a vulnerability assessment is necessary for identifying areas that are likely to be affected by pollution.

There are several methods for water resources vulnerability evaluation. The more frequent methods are based on overlay and index techniques, where different data parameters (recharge, soil, aquifer strata, etc.) are rated and superimposed to each other to produce a vulnerability map (Vrba and Zaporozec 1995; Gogu and Dassargues 2000). In some methods the rated data are also weighted for each parameter in order to reflect their relative importance in the evaluation. The criteria for selecting a particular method generally includes (a) data availability, as data scarcity is a habitual problem and (b) site geological conditions, since there are rock formations that require special attention due to their high solubility in water. Comparing the results obtained from two or more methods applied to a certain area, one can assist in evaluating their relative efficiency and provide a more comprehensive interpretation of the predicted

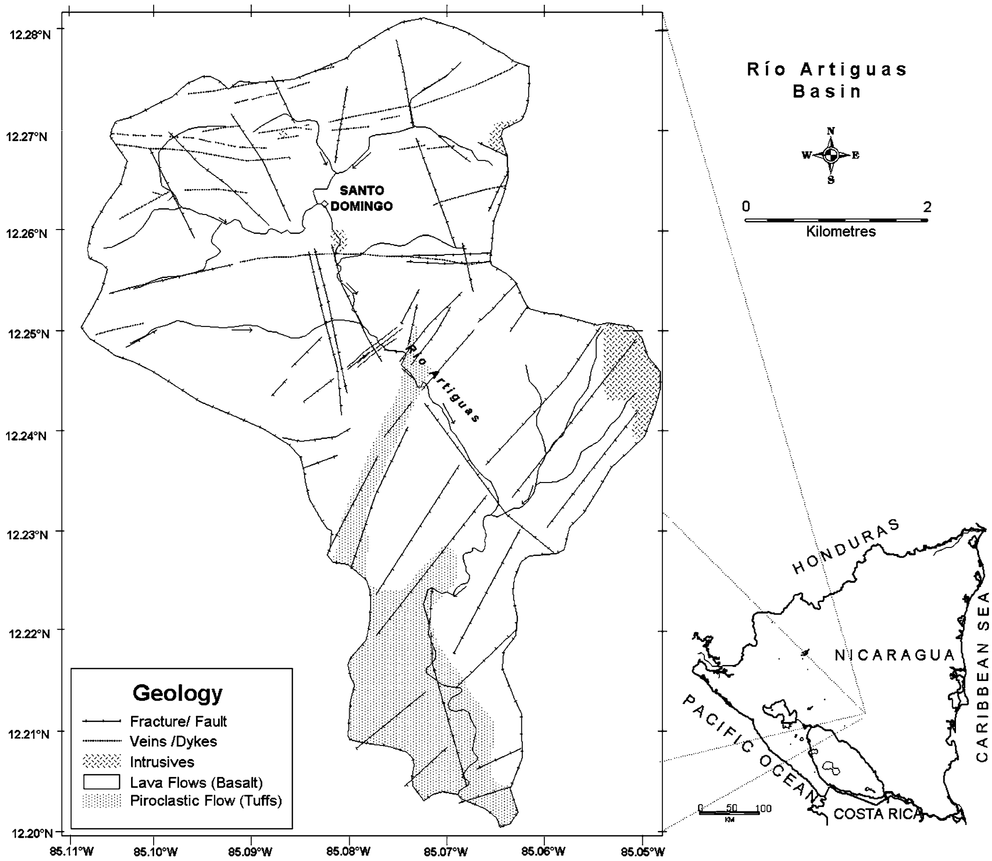

Fig. 1 Study area with its geological settings

vulnerability in that site. Examples of comparative case studies can be found in a number of reports (Ibe et al. 2001; Gogu and Dassargues 2003; Civita and De Maio 2004). Modifications to a vulnerability method are sometimes performed in order to consider geological and geographic factors that are found to be particularly relevant to the evaluation in a certain region (Secunda et al. 1998; Davis et al. 2002; Dixon 2005).

The aim of this article is to evaluate the groundwater intrinsic vulnerability in the Río Artiguas basin and contribute to a base of information for sustainable use of water resources for human activities, including prevention of further contamination derived from gold mining. The DRASTIC method (Aller et al. 1987) has been used to analyse the relative potential vulnerability within the basin. Additionally, the vulnerability was evaluated using the GOD method, which was originally formulated for use in areas with limited data availability (Foster 1987).

The work has been developed within the framework of a broad environmental program funded by the Swedish International Development Agency (Sida/SAREC). One of the main aims is to understand the environmental effects of mining activities in Nicaragua.

The study area: the hydrogeological significance of weathering and tectonics

The study area is the Rio Artiguas basin, located in the eastern part of the central highlands of Nicaragua. This basin has experienced a century of gold mining using the mercury method. A weather station located in the basin reports temperatures with a minimum of 15°C and a maximum of 34°C, for the period November 2004–March 2005. Historic average precipitations of ca. 2,400 mm/year have been recorded in the area by INETER (1991). The young drainage system for surface waters has developed under a structural control where faults, fractures and joints lead to a rectangular flow pattern.

Geologically, most of the Río Artiguas basin is covered by Tertiary volcanic rocks, mainly basalts and andesite lava flows. These lava flows are overlying rhyolitic–dacitic pyroclastic flows towards the south of the area (Hodgson 1972). There are gold bearing quartz veins embedded in these basalts and andesites lava flows, surrounded by hydrothermal alteration aureoles (Darce 1990). More acid rock types are found as plugs intruding the basalts and andesites. Tectonically, there is a distinct fracture trend in east–northeast directions where silica intruded to form the veins. These subvertical veins are often segmented by a semi-perpendicular fracturing trend in a northwest–southeast preferential orientation (Weinberg 1992; Ehrenborg 1996). Additionally, the 0.5–10 m wide veins are surrounded by alteration envelopes which gradually become fresh rock laterally and downwards from the quartz bodies. The combined perpendicular fracturing pattern is also affecting the morphology of the area, with drainage and hill alignments following the preferential fracture directions. The quartz veins are all located in the most upstream zones of Río Artiguas and extend outside the basin towards east and west.

The different rock formations present in the area have been exposed to strong physical and chemical weathering processes. It is hard to find fresh rock on the surface. The pyroclastic deposits are extremely weathered and it is likely that these deposits were exposed for long time before the lava flows were deposited. These basalt and andesite lava flows are less weathered than the pyroclastic rocks. Geological and geophysical surveys performed before this assessment indicates that the overall weathering thickness in the area varies from 1 to 3 m in general, and in some areas expands to 70 m (Mendoza 2002). The weathering thickness varies over short distances. These weathering layers consist of heterogeneous material ranging from leached and coarse grained to clay weathered rock (Mendoza et al. 2000). Dykes, veins and other intrusive bodies formed during late Tertiary have been less exposed to the strong tropical weathering than rocks surrounding them.

The quartz veins and tectonic zones, in combination with fracturing and weathering, are considered the major factors contributing to groundwater occurrence and transport. Consequently, the saturated zone is a composite horizon of both weathered layers and fractured bedrock. Figure 2 shows a hydrogeological model of the area; water infiltrating the weathered nonsaturated zone travels through the saturated zone but shortly discharges in a spring or along the streams. If water infiltrates through open fractures, tectonic contacts or bed contacts it can travel longer distances and eventually form regional groundwater flows. However, considering the basin area (28 km^2) and the high number of springs (99) it has been suggested that most of the groundwater is discharged into the springs, rather than forming large regional aquifers (Mendoza et al. 2005).

Methods for vulnerability assessment

The DRASTIC vulnerability assessment method assigns a value to each of seven parameters at a given geographic point or cell. Every parameter is then weighted in order to reflect its relationship with respect to the others and its likely contribution to transport of

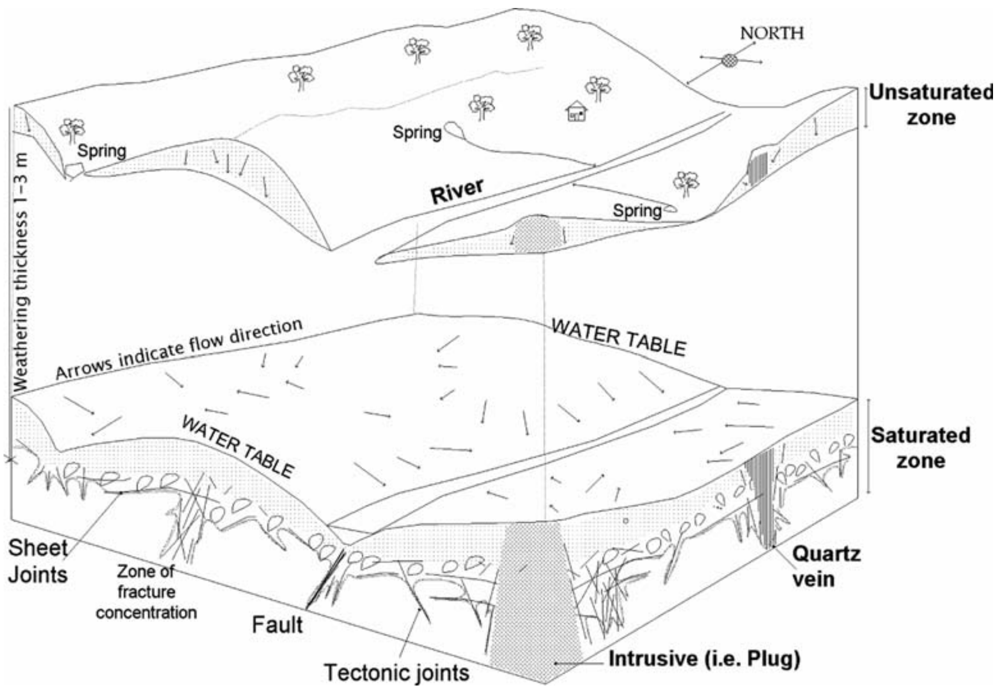

Fig. 2 Hydrogeological model of the Río Artiguas basin. The *upper part* represents the unsaturated zone and the *lower* the saturated zone

contaminants. The seven parameters are depth to groundwater (D), net recharge (R), aquifer media (A), soil media (S), topography (T), influence of the vadose zone (I) and hydraulic conductivity (C).

This system allows the user to determine a numerical value for any hydrogeological setting by using an additive model. The equation for determining the DRASTIC index is

$$D_R D_W + R_R R_W + A_R A_W + S_R S_W + T_R T_W + I_R I_W + C_R C_W = \text{DRASTIC index},$$

where R is the rating and W is the weight assigned to that parameter. For this vulnerability assessment the general equation formulated by Aller et al. (1987) is used

$$5D_R + 4R_R + 3A_R + 2S_R + T_R + 5I_R + 3C_R = \text{DRASTIC index}.$$

Since the hydrogeological role of geologic structures has been broadly studied and accepted (Forster and Evans 1991; Levens et al. 1994), geologic structures are likely to increase the vulnerability of highly fractured environments like the study area. Therefore, the DRASTIC index was modified to include the degree of influence that the length, connectivity and density of lineaments have in the vulnerability. Thus an additional parameter denominated lineament influence (M) was weighted using a coefficient of 5 and included in the equation as

$$\text{DRASTIC index} + 5M_R = \text{Modified DRASTIC index}.$$

The original DRASTIC Index does not propose classification ranges for the numerical values obtained as results. Therefore, a commonly used classification is used here, dividing the numerical values into five categories: very high vulnerability (vulnerability index >199), high vulnerability (160–199), moderate vulnerability (120–159), low vulnerability (80–119), and very low vulnerability (<79) (Civita and De Regibus 1995; Corniello et al. 1997).

The GOD method considers two basic factors to determine the aquifer pollution vulnerability: (a) the level of hydraulic inaccessibility of the saturated zone of the aquifer and (b) the contaminant attenuation capacity of the strata overlaying the saturated aquifer (Foster et al. 2002). However, in most cases those factors cannot be evaluated thoroughly due to data limitation. Thus, a simplification is required and the following parameters are considered (Foster 1987):

- Groundwater hydraulic confinement (groundwater occurrence), of the aquifer under consideration.
- Overlaying strata (vadose zone or confining beds).
- Depth to groundwater table or to groundwater strike in the case of confined aquifers. Figure 3 shows the GOD ratings according to different aquifer media, confinement degree and groundwater depth.

Overview of the input data for assessing the vulnerability

Considering the lack of background information in the area basic data had to be collected before carrying out this vulnerability assessment. The collected data included meteorological information, hydrochemical sampling of surface water and groundwater, hydrometric measurements, soil characterization, geological mapping, geophysical surveys and hydraulic permeability tests (Mendoza et al. 2005). The data collection and processing is considered part of the vulnerability assessment. The data selected for this assessment were organized in layers and grids for calculation in MapInfo and Vertical Mapper, respectively (MAPINFO 2000). Figure 4 presents a general idea of the data density by showing the locations of sample points used for this evaluation. The rates used for the different parameters as observed in the field are presented in Table 1. The following subsections give an overview of the input data used for each parameter of DRASTIC and the input data for each parameter of GOD.

Drastic

Depth to water

Static groundwater level measurements were made at 26 piezometers using both a sonic probe and permanently installed pressure transducers. Later, the absolute altitudes were measured by means of differential–GPS. Additionally, groundwater levels were measured at known discharge segments along the streams and in springs. Subsequently, these groundwater level data were Kriged, using the ground surface (digital elevation model, DEM) as an external drift, in order to estimate the groundwater surface for the entire basin (Deutsch and Journel 1992; Goovaerts 1997; Desbarats et al. 2002).

Net recharge

The net recharge was calculated using the chloride method (Allison and Hugues 1978; Gaye and Edmunds 1996). Water from springs, streams, observation wells and precipitation was analysed for chloride concentration and the precipitation was gauged at two locations in the area during 2002 and 2003. The results from these analyses indicate a net recharge high for the area, with values ranging from 84 mm in the central and low zones up to above 600 mm along the water divides. Since the mean value is 435 mm for the entire area, most of the area is classified at the highest rate in DRASTIC.

Aquifer media

The aquifer media is characterized by fractured and weathered lava flows that changes with depth to fractured hard rock. This aquifer media is typical within the first tens of meters of the subsurface profile at the hilltops and hillsides. As reaching the stream valleys the fractured basalts frequently outcrops.

Soil media

The soil media is mainly clay with variable contents of silt corresponding to the *Associations Orthoxic Tropudults and Typic Tropodults* (INETER 1973). In some areas in the south, a more silty clay soil can be found.

Topography

The area can be separated into three different morphological units, roughly equivalent to the geological units presented in Fig. 1. The central and southern parts of the basin present a low to moderate wavy relief with low smooth hills. The slopes in those areas range from 0 to 10% in general.

On the west, north and northeast borders of the basin the relief is more varied, with hilly areas, steep valleys and slopes higher than 10% in average. These areas are dominated by thick lava flows. Most of the alteration and quartz veins zones are located in this morphological unit. The third morphological unit corresponds to volcanic plugs having a high relief and is less eroded than the previous. The plugs and their surroundings have slopes steeper than 20°.

Impact of the vadose zone

In the hills, which are more exposed to weathering, the vadose zone is composed mainly by up to 2 m clay. This clay has more gravel content or coarser material towards the hillsides. There are some areas along the river terraces where most of the vadose zone is composed of fractured lava flows (basalt).

Hydraulic conductivity

The hydraulic conductivity conditions in the area derive primarily from the weathering extension and degree of fracturing. Slug tests at three of the observation wells installed in the area indicate that the hydraulic conductivities range from 5.7×10^{-6} m/s in the clay to

Fig. 3 The original GOD scheme (from Foster 1987)

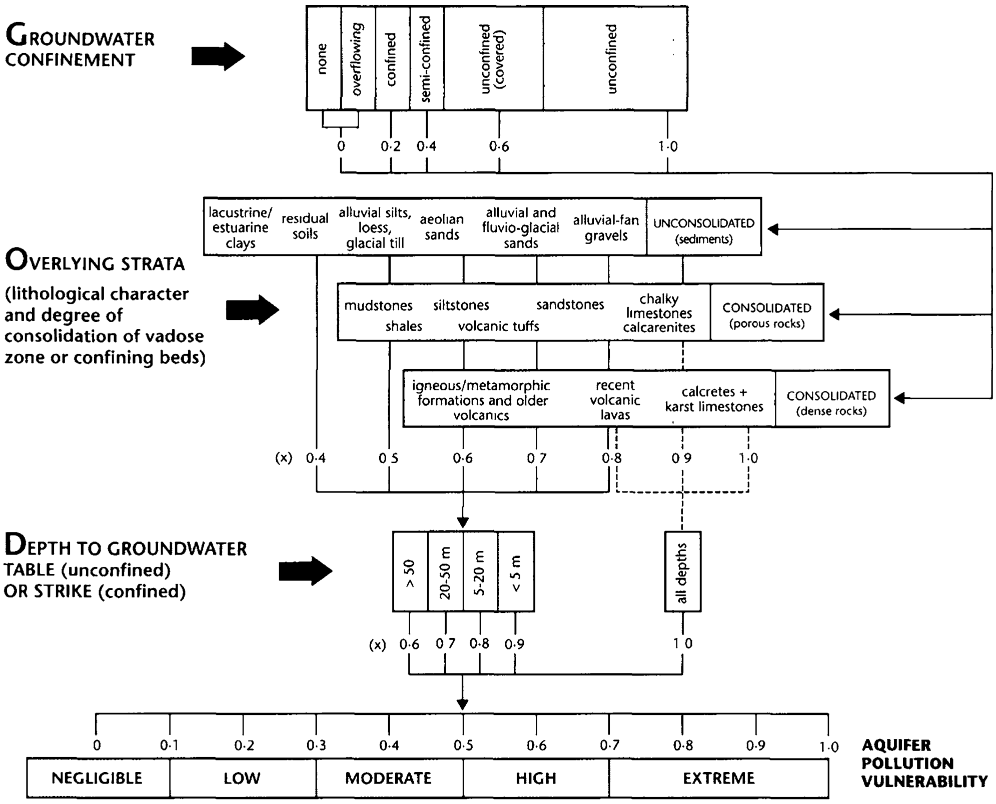

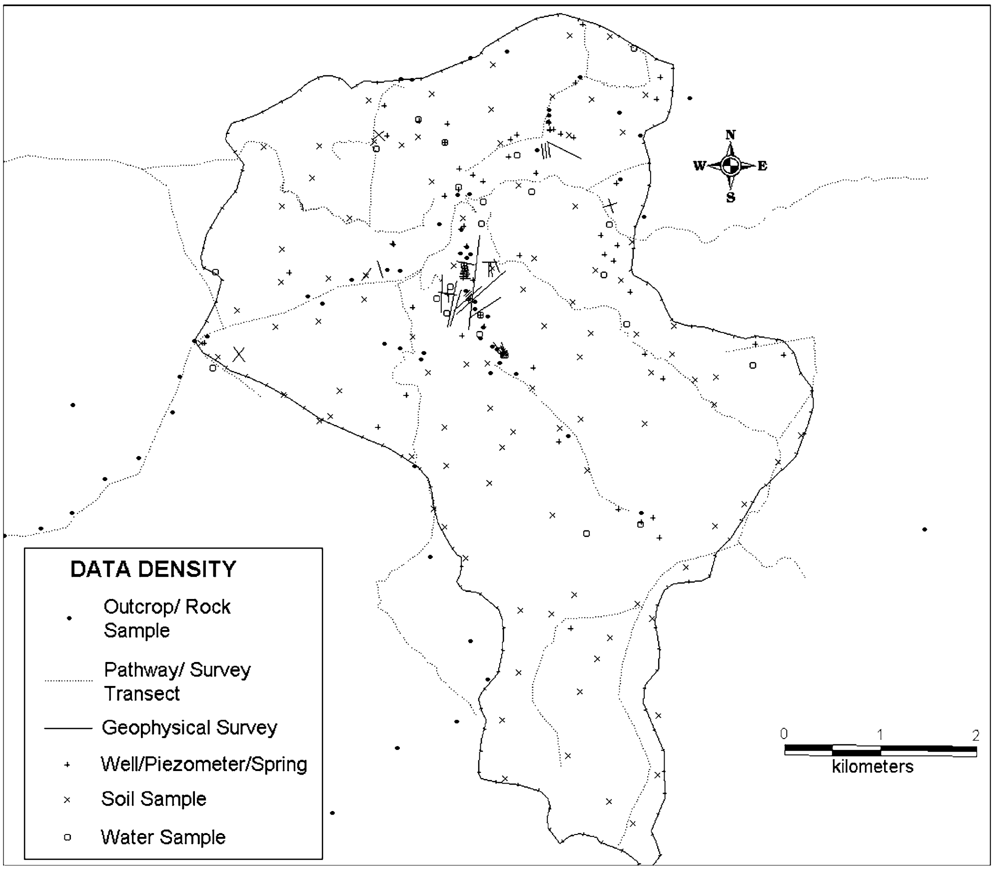

Fig. 4 Density of data collected for this vulnerability assessment

2.3×10^{-5} m/s in areas near a fractured basaltic dyke. Similarly, in hydraulic conductivity tests performed at the vicinities of the quartz veins areas, the observed values reached up to 2.8×10^{-5} m/s. Therefore, the hydraulic conductivities are expected to considerably increase along the quartz veins. Moreover, there are more than 2,800 m^3 of partly buried mining shafts and galleries along the north side of the basin, becoming another factor that locally contributes to increase the effective hydraulic conductivity.

Lineament influence

Fractures, faults and dykes (including quartz veins) were considered for the lineament influence analysis. The length, connectivity and density of lineaments were documented in field when possible and from aerial photointerpretation (scale 1:40,000). The length, connectivity and density were normalized independently and then combined in a single map shown in Fig. 5(*M*). The lineament influence was rated from 0 to 3.

GOD

Groundwater occurrence

The groundwater environment consists of weathering layers with heterogeneous material including coarse grained materials and weathered rock with high clay content. The contributions from coarse materials and clay weathered rock to the confinement of the aquifer are variable from hilltops to valleys. Ratings extending from 0.1, for horizons with higher clay contribution, to 1.0 for zones with major presence of fractured lava flow, were used to grade the different types of groundwater occurrence (see Table 1). Dykes and quartz filled fractures that were identified as active hydraulic zones during the field characterization were classified as unconfined units in this evaluation. Furthermore, a 20 m influence zone was delineated around veins and dykes as the weathering and fracturing extends out from the actual dyke bodies (Mendoza 2002). The youngest plug rock was classified 0.1 as neither fracturing nor advanced physical weathering is common there.

Table 1 Parameters and ratings used for DRASTIC and GOD, regarding the covered area

Parameter	Range/type	Rating	Area (km^2)
DRASTIC			
Depth to water (m) Weight = 5	0.0–1.6	10	8.6
	1.6–5.0	9	7.6
	5.0–10.0	7	6.4
	10.0–16.6	5	3.9
	16.6–25.0	3	1.5
	25.0–33.0	2	–
	33.0 +	1	–
Net recharge (mm) Weight = 4	0.0–50.8	1	–
	50.8–101.6	3	–
	101.6–177.8	6	–
	177.08–254	8	1.1
	254 +	9	26.9
Aquifer media Weight = 3	Igneus (Freshrock)	3	1.2
	Weathered igneous	4	21.7
	Weathered pyroclastics	6	1.0
	Basalt (Outcropping)	9	4.0
Soil media Weight = 2	Clay loam	3	4.3
	Clay	1	23.7
Topography (Percent slope) Weight = 1	0–2	10	1.6
	2–6	9	1.9
	6–12	5	7.5
	12–18	3	7.8
	18 +	1	9.2
Impact of vadose zone Weight = 5	Silt/clay	3	19.3
	Silt/clay with significant gravel	4	6.7
	Sand/gravel with significant silt and clay	6	1.4
	Lava flow	9	0.6
Hydraulic conductivity Weight = 3	5.7×10^{-6}–2.3×10^{-5} (clay and weathered rock)	1	23.1
	2.3×10^{-5}–10^{-4} (vicinities dykes and permeable basalt)	2	3.5
	$> 10^{-4}$ (river terraces)	6	1.4
Lineament influence	0.0–0.1	0	16.5
	0.1–0.5	1	9.1
	0.5–1.0	2	2.3
	1.0–1.5	3	0.1
GOD			
Groundwater occurrence	Non fractured (i.e. plugs)	0.1	1.2
	Unconfined	0.5	19.9
	Unconfined + fractured	0.6	4.7
	Unconfined + uncovered	1.0	2.2
Overlaying strata	Weathered zones	0.5	10.0
	Basalts + dykes	0.6	18.0
Depth to water	> 50	0.6	–
	20–50	0.7	0.9
	5–20	0.8	10.7
	< 5	0.9	16.4

Units in SI system

Overlaying strata

The lithological character of the overlaying strata was valued from 0.5 for the clay weathered materials to 0.6 for the fractured lava flows, which mostly outcrop in valleys and hilltops. All the dykes were rated as "igneous", 0.6.

Depth to groundwater

Most of the area has values from 0.7 (20–50 m) to 0.9 (< 5 m).

Results

Map layers related to each of the evaluated parameters were overlaid to produce a vulnerability map according to the corresponding evaluation method. The map layers for the different parameters used for DRASTIC are presented in Fig. 5 and the resulting vulnerability map is presented in Fig. 6. Low vulnerability areas cover approximately 13.9 km^2, moderate vulnerability areas represent 12.8 km^2 of the basin and areas with high vulnerability are mostly concentrated along the river valleys (1.3 km^2). There are no areas classified as having a very low and very high vulnerability.

The vulnerability map resulting from modifying DRASTIC to include the lineament influence is shown in Fig. 7. In this case, the vulnerability increased around the areas with geological structures, resulting in a 13% increase of areas with moderate vulnerability (14.3 km^2).

The resulting map using the GOD method is presented in Fig. 8. In this case, an area of 23.5 km^2 is classified as having a low vulnerability. Combined, moderate and high vulnerability areas cover around 4 km^2, mainly along major quartz veins, fractures and the river valley. The intrusive rocks represent small areas with negligible vulnerability.

Discussion

The maps resulting from DRASTIC and GOD methods differ in the vulnerability levels assigned to large extensions of the area. This can be explained by the different parameters and considerations involved in the map construction. DRASTIC considers more parameter which adds precision to the results (Gogu and Dassargues 2000; Rosén 1994) but can also suppress the relevance of particular factors in the vulnerability evaluation. Conversely, the simplicity of GOD allows for assigning higher values to a certain parameter according to the area characteristics but it can at the same time introduce bias into the indexing.

Fig. 5 Maps with all parameters used for DRASTIC index, including (*M*) lineament influence

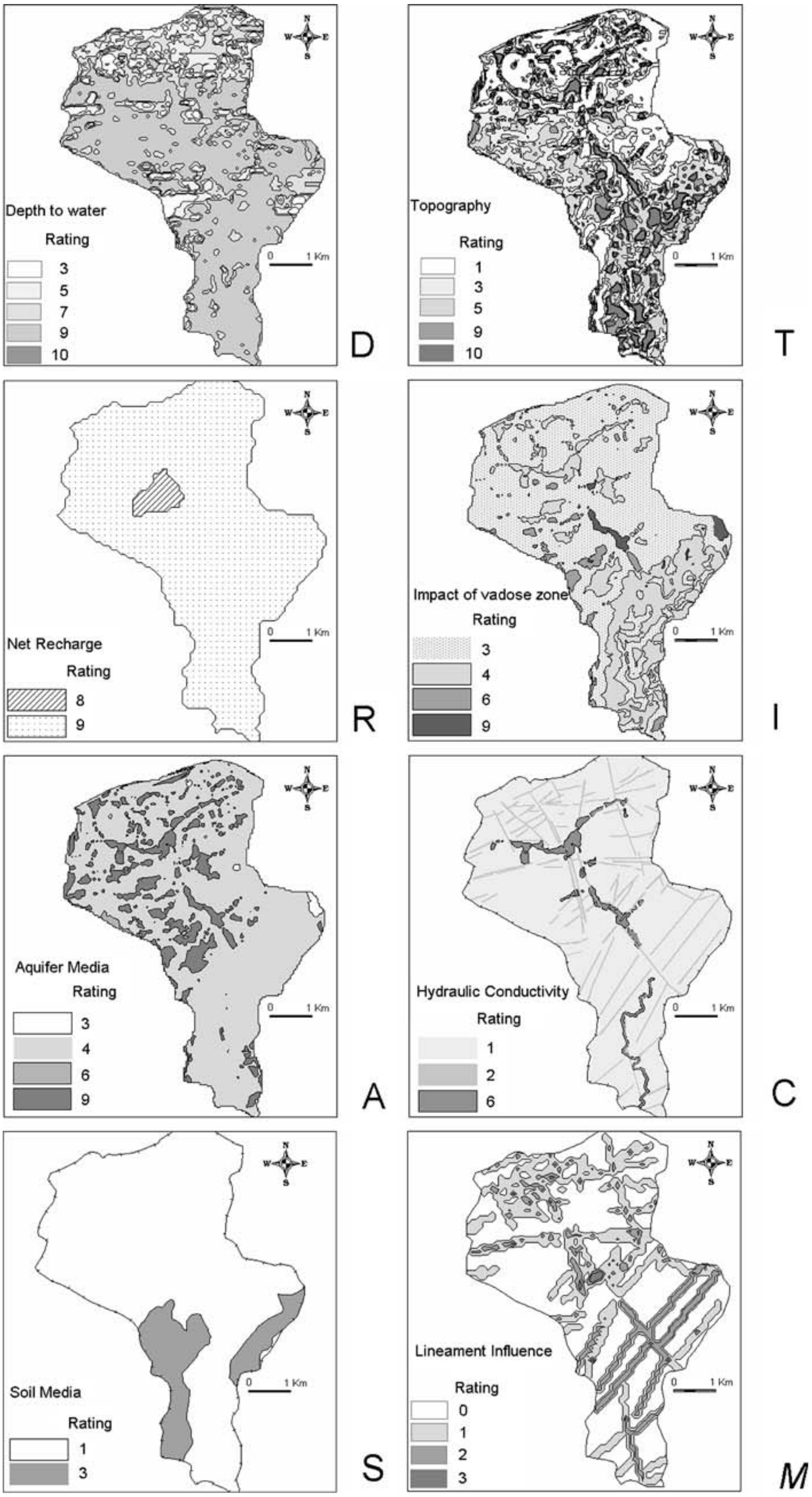

Fig. 6 Vulnerability map using DRASTIC

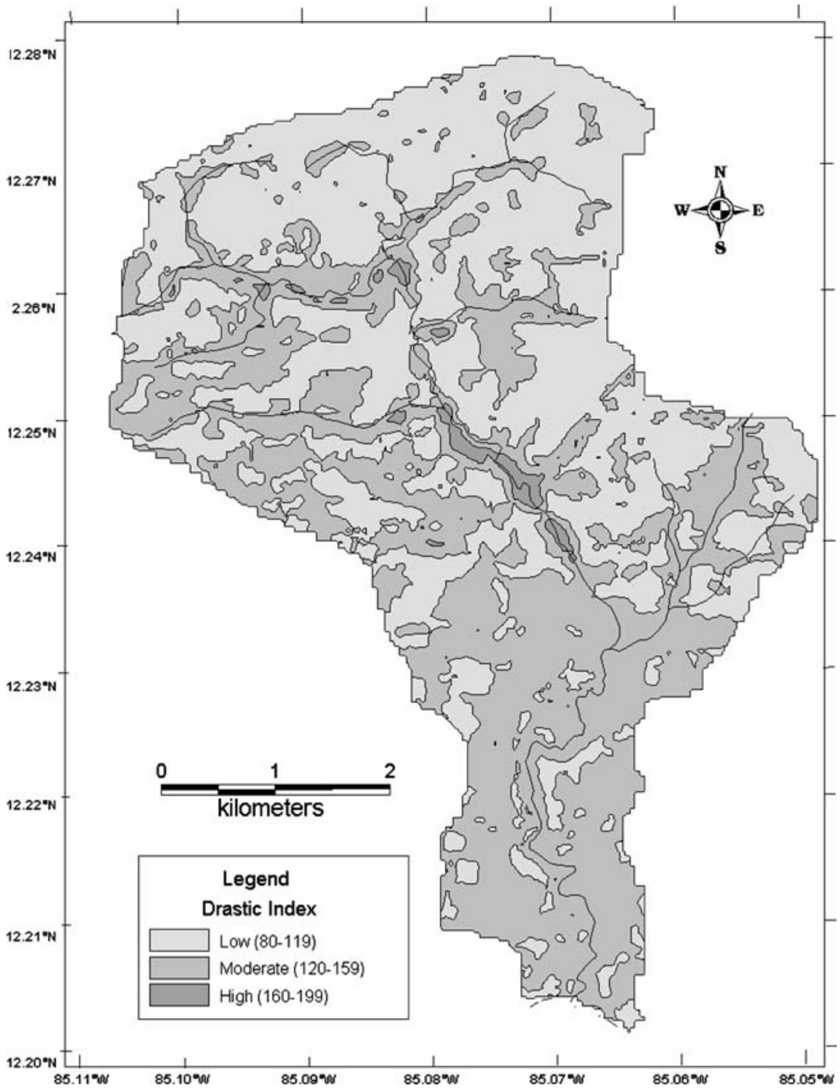

The main factors influencing the predicted vulnerability with the DRASTIC method are topography and depth to groundwater (see Table 1 and Fig. 5). The other parameters are not having strong influence as they change smoothly throughout the area. High slopes decrease the DRASTIC index, as theoretically a contaminant has less time to infiltrate at steep locations. Conversely, the south part of the basin exposes higher vulnerability as the slopes at those locations are less sharp. In the case of GOD, the depth to water was the parameter that had major influence in the overall result.

Distinguishing the vulnerability assigned to fractures/quartz veins from other materials by including the lineament influence in the DRASTIC index contributed to increase the predicted vulnerability index (See Fig. 7). Similarly, the relatively broad ranges related to the GOD ratings allowed to predict a relatively high vulnerability value for the highly fractured quartz vein areas (see Fig. 8).

The operation in underground mines can alter hydrogeological flow in highly fractured environments (Levens et al. 1994) and cause degradation of groundwater quality (Aller et al. 1987). However, both methods used in this research are designed to consider the vulnerability in relation to a contaminant released on the ground surface. Therefore, the results achieved here might underestimate the vulnerability with respect to contaminants released in the multiple shafts and galleries excavated in and around the gold bearing quartz veins.

In general, the hydraulic gradient induces groundwater discharge to the polluted river. However, previous works indicate that during periods of low precipitation the situation could be the inverse, with channel water infiltrating the near shallow aquifers due to a shift in the hydraulic

Fig. 7 Vulnerability map using the modified DRASTIC

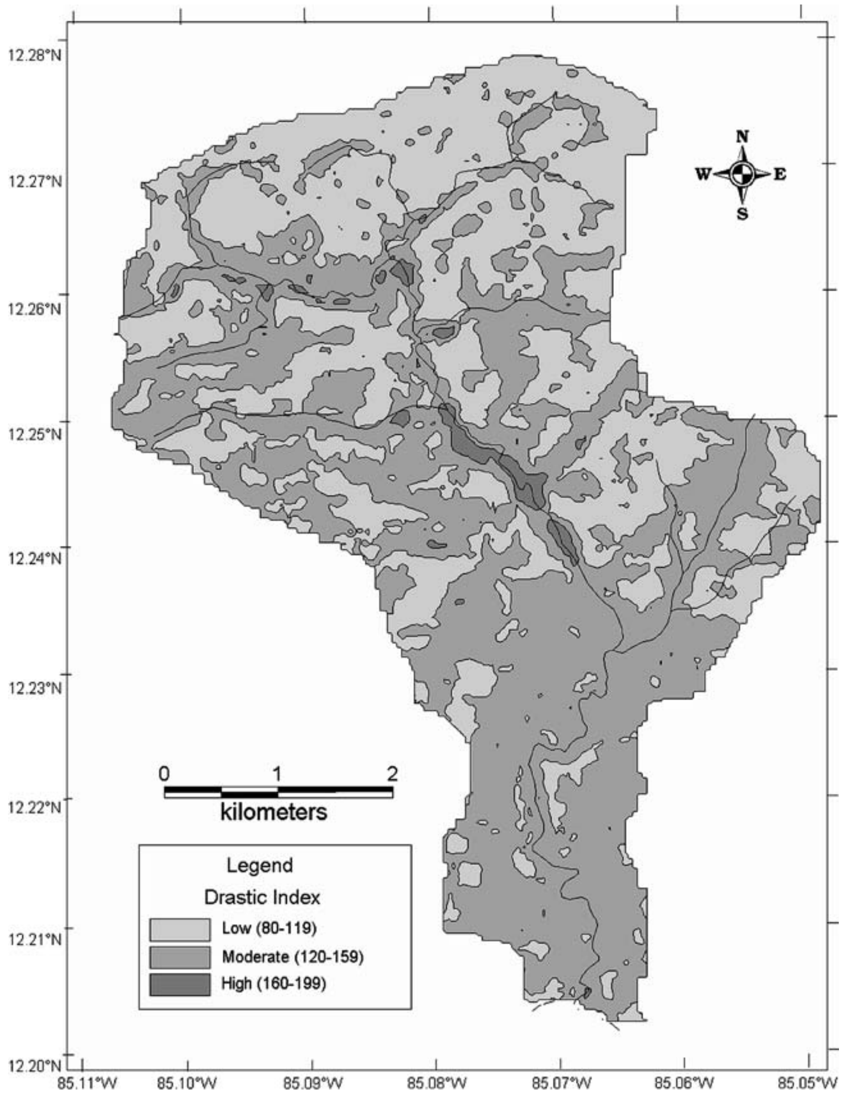

gradient (Grunander and Nordenberg 2004; Mendoza et al. 2004). This situation validates the relatively high vulnerability values assigned to the river valleys.

Conclusions

This work has compiled spatial data unavailable before developing the research project, except for historical precipitation records and geological background studies related to mining. The DRASTIC and GOD methods for vulnerability assessment were used to investigate potential groundwater vulnerability within the shallow aquifers composed of combined weathered horizons and fractured bedrock of the Río Artiguas basin. The DRASTIC index varied between 82 and 189, being classified into groups of low, moderate and high vulnerability. Moderate vulnerability areas cover most of the stream valleys and lowlands in the basin, with increasing vulnerability southwards. Including the lineament influence as an additional parameter in DRASTIC allowed for a better representation of the pollution potential associated with highly fractured areas.

The vulnerability assessment of the Río Artiguas area shows that the limited groundwater resources are susceptible to surface water pollution as areas with high vulnerability are concentrated along the river valleys. Therefore, those areas require special attention in a groundwater protection plan. Furthermore, a future risk assessment derived from these results might emphasize the risk in the valleys as household liquid wastes and mining tailings are continuously released into the streams.

There are large regions in Nicaragua where hydrogeological data are very limited and groundwater resources are under environmental stress. For those

Fig. 8 Vulnerability map using GOD

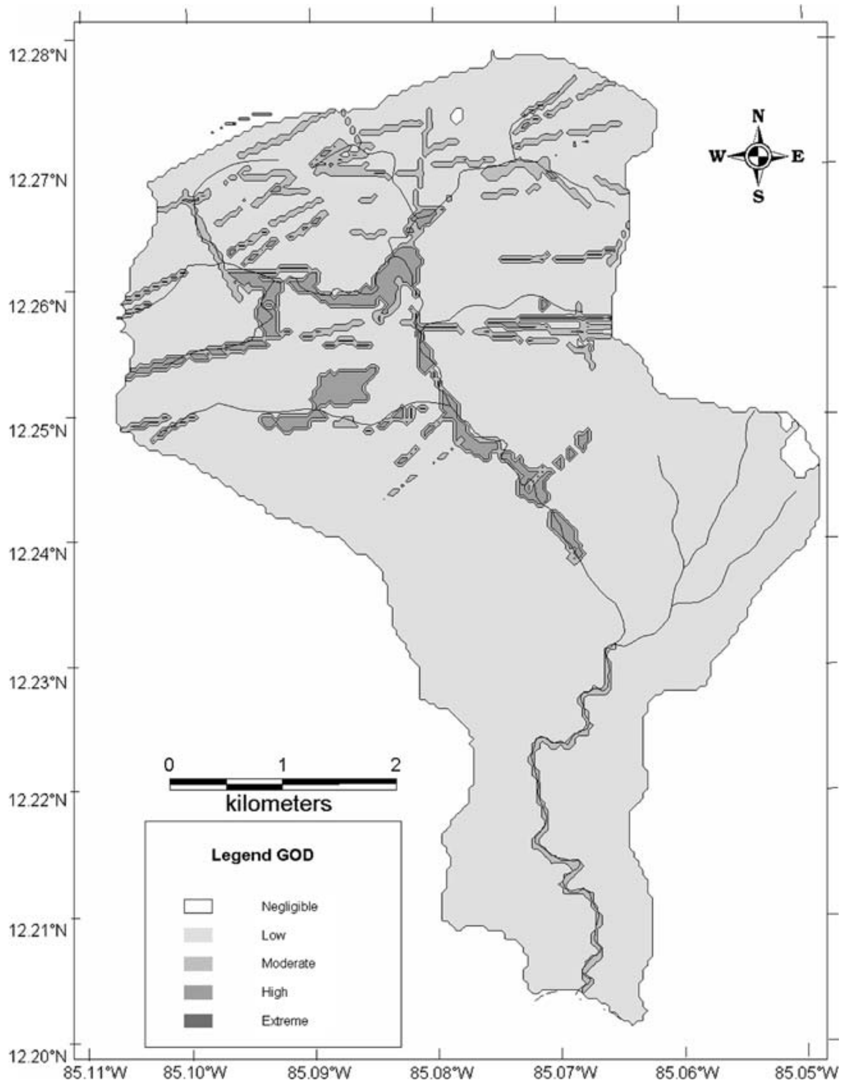

areas, the GOD method is an option that can provide a useful overview of the groundwater vulnerability until further hydrogeological data can be collected to produce more comprehensive vulnerability maps.

Acknowledgements This work was conducted as part of a multidisciplinary research program funded by the Swedish International Development Agency (Sida/SAREC). Technical and logistical support was provided by the Department of Engineering Geology at Lund University (Sweden) and Centro de Investigaciones Geocientíficas at UNAN-Managua, respectively. Dr. Torleif Dahlin offered valuable guidance. Emilio Pichardo, Meyling Herrera, Walter Espinoza, Martha Sánchez and Santiago Noguera collected important field data. Family *P*erez-*Mar*tínez is specially acknowledged as their assistance made fieldwork less difficult under the tropical conditions at Río Sucio. The contributions from three anonymous reviewers are acknowledged.

References

Aller L, Bennet T, Hehr JH, Petty RJ, Hackett G (1987) DRASTIC: a standardized system for evaluation groundwater pollution potential using Hydrogeologic Settings, U.S. Environmental Protection Agency, Ada. Ok, EPA/600/2-87-036, 455pp

Allison GB, Hugues MW (1978) The use of environmental chloride and tritium to estimate total recharge to an unconfined aquifer. Aust J Soil Res 16:181–95

Civita M, De Maio M (2004) Assessing and mapping groundwater vulnerability to contamination: The Italian "combined" approach. Geofísica Int 43(4):513–532

Civita M, De Regibus C (1995) Sperimentazione di alcune metodologie per la valutazione della vulnerabilità degli aquiferi (in Italian). Quad Geol Appl Pitagora Ed Bologna 3:63–71

Corniello A, Ducci D, Napolitano P (1997) Comparison between parametric methods to evaluate aquifer pollution vulnerability using GIS: an example in the "Piana Campana", southern Italy. In: Marinos PG, Koukis GC, Tsiambaos GC, Stournaras GC (eds) Engineering geology and the environment. Balkema, Rotterdam, pp 1721–1726

Darce M (1990) Mineralogic alteration patterns in volcanic rocks of the La Libertad gold mining district and its surroundings, Nicaragua. Econ Geol 85:1059–1071

Davis AD, Long AJ, Wireman M (2002) KARSTIC: a sensitivity method for carbonate aquifers in karst terrain. Environ Geol 42(1):65–72

Deutsch CV, Journel AG (1992) GSLIB geostatistical software library and user's guide. Oxford University Press, New York

Desbarats AJ, Logan CE, Hinton MJ, Sharpe DR (2002) On the kriging of water table elevations using collateral information from a digital elevation model. J Hydrol 255:25–38

Dixon B (2005) Groundwater vulnerability mapping: a GIS and fuzzy rule based integrated tool. Appl Geogr 25(4):327–347

Ehrenborg J (1996) A new stratigraphy for the Tertiary volcanic rocks of Nicaraguan Highlands. Geol Soc Am Bull 108(7):830–842

Foster SSD (1987) Fundamental concepts in aquifer vulnerability, pollution risk and protection strategy. In: van Duijvenbooden W, van Waegeningh HG (eds) TNO Committee on hydrological research, The Hague. Vulnerability of soil and groundwater to pollutants, Proc Inf 38, pp 69–86

Forster CB, Evans JP (1991) Hydrogeology of thrust faults and crystalline thrust sheets: results of combined field and modeling studies. Geophys Res Lett 18(5):979–982

Foster SSD, Hirata R, Gomes D, D'Elia M, Paris M (2002) Groundwater quality protection; a guide for water utilities, municipal authorities and environment agencies. The World Bank, Washington, p 103

Gaye CB, Edmunds WM (1996) Groundwater recharge estimation using chloride, stable isotopes and tritum profiles in sands of northwestern Senegal. Environ Geol 27:246–251

Gogu RC, Dassargues A (2000) Current trends and future challenges in groundwater vulnerability assessment using overlay and index methods. Environ Geol 39(6):549–559

Gogu RC, Dassargues A (2003) Comparison of aquifer vulnerability techniques. Application to the Néblon river basin (Belgium). Environ Geol 44:881–892

Goovaerts P (1997) Geostatistics for natural resources evaluations. Oxford University Press, New York

Grunander K, Nordenberg L (2004) Investigation of groundwater–surface water interaction in the drainage basin of the River Sucio, Nicaragua, MSc thesis, ISRN LUTVDG/TVTG-5090-SE, Lund University, Sweden, p 92

Hodgson G (1972) Mapa Geológico de La Libertad [Geological map of La Libertad] Catastro e Inventario de Recursos Naturales. Managua, Nicaragua (in Spanish)

Ibe KM, Nwankwor GI, Onyekuru SO (2001) Assessment of ground water vulnerability and its application to the development of protection strategy for the water supply aquifer in Owerri, Southeastern Nigeria. Environ Monit Assess 67:323–360

INETER (1973) Estudio Edafológico de la Cuenca del Río Escondido [Edaphology study of the Río Escondido basin]. Instituto Nicaragüense de Estudios Territoriales- Ministerio de Agricultura y Ganadería Departamento de Suelos y Taxonomía/Catastro, Nicaragua (in Spanish)

INETER (1991) Anuarios Meteorológicos (1990–1991) [meteorological charts]. Managua, Nicaragua (in Spanish)

Levens R, Williams R, Ralston D (1994) Hydrogeologic role of geologic structures. Part 1: The paradigm. J Hydrol 156(1–4):227–243

MapInfo (2000) Mapinfo professional ver. 6.0 software documentation. New York

Mendoza JA (2002) Geophysical and hydrogeological investigations in the Rio Sucio watershed, Nicaragua. Lic Thesis ISBN 91-972406-0-X, Lund University, Sweden, 60pp

Mendoza JA, Bjelm L, Dahlin T (2000) resistivity imaging as a tool for groundwater studies at Santo Domingo, central Nicaragua. Paper presented at the EEGS Bochum, Germany, 7–14 September 2000

Mendoza JA, Dahlin T, Barmen G (2004) Use of resistivity imaging in a surface water–groundwater interactions study. Paper presented at the XXXIII Congress IAH - 7° ALHSUD, Zacatecas City, Mexico, 11–15 October, 2004

Mendoza JA, Dahlin T, Barmen G (2005) Hydrogeological and hydrochemical features of an area polluted by heavy metals in central Nicaragua. Hydrogeol J. DOI 10.1007/s10040-005-0462-5

Rosén L (1994) A study of the DRASTIC methodology with emphasis on Swedish conditions. Ground Water 32(2):278–284

Secunda S, Collin ML, Melloul AJ (1998) Groundwater vulnerability assessment using a composite model combining DRASTIC with extensive agricultural land use in Israel's Sharon region. J Environ Manage 54:39–57

Vrba J, Zaporozec A (1995) Guidebook on mapping groundwater vulnerability. IAH, Int. Contrib. to Hydrogeol., 16 (1994). Heise, Hannover, p 131

Weinberg RF (1992) Neotectonic development of western Nicaragua. Tectonics 11:1010–1017

V

Mendoza JA, Cuadra S, Picado F, Barmen G, Jakobsson K, Bengtsson G. Ecological, groundwater and human health risk assessment in a mining region of Nicaragua. (Manuscript)

Ecological, Groundwater and Human Health Risk Assessment in a Mining Region of Nicaragua

Mendoza JA[1,2], Cuadra S[1,3], Picado F[1,4], Barmen G[2], Jakobsson K[3], Bengtsson G[4].

[1] Universidad Nacional Autónoma de Nicaragua, Apartado Postal 663, Managua Nicaragua
[2] Department of Engineering Geology, Lund University, 22100 Lund, Sweden
[3] Department of Occupational and Environmental Medicine, 221 85 Lund , Sweden.
[4] Department of Ecology Lund University, 22362 Lund, Sweden

---

Abstract

Risk assessment in disciplines like engineering, ecology and human health, is practically conducted independently from considerations to risk as regarded in other disciplines. This work attempts to integrate ecological, groundwater and human health risk assessments to mercury emissions. The relative risk of damages to stream biota, local inhabitants, and groundwater was calculated using hazard quotient approaches. When comparing our results a relatively higher risk from Hg emission is found for aquatic organisms, followed by groundwater and human health.

Key words: Risk; Human health risk; environmental risk; groundwater risk; pollution; mercury

---

Introduction

Risk assessment is the process by which the probability and magnitude of adverse effects is evaluated as a result of exposure to one or more stress factors. Risk assessment can be used to predict, compare, and manage environmental risk, and provide a quantitative basis for preventive or remedial action under uncertainty. One of the objectives of risk assessment is to compare and evaluate the realisation of different sources of hazard and weigh the benefits of reducing or eliminating the risk versus those of accepting it. For instance, environmental and human exposure to toxic chemicals can often be characterized by low doses of multiple chemicals, and a major challenge is to assess the potential risk from largely single-chemical databases. Although practical methods for the evaluation of the assumption of additivity of multiple chemicals have been developed, regulating authorities evaluate each chemical individually, and mixture effects are only considered via safety factors. Similarly, risk assessment in different disciplines, such as economics, engineering, environmental and human health risk, is practically conducted independently, but some efforts have been made to integrate them (Harvey et al., 1995; Cirone and Duncan, 2000; WHO, 2001; Suter, 2004).

One dimension for integration is the spatial scale. Ecological and human health risk assessment can be accommodated on a small, local scale level, e.g. when microbial soil respiration and blood levels of benzene in workers on a gasoline station are used as assessment endpoints, but preferably on a larger, e.g. watershed, level when they are integrated with groundwater vulnerability assessment. A watershed approach unifies the evaluation of the impacts of industrial discharges and agricultural activities on water quality, biota, and human welfare, and may be used to identify habitats, subareas, and communities within a region most at risk. Different models have been used to evaluate and compare risk at larger geographical areas, e.g. the Relative Risk Model (Landis and Weigers, 1997) combined with tiered procedures (Moraes and Molander, 2004), and weight-of-evidence approaches (Lowell et al., 2000).

Here we calculate the relative risk of mercury, released by gold mining in a Nicaraguan watershed, to stream biota, local inhabitants, and groundwater using hazard quotients approaches. Those are essentially applicable to large as well as small areas, they assume that toxicity can be obtained relative to a reference chemical, and they allow the comparison of risk from exposure to different stress factors (Zhang et al., 2001). The quotients are not measures of risk in a statistical sense, but when they are above 1.0, there are concerns about potential risks of adverse effects. The quotients are useful for screening purposes and can be evaluated as the probability of exceeding 1.0, but the values do not reflect effects on population-based metrics and are usually non-linear above 1.0 (Eaton and Klaassen, 1996; Kolluru, 1996).

In many developing countries in Central America, South America and Africa, mercury is used for amalgamation in mining of gold and other metals. Although gold mining plays an important role in the economic development, rural ecosystems in which mining activity has taken place have undergone dramatic deterioration (Salomons, 1995; Moreira, 1996). For instance, for more than one century the Sucio River located in central Nicaragua has received wastes containing mercury, lead, and cyanide from the gold mining industry in Santo Domingo and La Libertad, but also from artisanal activity (Belt, 1874). About 40 tons of mercury and 10 tons of lead have been released into the environment during the past 100 years of mining activity in Santo Domingo and La Libertad. Mercury concentrations in the Sucio River water are almost one order of magnitude higher than the permissible concentrations for human consumption (WHO, 1996), and the sediments are contaminated as far as 50 km downstream from the La Estrella plant (André et al., 1997). Metallic mercury is lost to the atmosphere through evaporation when gold particles in crushed ores are amalgamated with mercury, and when amalgam is burned. The frequency of burning was correlated with the levels of mercury in the blood (B-Hg) of gold miners and administrative workers (Cuadra et al., 2005). In general the B-Hg levels were much lower than those reported from others mining areas in Latin America, but they are in the same range as recent reports from others gold mining areas in Nicaragua. Occupational activities clearly influenced B-Hg levels in the miners and their families, whereas no correlation was observed between B-Hg and fish consumption. The general population sample from Santo Domingo had higher B-Hg levels than referents from a neighbouring mining town where Hg has not been used during the last 15 years. However, the risk for the general population without occupational or domestic mercury exposure needs to be better characterized.

The aim of this work was twofold: 1) to assess the risk of adverse effects of mercury on a) groundwater quality, b) the river ecosystem and especially fish, and c) humans in the watershed associated with the River Sucio; 2) use the assessment as a basis for recommendations on reducing and managing the environmental risks in the watershed.

Area description

The study area is a 28 km^2 basin located 177 km from the capital of Nicaragua, Managua. The Sucio River drains from North to South meandering along the steep topography of the basin. The altitude ranges from 400 m in the south to 800 m in the north. The tropical savannah climate meets with a tropical humid climate in this basin. There is a long rainy season, from May to December, and a dry season the rest of the year. The average precipitation is 2400 mm/yr (INETER, 1991), and the yearly temperature varies from 15 ℃ to 34 ℃ with humidity up to 80 % (Fig. 1).

The land use in the basin is primarily for cattle and crops for domestic consumption. There are sparse zones with rainforest, mainly along the stream valleys and near the springs. More than half the population in the basin (ca. 13000 inhabitants) live in the countryside areas. For these people, spring water or stream water is the most common source of domestic water.

Methodology

Groundwater risk assessment

The groundwater risk is regarded as a combination of the intrinsic vulnerability, the pollution hazards, and the socioeconomic value that water has for a given population or economic activity. This means that a combination of three maps; the vulnerability map, the hazard map, and the socioeconomic value map can be used to construct a risk map of groundwater pollution. The method used in this evaluation is adapted from Civita and De Maio (1997) and Ducci (1999) to the particular case of pollutants released from artisanal and small scale mining.

The vulnerability assessment used for this work was a modified version (Mendoza and Barmen, 2006) of the method DRASTIC (Aller et al., 1987). The method used the original seven parameters (depth to groundwater (D), net recharge (R), aquifer media (A), soil media (S), topography (T), influence of the vadose zone (I), hydraulic conductivity (C)) plus an additional parameter for the degree of fracturing, which is regarded as a factor enhancing the pollution transport. The map of vulnerability is presented in Figure 2a.

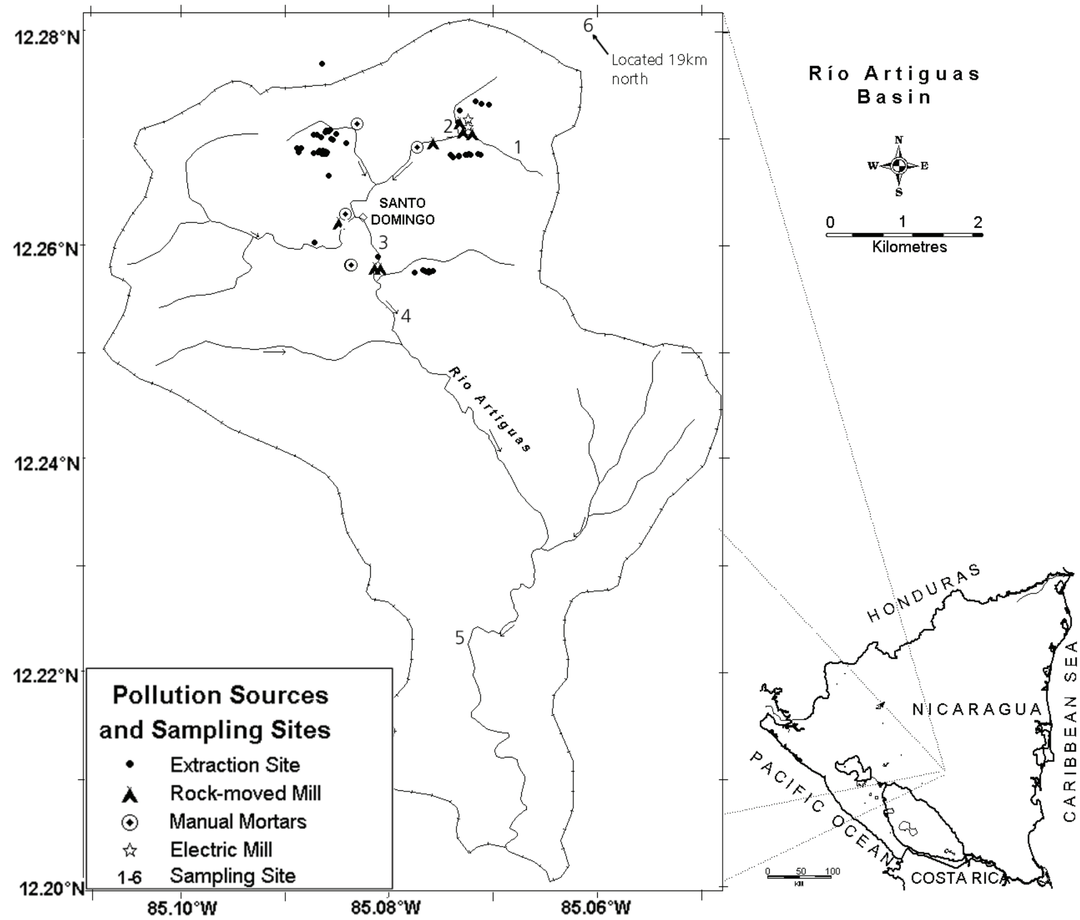

Fig. 1 Map of Río Artiguas (Sucio) basin showing the sampling points and pollution sources

The pollution hazard is identified as the mining mills, where Hg is used in the amalgamation process. There are different kinds of processing methods for gold refinement used in the area and each of them uses different amounts of Hg. Each plant or mill represents a different hazard since they use different methods for gold extraction. Every hazard has been ranked in the Danger of Contamination Index (DCI) (Table 1).

Table 1. Danger of Contamination Index (DCI) assigned to different methods for gold refining

DCI	Pollution source
1	Areas of the basin where mining has not been reported and there are no polluted sources of water
4	Tailings disposed at areas with groundwater discharge
5	Former mining areas
6	Current mining areas where Hg is occasionally handled
7	Manual mortar, commonly located by a stream
8	Mill moved by rocks
9	Electric mill and polluted river

There are 99 perennial springs and a few dug wells in the basin. A socioeconomic value was assigned to each catchment that supplies water to a given well or spring. The assigned value was based on the size of population using the water source and the commercial value (Table 2).

Table 2. Socioeconomic value classes (from Ducci 1999). Classes higher than medium are not included since they were not present in the area.

Class of the value	Description of the catchment
Medium	Well or spring supplying a population between 1000 and 10000 inhabitants or an industry with 10 to 99 workers.
Low	Spring supplying less than 1000 inhabitants or an industry with less than 10 workers

The criteria for linking the three maps (vulnerability, hazards and socio-economic values) were expressed in cross-tables (Civita and De Maio, 1997) (Table 3). The values for danger of contamination (Table 1), socioeconomic class (Table 2) and vulnerability are used to assign the risk value to every 50 x 50 m cell in the risk map.

Table 3. Cross-tables to evaluate the groundwater contamination risk (from Ducci, 1999). V: vulnerability degree; Vr:socioeconomic value; DCI:Danger of contamination index: vl: very low; l:low; m:medium; h: high; vh:very high; eh:extremely high.

V→	Very low				Low				Medium				High				Very high				Extremely high			
Vr→ DCI↓	l	m	h	vh	l	m	h	vh	l	m	h	vh	l	m	h	vh	l	m	h	vh	l	m	h	vh
1								vl			vl	vl			vl	l	vl	vl	l	m	vl	vl	m	h
2			vl			vl	vl	vl	vl	vl	vl	l	vl	vl	l	m	vl	vl	m	h	l	l	m	h
3	vl	vl	vl	vl	vl	vl	vl	l	vl	vl	l	l	vl	vl	l	m	vl	l	h	h	l	m	h	vh
4	vl	vl	vl	vl	vl	vl	l	l	vl	l	l	m	vl	l	m	h	l	m	h	vh	l	m	h	vh
5	vl	vl	l	l	vl	vl	l	m	vl	l	l	m	l	l	m	h	l	m	h	vh	l	h	vh	vh
6	vl	vl	l	m	vl	l	l	m	l	l	m	h	l	m	h	vh	l	h	vh	vh	l	h	vh	vh
7	vl	l	l	m	l	l	m	h	l	m	h	vh	l	m	h	vh	l	h	vh	eh	m	vh	vh	eh
8	l	l	m	h	l	l	h	vh	l	m	h	vh	l	h	vh	eh	m	vh	vh	eh	m	vh	eh	eh
9	l	m	h	vh	l	m	vh	eh	m	h	vh	eh	m	vh	eh	eh	m	eh	eh	eh	h	eh	eh	eh

Concentrations of Hg were determined in a group of spring water samples by inductively coupled plasma mass spectroscopy (ICP-MS). The results were then used to calculate the Hazard Quotient (HQ) for groundwater, estimated as the ratio between the Hg concentration found in the spring and the guideline of 1 μg l^{-1} for drinking water (WHO, 1996).

Ecological risk assessment

Frequency distributions of both water and sediment Hg concentrations were obtained from hourly water sampling at six sites along Sucio River and from the top 20 cm of sediment cores from the same sites. Hg was determined by ICP-MS. The BestFit 2.0d (Palisade Inc.) was used to fit probability distributions to the data. The aqueous concentrations of Hg were compared with both the acute toxicity of 2.4 μg l^{-1} and the chronic effect of 0.012 μg l^{-1} (96 h) criteria for freshwater aquatic life protection (USEPA, 1985). The interim sediment quality guidelines (ISQGs) for total Hg of 0.17 μg g^{-1} dry weight(dw) and the probable effect levels (PELs) of 0.486 μg g^{-1} dw in Canadian sediment quality guidelines for freshwater aquatic organism protection (CEQC/CCME, 1999) were used as benchmarks to deduce the HI for sediment.

The HI related to waterborne (C_w) and sediment bound (C_s) Hg was defined as: $HI_w = C_w / C_{w\ (\mathrm{guideline})}$ and $HI_s = C_s / C_{s\ (\mathrm{guideline})}$ respectively. $HI_w < 1$ infers that Hg concentrations in the river water are unlikely to give fatal or sublethal effects (survival, bioconcentration, etc) on sensitive species (0.012 µg l^{-1} is used as benchmark). When the guideline of 2.4 µg l^{-1} is used, it indicates the occurrence of fatal effects on sensitive aquatic organism; $RI_w = 1$ suggests a risk exits; $RI_w > 1$ indicates that most aquatic organisms including fish are threatened, and sensitive species undergo fatal and sublethal effects.

Hg content in fish was estimated using the lowest value of bioconcentration factor (BCF) reported by the literature (USEPA, 1985; WHO, 1990) for total inorganic Hg. BCF is defined as the ratio of Hg concentration in fish (C_{fish}) to its concentration in the river water (C_w). The methylmercury content in fish was assumed to be 80% of the total Hg (Huckabee et al, 1979; Bloom, 1992).
With the assumption that BCF does not change over time, the exposure to Hg in fish was expressed as

C_{fish} = BCF*C_w ; C_w (µg l^{-1}), where BCF = 1800 l kg^{-1} (USEPA, 1985; WHO, 1990).

Human risk assessment

People involved in gold mining and gold processing may have elevated inorganic Hg levels (Eisler, 2003, WHO, 1991). However, people in general are primarily exposed to methylmercury through the diet, especially fish, even when low fish consumption is assumed, and to elemental Hg vapours due to dental amalgams (Tchounwou et al., 2003; ATSDR, 1999).

The PDI (mg/(kg.day))was calculated from the total Hg fresh fish concentration (C_{fish}, µg/kg), the fish ingestion rate, FIR (kg/day), and the human body weight BW (kg). Data for FIR were the per capita fish consumption in the United States (USEPA, 2001) and the BW data came from the Santo Domingo inhabitants (n = 302).

PDI = C_{fish}*FIR/BW = BCF*C_w*FIR/BW, then the risk for human health related to consumption of Hg contaminated fish (*RFC*) is:

$$RFC = \mathrm{PDI}/\mathrm{TDI}$$

Similar procedures was followed to deduce the risk for human related to consumption of Hg contaminated fish using total Hg concentration quantified in 7 fishes caught in the Río Sucio (*RFC´*).

Data for total blood Hg in adults and children in non-miner´s families living in Santo Domingo (N=70), or in La Libertad, a mining community where Hg had not been used for amalgamation during the last 15 years (N=50), were obtained from (Cuadra, et al 2005) (Table 4). Data was also available from consumers of locally caught fish, living in Muelle de los Bueyes downstream the Santo Domingo area, (N=30), (Cuadra, 2006). The latter group was selected among female consumers of locally caught fish. Even if substantial additional contributions to the intake of total Hg can occur through air and water depending on the local Hg pollution load (ATSDR, 1999), we have assumed that the total blood Hg concentration is due mostly to the dietary intake of organic forms, particularly of methyl Hg (USEPA, 2001). Observed blood Hg levels were compared to a benchmark dose (BMD), derived from an analysis on a number of endpoints from three longitudinal prospective studies: the Seychelles Islands, the Faroe Islands, and the New Zealand studies (NRC, 2000).

At equilibrium, the concentration of Hg in blood reflects the daily intake (WHO, 1990). The accumulation and excretion of methyl Hg in humans measured in term of blood levels can be represented by a single-compartment model (WHO, 1990). The accumulation phase in the whole body or in a tissue compartment is described by the equation $A = (a / b)\,(1-\exp(-b \times t))$, where A= the accumulated amount, a= the daily uptake in the body (or organ), b= the elimination constant, and t= time. The elimination constant is related to the biological half-time ($T_{1/2}$) by the expression $T_{1/2} = \ln 2 / b$, and a is related to the daily dietary intake (d) by the expression $a = f \times d$, where f is the fraction of the daily intake taken up by the body (or organ). At a steady state, the accumulated amount (A) is given by A= a/b.

The steady-state Hg concentration in blood (C) in µg/l is related to the average daily dietary intake (in µg Hg) as follows

$$C = \frac{f \times d}{b} = \frac{0.95 \times 0.05 \times d}{0.01\,\text{days}^{-1} \times 5\,\text{litres}} = 0.95 \times d$$

It is assumed that 0.95 of the intake is absorbed, that 0.05 of the absorbed amount goes to the blood compartment, that the blood volume is around 8 % of the total body weight (5 litres in a 60 kg-subject) , and the elimination constant is 0.01 days^{-1}(WHO 1990). Then, the result is divided by the individual body weight (b.w.). Thus, the daily Hg intake was approximated from concentration data.

The hazard quotient (HQi) was defined as the radio between the estimate of chronic daily Hg intake and a methylmercury reference dose (RfD) (USEPA, 1989). The US Environmental Protection Agency (EPA) derived a RfD of 0.1 µg/kg/day for methylmercury in 2001, based on an extensive analysis by the National Research Council (NRC) of the National Academy of Sciences (NRC, 2000, Rice et al., 2003).The risk of having a hazard quotient (HQ_i) higher than one was estimated using odd ratios (OR) and 95% confidence intervals (95% CI) calculated by logistic regression (SPSS for Windows version 12.0.1). Age, sex, number of dental amalgams and fish consumption were considered as potential covariates. The change-in-estimate-method suggested by Greenland (1989) was used, with 10% change required for inclusion and 5% change for exclusion.

Table 4. Study subjects and background information (adapted from Cuadra et al. 2005; Cuadra, 2006)

Variables	**Santo Domingo[1] n=72**	**La Libertad[2] n=40**	**Muelle de los Bueyes[3] n=30**
	n (%)		
Sex			
Females	40 (55.6)	20 (50)	30 (100)
Males	32 (44.4)	20 (50)	
	Median (range)		
Age	27 (5-72)	27 (5-78)	20.5 (15-25)
Weight	59 (17-111)	52.5 (20-91)	56.5 (47-65)
		n (%)	
Eating fish (from all sources)	61 (85%)	33 (83%)	30 (100%)
(fish meals/week)		*Median (range)*	
	4 (1-7)	4 (1-7)	3 (1-7)
		n (%)	
Eating locally caught fish	36 (50%)	23 (58%)	30 (100%)
(fish meals/week)		*Median (range)*	
	4 (1-7)	4 (1-7)	3 (1-7)

[1]**Santo Domingo**, a small scale gold mining town in central Nicaragua, where Hg is still used for gold extraction.
[2]**La Libertad,** an equal size gold mining town where Hg has not been used during the last 15 years, located 10 Km west from Santo Domingo.
[3]**Mueye de los Bueyes**, located 50-70 km east from Santo Domingo and la Libertad. Populations from area consume fish from Mico and Rama rivers, which receive contribution from effluents originated at Santo Domingo and La Libertad area.

Results

In general, medium vulnerability areas cover most of the stream valleys and lowlands in the basin, with increasing vulnerability southwards (Figure 2a). The variability of vulnerability in the basin is mostly due to the steep topography and depth to groundwater. Areas with steep topography are less vulnerable to infiltration of pollutants than plain areas. The areas with medium socio-economic values coincide with those with the greatest hazard (largest DCI), that is, where the mining areas and the mills are located (Figure 2b). The risk map identifies some spots with a very high risk, such as the gold refining plants, and larger areas with a very low risk, e.g. where mining has been abandoned (Figure 2d). Most of the polluted river channel represents a medium level of risk.

The HI is low in most of the springs indicating that the pollution has not reached the springs and areas far away from the village and it is mostly concentrated around the gold refining plants and along the river. In all sampled springs, the concentrations of Hg are below the guideline of 1 μg l^{-1} for drinking water (WHO, 1996), and differ from the relatively higher concentrations found in the streams. The highest concentration (0.336 μg l^{-1}) was found in stream water near the largest pollution source in Santo Domingo.

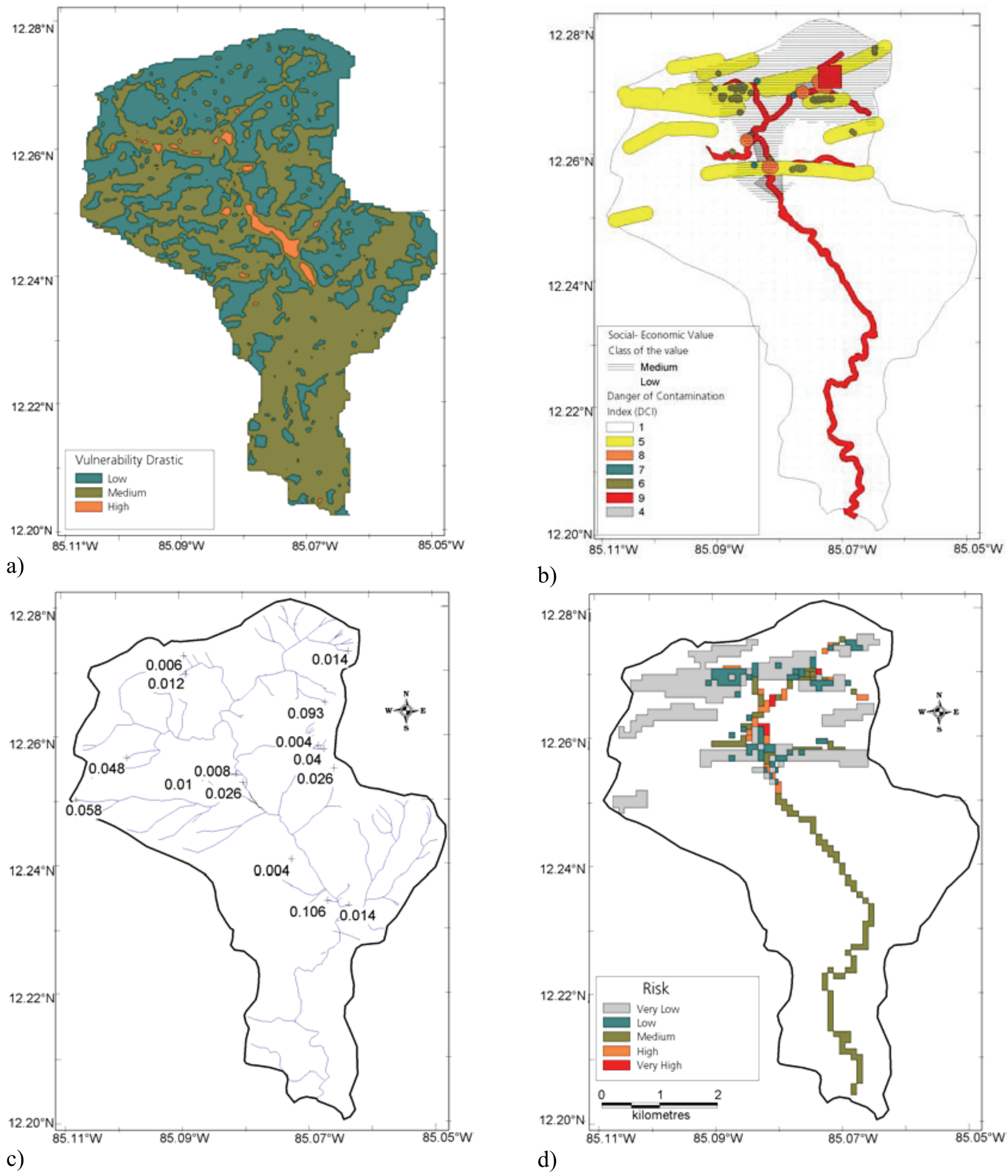

Fig. 2 Maps used for characterisation of the groundwater pollution risk a) Vulnerability map, b) the hazard and socioeconomic value map c) map with Hazard Quotient for the springs and d) the risk map.

Log-normal probability distributions were best (chi-square ranking) describing the observations of Hg concentrations in water and sediment at the six sites in the river, except in two cases when few data were available and uniform distributions were assumed.

The probability that Hg concentrations in the river water would exceed the guideline of 0.012 µg l^{-1} was 100% at all sites but less than 9% with respect to the acute toxicity guideline of 2.4 µg l^{-1} (Table 5). The probability that the sediment concentrations would exceed the guideline was 75% or higher, except at the most remote site (Table 7).

The risk that human health would be adversely affected by methylmercury concentrations in consumed fish-was less than 5% (Table 8).

Table 5. Probability density functions (PDF) for the parameters used to calculate the RQ's of ecological concern.

			PDF parameters		
Input variables	**Symbol**	**PDF**	**Mean (S. Dev)**	**Min.**	**Max.**
Water Hg concentration ($\mu g\ l^{-1}$)	C_w				
Site 1		Uniform		0.03	0.28
Site 2		[a]Lognormal truncated	1.07 (0.91)	0.30	4.92
Site 3		[a]Lognormal truncated	0.20 (0.17)	0.04	0.60
Site 4		[a]Lognormal truncated	0.61 (0.82)	0.05	2.19
Site 5		[a]Normal truncated	0.18 (0.07)	0.02	0.31
Site 6		Uniform		0.03	0.06
Sediment Hg concentration ($\mu g\ g^{-1}$ dw)	C_s				
Site 1		[a]Lognormal truncated	0.28 (0.16)	0.1	0.43
Site 2		[a]Lognormal truncated	4.35 (3.11)	2.05	7.88
Site 3		[a]Lognormal truncated	5.59 (0.66)	4.86	6.17
Site 4		[a]Lognormal truncated	9.10 (1.75)	7.71	11.07
Site 5		[a]Lognormal truncated	0.98 (0.21)	0.75	1.14
Site 6		[a]Lognormal truncated	0.07 (0.01)	0.07	0.08
Water Hg concentration-all sites ($\mu g\ l^{-1}$)	C_w	[a]Lognormal truncated	0.52 (0.75)	0.02	4.92
Fish Hg concentration ($\mu g\ kg^{-1}$ w.w)	C_{fish}	Uniform	233 (154)	30	420
Fish ingestion rate (kg day^{-1})	FIR	[a]Lognormal truncated	0.0001(0.0001)	0.0	0.1
Human body weight (kg)	BW	[a]Normal truncated	54.8 (19.9)	1.0	111.0

[a]Distributions were truncated at the minimum and maximum values of the data set.

Table 6. Risk Quotiens (RQ) based on Hg concentration in the river water and the guideline concentrations of 0.012 μg l^{-1} (96 h) and 2.4 μg l^{-1}.

Sampling site	***RI$_{w(0.012)}$*** Mean (S. Dev)	Min.	Max.	Probability exceeding guideline (%)
Site 1	12.81 (5.95)	2.50	23.00	100
Site 2	88.19 (79.27)	2.76	578.06	100
Site 3	15.61 (11.42)	0.79	83.05	100
Site 4	47.70 (43.60)	1.18	391.97	100
Site 5	15.03 (5.76)	0.00	37.83	100
Site 6	3.76 (0.72)	2.50	5.00	100
	RI$_{w(2.4)}$			
Site 1	0.06 (0.03)	0.01	0.11	0.0
Site 2	0.45 (0.40)	0.02	2.87	8.9
Site 3	0.08 (0.06)	0.00	0.41	0.0
Site 4	0.24 (0.21)	0.01	1.97	0.0
Site 5	0.08 (0.03)	0.00	0.19	0.0
Site 6	0.02 (0.0)	0.01	0.02	0.0

Table 7. Risk Quotiens (RQ) based on Hg concentration in river sediments and the guideline concentrations of 0.17 μg g^{-1} dw and 0.486 μg g^{-1} dw.

Sampling site	***RI$_{s(0.170)}$*** Mean (S. Dev)	Min.	Max.	Probability exceeding guideline (%)
Site 1	1.48 (0.58)	0.59	2.93	76
Site 2	21.86 (11.40)	1.55	52.90	100
Site 3	32.88 (3.85)	21.97	44.96	100
Site 4	37.74 (2.77)	23.85	41.17	100
Site 5	5.90 (1.15)	4.11	11.56	100
Site 6	0.41 (0.06)	0.25	0.66	0
	RI$_{s(0.486)}$			
Site 1	11.50 (4.35)	8.02	16.29	76
Site 2	0.52 (0.20)	0.20	1.03	100
Site 3	7.61 (3.97)	8.02	16.29	100
Site 4	13.19 (0.97)	8.63	14.40	100
Site 5	2.07 (0.40)	1.44	4.06	100
Site 6	0.14 (0.02)	0.07	0.23	0

Table 8. Risk for human health related to Hg contaminated fish (RFC) based on a calculation of the personal intake from bioconcentration of Hg from the water, fish consumtion and human body weight.

Sampling site	***RFC*** Mean (S. Dev)	Min.	Max.	Probability exceeding benchmark (%)
All sampling site	0.21 (0.5)	0.0	12.7	4
	RFC´			
	0.06 (0.12)	0.0	3.1	0.2

Observed blood Hg levels, estimated dietary daily intake (DI) and the proportion of individual exceeding the EPA reference dose (RfD) expressing by a hazard quotient (HQ) > 1, are given in Table 9. All subjects, including women of childbearing age, had blood Hg levels below 58 μg/L, the lower limit for a benchmark dose. Overall, 8 out of 142 investigated subjects had levels between 5.8 and 35 μg/L, and only one subject exceeded 35 μg/L.

Only one individual from La Libertad had a HQ >1. In contrast, 5 (7%) subjects from Santo Domingo and 7 (23%) subjects from Muelle de los Bueyes had HQ >1. The young women with moderate to high fish consumption from Muelle de los Bueyes had an increased risk of exceeding the RfD, in comparison to the non-occupationally exposed population from Santo Domingo.

Table 9. Hg pollution from gold mining activities in Santo Domingo Chontales and its local and regional impact on human populations. Blood samples were analyzed by cold vapour atomic fluorescence spectrometry to estimate total blood Hg concentration (Total B-Hg).

Indicators		**Santo Domingo**[1]	**La Libertad**[2]	**Muelle de los Bueyes**[3]
Number of samples		72	40	30
Total B-Hg, µg/L	Median (Range)	1.4 (nd-50)	0.84 (0.24-14)	1.99 (0.4-11)
Estimated dietary daily intake, µg/kg b.w. (DI)	Median (Range)	0. 03 (<0.007-0.7)	0.02 (0.004-0.16)	0.04 (0.01-0.19)
Hazard quotient (HQ)	Median (Range)	0.28 (0.02-6.96)	0.21 (0.04-1.58)	0.37 (0.08-1.89)
Proportion of cases with HQ >1 (95% CI)	N (%; 95% CI)	5 (6.9 % ; 2.7-14.5)	1 (2.5 % ; 0.3-11)	7 (23 % ; 11-40)
Odds ratio for a hazard quotient (HQ_i) >1	OR (95% CI)	---	0.3 (0.04-3)[4]	7.8 (1.7-36)[5]

[1]**Santo Domingo**, a small scale gold mining town in central Nicaragua, where Hg is still used for gold extraction.
[2]**La Libertad,** an equal size gold mining town where Hg has not been used during the last 15 years, located 10 Km west from Santo Domingo.
[3]**Mueye de los Bueyes**, located 50-70 km east from Santo Domingo and la Libertad. Populations from area consume fish from Mico and Rama rivers, which receive contribution from effluents originated at Santo Domingo and La Libertad area.
[4]Risk of having a hazard quotient (HQ_i) >1. La Libertad vs. Santo Domingo. None of the potential covariates changed the effect estimate by >10%. Thus, an only crude estimate is reported.
[5]Risk of having a hazard quotient (HQ_i) >1. Downstream communities vs. Santo Domingo, adjusted by fish consumption. None of the others potential covariates changed the effect estimate by >10%.

Discussion

The resultant risk map is explained by the fact that the high vulnerability areas, the larger hazards and the groundwater zones with higher economic values coincide in some parts of the basin. The relatively high vulnerability in the south of the basin has also an effect on the resultant risk map with medium risk in those areas (see Figure 2c). This result is also hydrologically important, since contaminants will tend to move in the drainage direction, in this case from north to south. Therefore, higher risk should be observed downstream from the pollution sources.

The Hazard quotient based on Hg concentrations found in the springs support the map of risk produced in this evaluation. The main risk is concentrated along the river channel. Mendoza et al. (2004) shows that there are areas along the polluted river where connections between the river and the nearby shallow aquifers can facilitate infiltration of pollutants.

The risk of pollution is of concern when analysing the position of the groundwater supply sources for the population. The main source of water supply is located only 100 m away from the polluted river, in an area with medium risk of pollution. Some other sources are also located close to mills and mining areas.

This risk of groundwater pollution represents the risk as a point in the timescale. This means that the risk changes as the hazards does with time. Installation or removal of gold processing plants has an effect on increasing or reducing the risk, respectively. In the same way, the concentrations of Hg in water of the drainage system are a function of the variability in the emission sources and the changes in flow of the river.

Because a large number of aquatic organisms could exist in the river and the Hg concentrations in the river are time and spatial dependent, a single dose-organism response relationship could not be derivate from the field data. However, the calculated RI's suggest (Tables 3 and 4) that aquatic organisms are affected by the relative high Hg concentration in the Sucio river (Table 2). Freshwater organisms such as insects and macro invertebrates are high sensitive to Hg compounds and their susceptibility to Hg vary greatly (WHO, 1989). These can obtain Hg from food, water and sediment and they accumulate Hg with continuo sources of exposure (Huckabee et al., 1979). Toxicity tests on freshwater sensitive organisms result in a wide range of BCF values. Reported BCF are from 138 to two orders of magnitude up (WHO, 1989). High BCF indicates that most of the Hg is transferred from the water to the organisms. For instance, physiological and biochemical disruptions are sublethal effects commonly observed on freshwater sensitive species. Generally, lethal concentrations of total Hg to sensitive and representative aquatic organisms vary from 0.1 to 2.0 μg l^{-1} (Eisler, 2000).

Since a concentration of 0.012 μg/l is an overprotective life criterion related to the Hg concentration in the water, the Monte Carlo simulation showed high risk indices (Table 3). Even though, the Hg concentrations in the water resulted to be below of the benchmark value (Table 3) which is related to sublethal and lethal effects on sensitive organisms, the risk indices related to the Hg in the sediments indicate a high risk for benthic organisms living at those sites located close to the Hg sources (Table 4).
Most of the Hg in surface waters and sediments is typically inorganic, but the Hg accumulated in fish is almost entirely Methylmercury (Huckabee et al., 1979; Bloom, 1992). Results of Monte Carlo simulations estimating the risk for human health related to the consumption of Hg contaminated fish (which are considered the primary source of Hg in the human diet (Clarkson, 1992)), show that dietary Hg exposure posed a very low risk to St Domingo entire population (Table 5). Nevertheless, the risk is overestimated. It can be high if only the susceptible population (children, pregnant women) is considered in the risk deduction.

A similar conclusion can be drawn from the observations in humans in the area. A cord blood Hg level of 85 μg/L (lower 95% confidence bound = 58 μg/L) has been associated with subtle fetal neurodevelopmental effects (NRC, 2000). We observed that all subjects, including women of childbearing age, had levels below 58 μg/L but 6 % had levels between 5.8 and 58 μg/L; that is, levels within a factor of 10 of a benchmark dose. The cord blood/maternal blood ratio is however likely to be higher than 1 – a recent estimate is 1.7 (SD 0.9) (Stern and Smith 2005). Thus, the benchmark dose lower 95% confidence bound expressed as maternal blood level would be lower, approximately 35 μg/L. We observed only one subject from Santo Domingo exceeding this value, and no one from the other sampling sites.

EPA has set an oral reference dose, a daily dose considered to be safe) for methyl Hg of 0.1μg/kg/day, derived in part from blood levels in outcome studies. However, a specific value for the blood Hg concentration that corresponds to the RfD has not been established (Rice, 2004). Nevertheless, when calculating the oral daily intake (μg of Hg/Kg/day) based upon the Total B-Hg concentration, we observed that up to 9% of all individual from the three investigated areas had an estimated DI > 0.1 μg/Kg/day (not presented in tables). For subjects from Santo Domingo the estimated DI may overestimate the true DI from fish, as there may be an additional environmental exposure to inorganic mercury. Another caveat is that the study population is aged 5-78, and we introduced a standard blood volume of 5 litres for all subjects. This is an oversimplification which leads to a too high estimated DI in many subjects.

Fish from Rama and Mico rivers is an important part of the diet for segments of the population in the investigated area. Effluents from La Libertad contribute to Mico River, and effluents from Santo Domingo (Río Artigua also called Rio Sucio) are contributors of Siquia rivers, which joins Rama River few kilometers downstream Muelle de lo Bueyes.. The B-Hg levels observed in our sample of young women consuming locally caught fish did not exceed the benchmark dose lower limit. However, it has to be kept in mind that there is no evidence of a threshold effect for the neurodevelopmental effects of methyl mercury. At present the amount of fish from Rama and Mico River consumed by the general population is unknown. The size of the most susceptible population in the area is substantial. In 2002, there were 463 births in Muelle de los Bueyes, and 310 births in Santo Domingo (INEC, *unpublished data*)

Conclusions

Fatal or sublethal effects on sensitive species (in the Río Sucio) are expected due to long term of waterborne mercury exposure. In the river, sediments are the main mercury source to aquatic organisms. Those downstream sediments, which are far away of the sites where mercury is released, do not represent any risk for aquatic life in the river. The risk for groundwater pollution from Hg is mainly concentrated around the mining town of Santo Domingo, since the main pollution sources are located there and that part of the area is vulnerable to pollution. The risk extends from the village along the river channel. The pollution can reach the aquifers in the extent that the aquifers are interconnected with the river channel. Despite the reported concentrations of mercury in fish are relatively high, the risk for humans related to consumption of Hg contaminated fish is not a major concern. However, young women should be advised to avoid high consumption of locally caught fish before and during pregnancy.

References

Aller L, Bennet T, Hehr JH, Petty RJ, Hackett G (1987) DRASTIC: A Standardized System for Evaluation Groundwater Pollution Potential using Hydrogeologic Settings, U.S. Environmental Protection Agency, Ada. Ok, EPA/600/2-87-036, 455 p.

André L, Rosén K, Torstendahl J (1997) Minor field study of mercury and lead pollution from gold refining in central Nicaragua. MSc thesis ISBN 1402-1617 Luleå University of Technology, Sweden, 154p

ATSDR (1999) Toxicological profile for mercury. Agency for Toxic Substances and Disease Registry, Atlanta, GA: U.S. Department of Health and Human Services, Public Health Service. Available from: http://www.atsdr.cdc.gov/toxprofiles/tp46.html [Accessed on March 31, 2006]

Belt T (1874). The Naturalist in Nicaragua; A Narrative of Residence at the Gold Mines of Chontales; Journeys in the Savannahs and Forest. London, J. S. Dent and Sons

Bloom NS (1992) On the chemical form of mercury in edible fish and marine invertebrate tissue. Canadian Journal of Fisheries and Aquatic Sciences. 49: 1010–1017

CEQC/CCME (1999) Canadian Environmental Quality Guidelines/Canadian Council of Ministers of the Environment

Cirone PA, Duncan B (2000) Integrating human health and ecological concerns in risk assessments. Journal of Hazardous Materials 78: 1-17

Civita M, De Maio M (1997) Assessing groundwater contamination risk using ARC/INFO via GRID function, Proceedings of ESRI Conference 1997, San Diego, USA

Clarkson TW (1992) Mercury: Major issues in environmental health. Environ. Health Perspect., 100: 31–38

Cuadra SN, Delgado A, Alfonso A, Lundh T, Jakobsson K (2005), Mercury exposure in the small-scale gold mining sector, Santo Domingo and La Libertad, Chontales, Nicaragua. Presented at III Conference on Occupational and Environmental Health in the Americas, Alajuela, Costa Rica

Cuadra SN (2006) Preliminary report on Mercury exposure and fish consumption in young women from Muelle de Los Bueyes, a rural town downstream central mining area of Nicaragua. Presented at XIV University Scientific Conference, National Autonomous University of Nicaragua (UNAN Managua), Managua.

Davidson PW, Myers GJ, Weiss B (2004), Mercury Exposure and Child Development Outcomes. Pediatrics 113: 1023-9

Ducci D (1999) GIS Techniques for Mapping Groundwater Contamination Risk. Natural Hazards 20(2-3):279-294

Eaton DL, Klaassen CD (1996) Principles of toxicology. In Klaassen, C. D. (ed), Casarett&Doull's Toxicology, 5th ed. Pp 13-33. McGraw-Hill, NY, USA.

Eisler R (2003), Health risk of gold miners. Environmental Geochemistry and Health 25: 325-45

Eisler E (2000) Health Hazard to Humans, Plants and Animals – Handbook of Chemical Risk Assessment. Lewis Publisher. Boca Raton, London New York Washington DC

Greenland H (1989) Modelling and variable selection in epidemiologic analysis. Am J Public Health 79: 340-9

Harvey T, Mahaffey KR, Vasquez S, Dourson M (1995) Holistic risk assessment: An emerging process for environmental decisions. Regulatory Toxicology and Pharmacology 22, 110-117

Huckabee JW, Elwood JW, Hildebrand SG (1979) Accumulation of mercury in freshwater biota. Pages 277-302 in J. O. Nriagu (ed.). The Biogeochemistry of Mercury in the Environment. Elsevier/North-Holland Biomedical Press, NY.

INEC (unpublished data) Demographic survey by the Instituto Nacional de Estadísticas y censos. INEC, Managua, Nicaragua

INETER (1991) Anuarios Meteorológicos (1990, 1991) [meteorological charts] Catastro e Inventatio de Recursos Naturales, Nicaragua

Kolluru R (1996) Health risk assessment: principles and practices. In: Kolluru, R, Bartell, S, Pitblado, R et al. (eds), Risk Assessment and Management Handbook, McGraw-Hill, NY, USA. pp 10.3-10,59

Lacerda (2003) Updating global Hg emissions from small-scale gold mining and assessing its environmental impacts Environmental Geology 43:308–314

Landis WG, Weigers JA (1997) Design considerations and a suggested approach for regional and comparative ecological risk assessment. Human and Ecological Risk Assessment 3:287-297

Lowell RB, Culp JM, Dubé MG (2000) A weight-of-evidence approach for northern river risk assessment: integrating the effects of multiple stressors. Environmental Toxicology and Chemistry 19:1182-1190

Mendoza JA, Dahlin T, Barmen G (2004) Use of resistivity imaging in a surface water –groundwater interactions study. Procc. XXXIII International Association of Hydrogeology IAH & VI ALHSUD Congress 11-15 October, 2004, Zacatecas City, Mexico

Mendoza JA, Barmen G (2006) Assessment of groundwater vulnerability in the Río Artiguas basin, Nicaragua. Environmental Geology, DOI 10.1007/s00254-006-0233-1

Moraes R, Molander S (2004) A procedure for ecological tiered assessment of risks (PETAR). Human and Ecological Risk Assessment 10:349-371

Moreira JC (1996). "Threats by Heavy Metals: Human and Environmental Contamination in Brazil." The Science of the Total Environment. **188** Suppl**.**(1): S61-S71

NRC (2000) Toxicological effects of methylmercury, Committee on the Toxicological Effects of Methylmercury, Board on Environmental Studies and Toxicology,Commission on Life Sciences, National Research Council, National Academy Press, Washington, DC.

Rice DC, Schoeny R, Mahaffey K (2003) Methods and rationale for derivation of a reference dose for methylmercury by the U.S. EPA. Risk Analysis 23: 107-15

Salomons W (1995) Environmental Impact of Metals Derived from Mining Activities: Processes, Predictions, Prevention. Journal of Geochemical Exploration 52: 5-23

Stern AH, Smith AE (2005) An assessment of the cord blood/maternal blood methylmercury ratio: implications for risk assessment. Environ Health Perspect 111:1465-70

Suter GW II (2004) Bottom-up and top-down integration of human and ecological risk assessment. Journal of Toxicology and Environmental Health, Part A 67, 779-790

Tchounwou PB, Ayensu W K, Ninashvili N, Sutton D (2003) Environmental exposure to mercury and its toxicopathologic implications for public health. Environ Toxicol 18: 149-75

USEPA (1985) Ambient Aquatic Life Water Quality Criteria for Mercury, U.S. Environmental Protection Agency, Office of Research and Development, Duluth, MN. PB85-22745

USEPA (1989) Risk Assessment Guidance for Superfund: Volume 1-Human Health Evaluation Manual,, US Environmental Protection Agency (EPA), Office of Emergency and Remedial Response, Washington, D.C.

USEPA (2001) Methylmercury (MeHg) (CASRN 22967-92-6). Washington, DC: Integrated Risk Information System, U.S. Environmental Protection Agency (U.S. EPA)

WHO (1989) Mercury Environmental Aspects, World Health Organization, Geneva: Environmental Health Criteria #86

WHO (1990) Environmental health criteria 101: Methylmercury, World Health Organization (WHO), International Programme on Chemicals Safety (IPCS), Geneva

WHO (1991) Environmental Health Criteria 118: Inorganic mercury, World Health Organization (WHO), International Programme on Chemicals Safety (IPCS), Geneva

WHO (1996) Guidelines for drinking-water quality, 2 nd ed. Vol.2 Geneva, 940-949

WHO (2001) Report on integrated risk assessment. WHO/IPCS/IRA/01/12 Geneva, Switzerland, World Health Organization

Zhang Q, Crittenden JC, Mihelcic JR (2001) Does simplifying transport and exposure yield reliable results? An analysis of four risk assessment methods. Environmental Science &Technology 35: 1282-1288.